

Understanding the
role of histone H3.3
and its chaperone
ATRX in the
maintenance of
chromatin integrity

Chang Tsz Man

Submitted in total fulfillments of the
requirements of the degree of

Doctor of Philosophy

October 2015

Department of Biochemistry
and
Molecular Biology

Monash University

© The author 2015. Except as provided in the Copyright Act 1968, this thesis may not be reproduced in any form without the written permission of the author.

I certify that I have made all reasonable efforts to secure copyright permissions for third-party content included in this thesis and have not knowingly added copyright content to my work without the owner's permission.

TABLE OF CONTENTS

LIST OF FIGURES	1
LIST OF SUPPLEMENTARY FIGURES	3
LIST OF TABLES	4
LIST OF SUPPLEMENTARY TABLES	5
LIST OF PUBLICATIONS	6
SUMMARY	7
LIST OF ABBREVIATIONS	9
GENERAL DECLARATION	11
ACKNOWLEDGEMENTS	13
CHAPTER 1.....	14
INTRODUCTION	14
1.1 THE ROLE OF TELOMERE IN THE MAINTENANCE OF GENOME STABILITY.....	15
<i>1.1.1 Shelterin and its role in the maintenance of telomere and genome integrity.....</i>	<i>16</i>
(i) Telomere capping and suppression of DDR signalling	17
(ii) Telomere replication	19
(iii) Homeostasis of telomere length.....	20
(iv) Maintenance of genome integrity during mitosis	21
<i>1.1.2 The importance of telomere transcription to the maintenance of telomere integrity</i>	<i>22</i>
<i>1.1.3 The epigenetic state of telomeres and its role in the maintenance of telomere length</i> <i>and genome stability.....</i>	<i>28</i>
<i>1.1.4 The ALT pathway – a model to illustrate the association between the maintenance</i> <i>of telomere integrity and tumorigenesis</i>	<i>34</i>
1.2 THE ROLE OF HISTONE POST-TRANSLATIONAL MODIFICATIONS TO THE MAINTENANCE OF GENOME STABILITY	38
<i>1.2.1The function of histone phosphorylation and methylation in the regulation of gene</i> <i>transcription and chromatin organization</i>	<i>42</i>
<i>1.2.2 The role of histone modifications in DNA damage signalling and repair</i>	<i>44</i>
1.3 THE ROLE OF HISTONE VARIANTS IN THE MAINTENANCE OF CHROMATIN INTEGRITY ...	48
<i>1.3.1 Replication independent role of H3.3.....</i>	<i>52</i>

1.3.2 <i>The role of H3.3 in the establishment of epigenetic reprogramming during embryonic development</i>	53
1.3.3 <i>The function of H3.3 in the dynamics of chromatin organization and the maintenance of chromatin integrity</i>	55
1.4 THE ROLE OF HISTONE MODIFICATIONS ON H3.3 IN THE REGULATION OF GENOME STABILITY AND CANCER DEVELOPMENT	59
CHAPTER 2	62
PML-NBS PROVIDE A PLATFORM FOR THE ASSEMBLY OF H3.3 AND ATRX TO MAINTAIN TELOMERE CHROMATIN IN PLURIPOTENT MOUSE EMBRYONIC STEM CELLS	62
2.1 OVERVIEW	63
2.2 MATERIALS AND METHOD	65
2.2.1 <i>Cell lines</i>	65
2.2.2 <i>Antibodies</i>	66
2.2.3 <i>Cell-cycle analysis</i>	66
2.2.4 <i>Immunofluorescence analysis and Telomere-FISH analysis</i>	67
2.2.5 <i>siRNA transfection and real time PCR analysis</i>	67
2.2.6 <i>CO-FISH assay</i>	71
2.2.7 <i>Cell extracts and Western Blot analysis</i>	71
2.3 RESULTS	72
2.3.1 <i>PML-NB is associated with the telomeres in pluripotent mESC during S-phase</i>	72
2.3.2 <i>Loss of PML-NB assembly leads the induction of telomere dysfunction</i>	78
2.3.3 <i>The disassembly of PML-NB affects the loading of H3.3 and ATRX to the telomere in mES cells</i>	84
2.3.4 <i>The telomere associated PML-NB is functionally different from the ALT associated PML-NB (APB) in ALT positive cancer cells</i>	90
2.4 DISCUSSION	106
CHAPTER 3	111
CHK1-DRIVEN HISTONE H3.3 SERINE 31 PHOSPHORYLATION MAINTAINS CHROMATIN DYNAMICS AND CELL SURVIVAL IN HUMAN ALT CANCER CELLS	111
3.1 OVERVIEW	112

3.2 MATERIALS AND METHODS	114
3.2.1 Cell cultures.....	114
3.2.2 Antibodies and inhibitors	115
3.2.3 Cell-cycle analysis.....	116
3.2.4 RNAi transfection and quantitative RT-PCR.....	116
3.2.5 Cell extracts and Western blot analysis	119
3.2.6 Immunofluorescence analysis.....	119
3.2.7 Immunoprecipitation and in vitro kinase assay.....	120
3.2.8 Exome sequencing of H3F3A and H3F3B genes	121
3.2.9 Over-expression of pcDNA4/TO/myc HisA N-terminal myc-tagged H3.3 S31A plasmid in ALT cancer cells	124
3.3 RESULTS	126
3.3.1 ALT cancer cells show intense and aberrant H3.3S31ph staining on chromosome arms at mitosis.....	126
3.3.2 Loss of ATRX function does partially contribute to the aberrant H3.3S31ph staining on chromosome arms in ALT cancer cells	138
3.3.3 The altered H3.3 S31 phosphorylation staining pattern in ALT cancer cells is not caused by any underlying mutation in the H3.3 alleles or a differential expression of H3.3 at the protein level.....	142
3.3.4 A delay in mitotic progression contributes to the elevated and extensive H3.3S31ph staining on metaphase chromosome arms in ALT cancer cells	152
3.3.5 Up-regulated CHK1 kinase activity drives H3.3S31 phosphorylation in ALT cancer cells.....	164
3.3.6 Loss of H3.3S31 phosphorylation on the chromosome arms affects the viability of ALT cancer cells by the activation of DDR during mitosis	180
.....	188
3.3.7 Substitution of the Serine with an Alanine residue at Position 31 led to an increase in DNA damage on chromosome arms in ALT cancer cells.....	190
3.4 DISCUSSION	196
CHAPTER 4.....	204
CONCLUSION AND FUTURE DIRECTIONS.....	204
REFERENCES	232

LIST OF FIGURES

FIGURE 1.1 THE TELOMERE STRUCTURE.	26
FIGURE 1.2 THE HETEROCHROMATIC NATURE OF TELOMERE CHROMATIN.....	32
FIGURE 2.1 THE LOCALIZATION OF PML-NB AT THE TELOMERE IS DEPENDENT ON THE CELLULAR PLURIPOTENT STATE.....	74
FIGURE 2.2 LOSS OF PML-NB ASSEMBLY INDUCES TELOMERE DAMAGE IN ES129.1 CELLS	81
FIGURE 2.3 THE DISASSEMBLY OF PML-NB AFFECTS THE DEPOSITION OF ATRX AND H3.3 TO THE TELOMERE IN ES129.1 CELLS	87
FIGURE 2.4 LOCALIZATION OF DDR SIGNALLING PROTEINS TO THE TELOMERES AND PML- NB IN ES129.1 CELLS.....	92
FIGURE 2.5 THE REMOVAL OF MRE11 PROTEIN DOES NOT AFFECT THE ASSEMBLY OF PML- NB AT THE TELOMERE IN ES129.1 CELLS	95
FIGURE 2.6 LOSS OF THE NBS1 PROTEIN DOES NOT AFFECT THE ASSEMBLY OF PML-NB AT THE TELOMERE IN ES129.1 CELLS	99
FIGURE 2.7 NO INCREASE IN THE FREQUENCY OF T-SCE IN PML RNAI-DEPLETED M _{ES} CELLS	103
FIGURE 3.1 LOCALISATION OF H3.3S31PH AT HETEROCHROMATIC REGIONS IN NON-ALT CANCER CELL LINES.....	128
FIGURE 3.2 ABERRANT LOCALIZATION OF H3.3 S31PH ON CHROMOSOME ARMS IN ALT CANCER CELLS.....	131
FIGURE 3.3 SPECIFICITY OF THE H3.3 SERINE 31 PH ANTIBODY STAINING.....	135
FIGURE 3.4 LOSS OF ATRX EXPRESSION CORRELATES WITH THE ALTERED H3.3S31PH STAINING ON CHROMOSOME ARMS IN HUMAN ALT CANCER CELL LINES.....	139
FIGURE 3.5 EXOME SEQUENCING OF <i>H3F3A</i> ALLELE FOR ALT CANCER CELLS.....	145
FIGURE 3.6 NO ASSOCIATION BETWEEN H3.3 EXPRESSION AND ALTERED H3.3 SERINE 31PH DYNAMICS IN ALT CANCER CELLS	149
FIGURE 3.7 PROLONGED MITOTIC PROGRESSION LED TO THE DE-LOCALIZATION OF H3.3S31PH ON CHROMOSOME ARMS IN PLURIPOTENT M _{ES} CELLS	154
FIGURE 3.8 HUMAN ALT CANCER CELL LINES ARE BURDENED WITH SEVERE GENOME INSTABILITY.	157

FIGURE 3.9 ASSOCIATION OF PROLONGED MITOTIC PROGRESSION WITH ABERRANT H3.3S31PH STAINING PATTERN IN ALT CANCER CELL LINES.	161
FIGURE 3.10 CHK1 KINASE MEDIATES THE PHOSPHORYLATION OF H3.3S31 IN ALT CANCER CELL LINES.....	167
FIGURE 3.11 DEPLETION OF CHK1 AFFECTS THE CELL-CYCLE DISTRIBUTION IN ALT CANCER CELLS.....	173
FIGURE 3.12 CHK1 INHIBITION LED TO REDUCED PHOSPHORYLATION OF H3.3S31 IN ALT CANCER CELL LINES.....	177
FIGURE 3.13 INHIBITION OF CHK1 ACTIVITY IN MITOTIC ALT CANCER CELL LINES INDUCES DDR SIGNALING AND AFFECTS CELL VIABILITY.	183
FIGURE 3.14 SUBSTITUTION OF THE H3.3 SERINE TO AN ALANINE RESIDUE ALTERS THE STAINING LEVEL OF H3.3S31PH AND INDUCES DDR SIGNALING IN ALT CANCER CELLS	192
FIGURE 4.1 PROPOSED MODEL OF H3.3S31PH IN THE REGULATION OF CHROMATIN INTEGRITY	211

LIST OF SUPPLEMENTARY FIGURES

SUPPLEMENTARY FIGURE 1 THE SYNCHRONIZATION OF ES129.1 CELLS BY A SINGLE THYMIDINE TREATMENT PROTOCOL.....	110
SUPPLEMENTARY FIGURE 2 SEQUENCING CHROMATOGRAMS OF THE pCDNA4/TO/HIS3-MYC-TAGGED H3.3S31A CONSTRUCT	202
SUPPLEMENTARY FIGURE 3 THE LOCALIZATION OF H3.3S31PH ON CHROMOSOME ARM IN OS CANCER CELLS	215
SUPPLEMENTARY FIGURE 4 LOW LEVELS OF APB IN OS CANCER CELL LINES	219
SUPPLEMENTARY FIGURE 5 OS CANCER CELLS ARE BURDENED WITH HIGH LEVELS OF DNA DAMAGE	223
SUPPLEMENTARY FIGURE 6 INHIBITION OF CHK1 ACTIVITY DOES NOT LEAD TO A SIGNIFICANT REDUCTION OF H3.3S31PH AT THE TELOMERES	226
SUPPLEMENTARY FIGURE 7 PHOSPHORYLATION OF H3.3 SERINE 31 RESIDUE BY THE AURORA A AND AURORA B KINASES	229

LIST OF TABLES

TABLE 1.1 PREVALENCE OF ALT AND ATRX MUTATIONS IN VARIOUS CANCER SUBTYPES	37
TABLE 1.2 MAJOR HISTONE MODIFICATIONS ON CANONICAL HISTONE H3.....	40
TABLE 1.3 HISTONE VARIANTS AND THEIR CELLULAR FUNCTION.....	50
TABLE 2.1 siRNA SEQUENCE FOR PML, MRE11 AND NBS1 DEPLETION IN ES129.1 CELLS	69
TABLE 2.2 PRIMERS USED FOR QUANTITATIVE PCR ANALYSIS FOR PML, MRE11 AND NBS1 siRNA.....	70
TABLE 3.1 siRNA SEQUENCE FOR CHK1 DEPLETION IN HUMAN ALT CANCER CELLS	118
TABLE 3.2 PRIMERS USED FOR CHK1 QUANTITATIVE RT-PCR	118
TABLE 3.3 PRIMERS USED FOR PCR AMPLIFICATION	122
TABLE 3.4 PRIMERS FOR SEQUENCING <i>H3F3A</i> AND <i>H3F3B</i> ALLELES.....	123

LIST OF SUPPLEMENTARY TABLES

SUPPLEMENTARY TABLE 1 ALT CANCER CELLS HAVE ELEVATED CHK1 ACTIVITY
COMPARED TO NON-ALT CELLS. 203

SUPPLEMENTARY TABLE 2 CHK2 ACTIVITY IS HIGHER IN SOME ALT CANCER CELLS..... 203

LIST OF PUBLICATIONS

ACCEPTED MANUSCRIPT

PML bodies provide an important platform for the maintenance of telomeric chromatin integrity in embryonic stem cells.

Chang FT, McGhie JD, Chan FL, Tang MC, Anderson MA, Mann JR, Andy Choo KH, Wong LH.

Nucleic Acids Res. 2013 Apr;41(8):4447-58.

CHK1-driven histone H3.3 serine 31 phosphorylation is important for chromatin maintenance and cell survival in human ALT cancer cells.

Chang FT, Chan FL, R McGhie JD, Udugama M, Mayne L, Collas P, Mann JR, Wong LH.

Nucleic Acids Res. 2015 Mar 11;43(5):2603-14.

Histone variant H3.3 provides the heterochromatic H3 lysine 9 tri-methylation mark at the telomeres

Udugama M, **Chang FT**, Chan FL, Tang M, Pickett HA, McGhie JD, Mayne L, Collas P, Mann JR, Wong LH

Nucleic Acids Res. 2015 Aug 24. pii: gkv847. [Epub ahead of print]

SUMMARY

Histones and their associated post-translational modifications (PTM) play an essential role in regulating chromatin dynamics. In addition to the canonical histone family, histone variants have also emerged as key players in regulating chromatin structure and dynamics and governing cellular integrity. For example, recent studies have identified frequent mutations of not only histone variant H3.3 at specific key residues, but also its chaperones Alpha-Thalassemia Mental Retardation X-linked (ATRX) and DAXX (Death-associated protein 6) in human cancers. In particular, mutations of the ATRX genes is found to be closely associated (>90% mutation rate) in human cancers that maintain the telomere length by a recombination based mechanism, known as the Alternative Lengthening of Telomeres (the ALT pathway).

The function of ATRX is required for mediating the deposition of H3.3 at heterochromatin including the telomeres and pericentric DNA repeats. Although it has been well documented that ATRX is important for the maintenance of a heterochromatic state at these repeats such as the telomeres, much remains unknown of the pathway and nuclear platform that promote ATRX binding and H3.3 deposition at telomeres. Furthermore, it is also unclear whether ATRX inactivation can further affect H3.3 deposition and its PTM profile at other genomic regions or in the global genome. In this study, I investigated the assembly pathway essential for binding of ATRX and deposition of H3.3 at telomeres in pluripotent mouse embryonic stem cells (mESC). I showed a novel role of Promyelocytic nuclear bodies (PML-NB) in regulating the assembly of H3.3 by ATRX at the telomeres. In mouse ES cells, the association of telomeres with these nuclear bodies is important for the propagation of a unique telomeric chromatin state which is important for maintaining the mESC pluripotent state. More importantly,

my study shows that these nuclear bodies are functionally distinct to the ALT-associated PML nuclear bodies found in human ALT cancers. Considering the high inactivation frequency of ATRX reported in these telomerase deficient cancers, this project also examined the effect of ATRX loss of function on the distribution and PTM of H3.3 through the investigation of the profile of Serine 31 phosphorylation on H3.3 (H3.3S31ph). H3.3S31ph is normally a histone mark associated with heterochromatic repeats including the telomeres and pericentric DNA repeats in mitotic cells. However, in ALT cancer cells, H3.3S31 phosphorylation is found to be extremely high across the entire chromosome arms. This aberrant localisation of H3.3S31ph correlates with the loss of ATRX expression and is driven by the high level of endogenous CHK1 activity in these cancer cells. Together, this study has examined the role of ATRX and H3.3 in the regulation of chromatin integrity in two different cellular settings: the normal and disease cell state. Findings from this study have provided novel insights into the mechanism underlying H3.3 deposition at telomeres in normal cells, and the impact of ATRX inactivation on H3.3 PTM profile, and its contribution to disease development in cancer cells.

LIST OF ABBREVIATIONS

ALT	Alternative Lengthening of Telomeres
APB	ALT associated PML-NB
ATM	Ataxia telangiectasia mutated
ATR	ATM and Rad3 related
ATRX	Alpha Thalassemia Mental Retardation X-linked protein
AukB	Aurora B kinase
CHK1	Checkpoint kinase 1
CHK2	Checkpoint kinase 2
Cr6	Crest 6
DAXX	Death associated domain 6 protein
DDR	DNA damage response
Dnmt	DNA methyltransferase
DSB	Double-stranded breaks
H3	Histone H3
H3.3	Histone variant H3.3
H3.3S31ph	H3.3 Serine 31 phosphorylation
HDR	Homology directed repair
HP1	Heterochromatin Protein 1
HR	Homologous Recombination
mESC	mouse Embryonic stem cell
Mre11	Meiotic Recombination 11 homolog A
MRN	Mre11-Rad50-Nbs1
Nbs1	Nijmegen Breakage Syndrome 1
NHEJ	Non-homologous End-Joining
PML	Promyelocytic leukemia protein

PML-NB	PML nuclear bodies
PTM	Post-translational modification
Suvar	Suppressor of variegation
TERRA	Telomere repeat containing RNA
TIF	Telomere damage induced foci
T-SCE	Telomere sister chromatid exchange
TRF1	Telomere Binding protein 1
TRF2	Telomere Binding protein 2
53BP1	p53 binding protein
γ H2AX	H2A phosphorylated Serine 139

GENERAL DECLARATION

Monash University

Declaration for thesis based or partially based on conjointly published or unpublished work

General Declaration

In accordance with Monash University Doctorate Regulation 17.2 Doctor of Philosophy and Research Master's regulations the following declarations are made:

I hereby declare that this thesis contains no material which has been accepted for the award of any other degree or diploma at any university or equivalent institution and that, to the best of my knowledge and belief, this thesis contains no material previously published or written by another person, except where due reference is made in the text of the thesis.

This thesis includes 2 original papers published in peer reviewed journals. The core theme of the thesis is to understand the function of H3.3 and its chaperone protein ATRX in the regulation of chromatin integrity in pluripotent mouse embryonic stem cells and ALT cancer cells. The ideas, development and writing up of all the papers in the thesis were the principal responsibility of myself, the candidate, working within the Department of Biochemistry and Molecular Biology under the supervision of Dr. Lee H Wong

The inclusion of co-authors reflects the fact that the work came from active collaboration between researchers and acknowledges input into team-based research.

In the case of Chapters 2 and 3 my contribution to the work involved the following:

Thesis chapter	Publication title	Publication status	Nature and extent of candidate's contribution
2	PML bodies provide an important platform for the maintenance of telomeric chromatin integrity in embryonic stem cells.	Published	Experimental planning and analysis for all immunofluorescence analyses (50% of the manuscript); co-author performed ChIP and FISH experiments in the manuscript. Manuscript preparation and editing.
3	CHK1-driven histone H3.3 serine 31 phosphorylation is important for chromatin maintenance and cell survival in human ALT cancer cells.	Published	Planned, performed and conduct 90% of all experiments presented in the manuscript. Manuscript preparation and editing.

I have renumbered sections of submitted or published papers in order to generate a consistent presentation within the thesis.

Signed:



Date: 1st October 2015

ACKNOWLEDGEMENTS

Foremost, I would like to express my sincere gratitude to my supervisor and mentor, Dr Lee Wong for her guidance and patience during my candidature. Without her due support, this candidature would not have come to this fruitful completion.

Next, I would like to thank all members of the Epigenetics and Chromatin Lab, including Dr Lyn Chan, Dr Jane Lin, Dr Maheshi Udugama and Dr Hsiao Voon for their continual support. It has been a memorable experience with you all during the past two years following our relocation to Monash University.

I would also like to take this opportunity to thank all past and current members of the Chromosome Research Laboratory at the Murdoch Childrens Research Institute for all their friendship and kindness.

Lastly, I would like to express my gratefulness to my family and my companion, Dr Jason Tang, for his patience and understanding during my rough four years of the PhD training.

Chapter 1

Introduction

1.1 The role of telomere in the maintenance of genome stability

The telomere structure is maintained by a six-subunit protein complex known as the Shelterin (de Lange, 2005). This nucleoprotein complex shields the chromosome ends from the activation of the DNA damage response (DDR) signalling; however, it is irony that normal telomere maintenance also requires transient recruitment of proteins involved in DDR signalling. These include the ATM kinase, the Mre11a-Rad50-Nbs1 (MRN complex) and the Fanconi anemia (FA) proteins, as well as the RecQ family of DNA helicases such as Bloom and Werner's syndrome proteins (Bohr, 2008; Paeschke et al., 2010; Verdun et al., 2005). These DDR signalling proteins and helicases are important regulators of telomere biology and genome stability. Inactivation of these proteins, such as that observed in cells derived from patients with Bloom and Werner's syndrome, lead to increase in the frequency of telomere fragility and chromosome aberrations. Together, these promote the development of premature cellular arrest and predisposes to tumourigenesis (Blasco, 2005; Bohr, 2008). In addition, it is well documented that the role of these DDR signalling proteins also play significant roles in cancers which regulate the telomere length by a recombination based mechanism known as the Alternative Lengthening of Telomeres (ALT pathway). In these telomerase deficient cancer cells, the assembly of the ALT associated PML nuclear bodies (APB) was found to be dependent on these DDR signalling proteins. It has been shown that the removal of the MRN complex results in substantial reduction in telomere DNA recombination or telomere sister chromatic exchange (T-SCE) and cell survival of these cancers cells (Jiang et al., 2005; Wu et al., 2003; Zhong et al., 2007). Considering the importance of telomere biology in cancer development, this section will address the interdependence between telomere structure, length and epigenetic chromatin environment to the maintenance of telomere integrity.

1.1.1 Shelterin and its role in the maintenance of telomere and genome integrity

The telomeric region is made up of repetitive TTAGGG sequences. During telomere synthesis, conventional DNA polymerases are unable to replicate the telomeric DNA distal to the last Okazaki fragment. In cancer cells, this end-replication problem is overcome by the function or activity of telomerase complex (a terminal transferase and a ribonucleoprotein) that adds DNA sequence repeats to the 3' end of DNA strands in the telomere regions. At the very distal end of the telomere is a protruding G-overhang single-stranded DNA. This 3' end single-stranded DNA invades into the double stranded portion of the telomeric tract, leading to the formation of a displacement loop (D-loop) and the t-loop structure (Griffith et al., 1999) (Figure 1.1). The Shelterin complex plays a critical role in promoting the formation of the t-loop which mediates the protective function of telomeres. Shelterin is made up of 6 subunits: telomere repeats associated factor 1 and 2 (TRF1 and TRF2), Protector of telomeres protein 1 (POT1), TRF1 interacting protein 2 (TIN2), TIN2 organising protein 1 (TPP1) and Repressor of activator protein 1 (Rap1) (de Lange, 2005). The importance of the Shelterin complex in mediating telomere structural maintenance and chromosome end protection is evident by the substantial increase in DNA damage markers (e.g. γ H2AX) following the disruption of Shelterin components such as TRF2 and TRF1 (Martinez et al., 2009; Takai et al., 2003). The formation of these telomere damage foci (TIF) indicates that DDR signalling is activated as the chromosome ends are recognized as double-stranded breaks (DSB) or damaged DNA sites (Palm and de Lange, 2008). In p53 proficient cells, the activation of DDR signalling leads to cellular arrest and apoptosis (Takai et al., 2003). In most cancer cells where the p53 checkpoint is lost, the persistent telomere damage can either result in a mitotic bypass or delay in mitotic progression (Davoli et al., 2010; Stagno d'Alcontres

et al., 2014). This leads to the formation of multinucleated cells that underlies the development of genome instability during tumourigenesis (Davoli et al., 2010).

(i) Telomere capping and suppression of DDR signalling

Telomeric DNA damage is generally repaired by two major mechanisms: the template dependent Homology directed Repair (HDR) and the error prone classical Non-Homologous End Joining (NHEJ). This leads to downstream recruitment of signalling proteins such as the Ataxia Telangiectasia mutated (ATM) and the Ataxia Telangiectasia and Rad3 related (ATR) (Shiloh, 2003). In addition to the canonical repair mechanisms, the removal of all Shelterin subunits have indicated the involvement of other pathways, including the microhomology directed alternative NHEJ and resection repair (Sfeir and de Lange, 2012). Activation of the DDR signalling pathway is generally repressed by the Shelterin complex under physiological conditions (Denchi and de Lange, 2007). During telomere replication, the transient exposure of the G-overhang and the duplex portion of the telomeres can lead to activation of the DDR signalling. Furthermore, some of these damage proteins including the ATM and MRN complex are actively recruited to facilitate the processing and the maturation of the t-loop structure following telomere replication (Palm et al., 2009; Verdun et al., 2005; Yang et al., 2005; Zhu et al., 2000).

The TRF1 and TRF2 are two Shelterin components which bind to the duplex portion of the telomeric DNA tract. Although these subunits contain similar Myb-DNA binding domains at the C-terminal, the difference in their N-terminal TRF homology (TRFH) domain indicates these two subunits have different roles in mediating telomere protection (Broccoli et al., 1997). In addition to its role in repressing ATR signalling, TRF1 is known to have unique roles during telomere replication (refer to later section (Sfeir et al., 2009)). On the other hand, the TRF2 subunit mediates telomere protection via two

different mechanisms: the repression of NHEJ pathway to prevent chromosome fusions (van Steensel et al., 1998), as well as the suppression of ATM activation to prevent the downstream DDR signalling (Karlseder et al., 2004; Okamoto et al., 2013).

Indeed, the ability of TRF2 to mediate telomere end protection is regulated by the TIN2 subunit (Frescas and de Lange, 2014; Kim et al., 2004). The TIN2 subunit comprises of binding sites for TRF1, TRF2 and the TPP1 subunits. It acts as an intermediary that links the TRF1 and TRF2 subunits to the TPP1/POT1 complex (Takai et al., 2011). During telomere replication, TIN2 promotes the assembly of the POT1/TPP1 heterodimers on the single-stranded telomeric tract to prevent its recognition by the Replication Protein A (RPA) and subsequent downstream activation of ATR signalling (Hockemeyer et al., 2007; Hockemeyer et al., 2005; Takai et al., 2011; Wu et al., 2006; Zimmermann et al., 2014). Besides its interaction with TIN2, TRF2 also recruits the Rap1 subunit during telomere replication. The transient localisation of TRF2/Rap1 complex to the blunt-ended telomeric tract after the replication process serves to regulate the activation of the NHEJ pathway mediated by the DNA dependent protein kinase (DNA-PK) (Bombarde et al., 2010). Unlike the TIN2 subunit, loss of Rap1 does not affect the localisation of other Shelterin subunits (Frescas and de Lange, 2014; Martinez et al., 2010). Furthermore, the removal of the Rap1 subunit also does not result in a substantial increase in telomere fusion. This indicates the function of TRF2 in repressing ATM signalling is independent of the Rap1 subunit and more importantly, Rap1 is not involved in establishing the telomere capping (Martinez et al., 2010; Sfeir et al., 2010). Nevertheless, an increase in telomere DNA recombination and the fragile telomere phenotype is observed in Rap1-null cells, indicating Rap1 is involved in maintaining other aspects of the telomere structural organization and function (Martinez et al., 2010; Sfeir et al., 2010).

(ii) Telomere replication

The origin of telomere replication is known to initiate at the sub-telomeric region which is highly methylated and consists of repetitive sequences (Sfeir et al., 2009). Due to the nature of the telomeric sequences, they are known to be poor templates for the DNA replication machinery. Furthermore, recent evidence has suggested the propensity of secondary structures, such as G-quadruplex to form at the G-rich telomeric tract (Lipps and Rhodes, 2009; Sfeir et al., 2009). The formation of these G4 structures can affect the normal progression and results in subsequent stalling of the replication fork. In a study by Rizzo et al (2009), DDR signalling mediated by the ATR pathway is activated following the treatment with G4 stabilizing drug. Furthermore, the persistence of these structures also disrupts the binding of the Shelterin subunits on the replicating telomere tract (Rizzo et al., 2009).

Replication stalling at the telomeric tract is manifested by the presence of multi-telomeric DNA signals on the sister chromatid of metaphase chromosome spreads known as the fragile telomere (Sfeir et al., 2009). The Shelterin complex, in particular the TRF1 subunit is shown to play an important role in suppressing the occurrence of fork stalling at the telomeres. Consistent with this, the telomere fragility phenotype was most prominent following the removal of the TRF1 subunit and members of the RecQ family of DNA helicases including the Regulator of Telomere Length (RTEL1) and Bloom (BLM) protein (Deng et al., 2013; Sfeir et al., 2009; Vannier et al., 2012). During telomere replication, the recruitment of these DNA helicases by the TRF1 and TRF2 subunits promote dismantling of both the t-loop and D-loop structure (Opresko et al., 2004; Sarek et al., 2015; Vannier et al., 2012). Furthermore, the ability of these DNA helicases to unwind G-rich DNA templates *in vitro* suggests their potential role in resolving G4 structures to minimize the replication stalling at the fragile telomeric sites

(Mohaghegh et al., 2001). Indeed, both BLM and WRN proteins have been implicated in the removal of G4 structures that arise during the lagging strand synthesis (Crabbe et al., 2004; Zimmermann et al., 2014). Furthermore, a substantial increase in the level of BLM and WRN was found to be present on replicating telomeres following the stabilization of G4 structures, further indicating the importance of these helicases in resolving these replication intermediates (Rizzo et al., 2009). Furthermore, the recruitment of the TIN2/POT1/TPP1 complex to the G-rich strand mediated by TRF1 subunit to avert the activation of ATR signalling (Zimmermann et al., 2014). Together, this indicates the Shelterin complex functions at different aspects to repress replication stalling during telomere synthesis.

(iii) Homeostasis of telomere length

The role of Shelterin in the maintenance of telomere integrity is not limited to the replication process. Several studies have also established an important function of the Shelterin complex in regulating telomere length and the maintenance of genome stability (Blanco et al., 2007; Martinez et al., 2009; Munoz et al., 2005). For example, the TIN2/TPP1 complex has been reported to regulate the recruitment of the telomerase enzyme (Abreu et al., 2010). In a subgroup of patients with Dyskeratosis Congenita (DC) with TIN2 mutation, loss of telomere cohesion has been shown to affect the binding of the telomerase enzyme and leads to rapid telomere attrition (Canudas et al., 2011). Both TRF1 and TRF2 subunits are known to be negative regulators of the telomere length (Smogorzewska et al., 2000; van Steensel and de Lange, 1997). This is evident by the rapid telomere shortening following the over-expression of TRF1 or TRF2 subunits. In earlier studies, the increase in telomere attrition has been attributed to the stabilization of the t-loop structure, which can interfere with the binding of the telomerase enzyme (Smogorzewska et al., 2000; van Steensel and de Lange, 1997). Interestingly, recent

investigations with targeted over-expression of these two subunits at the epidermal cells have argued that aberrant telomere processing is likely to be the underlying cause of the telomere shortening phenotype (Muñoz et al., 2009; Munoz et al., 2005). Although over-expression of the dominant negative allele of TRF1 is shown to induce telomere elongation (van Steensel and de Lange, 1997), no significant change in telomere length was detected following the deletion of TRF1 in mouse models or targeted removal of TRF1 in skin epithelial cells (Karlseder et al., 2003; Muñoz et al., 2009). Nevertheless, the persistent induction of DDR signalling at these critically short telomeres or de-protected telomeres have contributed to the induction of genome instability (Beier et al., 2012; Martinez et al., 2009; Munoz et al., 2005). Furthermore, a substantial increase in the frequency of telomere sister chromatid exchange (T-SCE) and the presence of APB, which are hallmarks associated with ALT cancers are also detected (Blanco et al., 2007; Muñoz et al., 2009). These findings show that the altered binding dynamics of these Shelterin subunits at telomeres can predispose cells to cancer development.

(iv) Maintenance of genome integrity during mitosis

Besides its regulatory role during telomere replication in S-phase, the Shelterin complex is also involved in the maintenance of chromatin integrity at mitosis. The spindle assembly checkpoint (SAC) ensures proper chromosome alignment prior to the segregation at the metaphase-to-anaphase transition. Several molecular players including the Aurora kinase family (reviewed in (Carmena et al., 2009) and the TRF1 subunit is implicated in the regulation of chromosome segregation and mitotic progression. In addition to its interaction with proteins that regulates the mitotic spindle checkpoint (Muñoz et al., 2009; Nakamura et al., 2001), a study by Ohishi et al indicated the chromosome misalignment regulated by the Aurora A kinase is mediated by the TRF1 protein (Ohishi et al., 2010). Furthermore, TRF1 is required for the localisation of Aurora

B kinase to mediate centromere cohesion and prevent subsequent chromosome segregation defect (Ohishi et al., 2014). In addition to the surveillance on the proper microtubule attachment to the kinetochore prior to chromosome segregation, a recent study has reported a telomere-based monitoring mechanism to ensure the chromosome integrity during mitosis (Hayashi et al., 2012). Following prolonged mitotic arrest, the uncoupling of TRF2 from the telomeres results in telomere de-protection and DDR signalling. The subsequent cell-cycle arrest following mitotic exit ensures the damage is repaired before further progression (Hayashi et al., 2012). In conclusion, the Shelterin complex mediates telomere protection by regulating the activation of DDR and telomere length homeostasis during the process of telomere synthesis. Furthermore, the extra-telomeric roles of these Shelterin subunits such as the TRF1 and Rap1 indicate a more genome-wide role of this complex in the maintenance of the telomere integrity.

1.1.2 The importance of telomere transcription to the maintenance of telomere integrity

The telomeric tract has long been considered transcriptionally inert as the expression of inserted reporter genes into telomeres and neighbouring subtelomeric regions are inhibited (Baur et al., 2001). This Telomere position effect (TPE) was first uncovered in *Drosophila melanogaster* and demonstrated the repressive chromatin state of the telomeric region. However, the identification of telomere repeats associated RNA (TERRA) has changed the view on the transcription status of the telomeric region (Azzalin et al., 2007; Schoeftner and Blasco, 2010). These telomeric RNAs, which are transcribed from the subtelomeric region during S-phase, are known to play an important role in the maintenance of telomere integrity. This is evident by the increase in the number of TIF at telomeres following the depletion of TERRA (Deng et al., 2009). In

addition to the recruitment of DNA replication factors, the interaction between TERRA and TRF2 also promotes the binding of factors such as the Heterochromatin protein family (HP1) required for the establishment of the heterochromatin state (Deng et al., 2009).

Although these non-coding telomere transcripts are important regulators of telomere structure and integrity, there is growing evidence to suggest that the aberrant accumulation of TERRA can affect the kinetics of telomere replication and maintenance of telomere length (Maicher et al., 2012). During telomere synthesis, the single-stranded telomere DNA can be recognized by two different proteins: Replication Protein A (RPA1) which is involved in the activation of DDR signalling, and the Shelterin complex, POT1 subunit (Hockemeyer et al., 2005). The presence of telomeric RNA facilitates the exchange of RPA1, and promotes the binding of POT1 to the single-stranded telomeric tract to avert the activation of DDR signalling (Flynn et al., 2011). It is known that the presence of TERRA plays an important role in the formation of telomere capping; however, the tendency of these non-coding RNA transcripts to form RNA-DNA hybrids or R-loop can pose challenges to the replication machinery (Aguilera and Garcia-Muse, 2012; Arora et al., 2014; Maicher et al., 2012). Furthermore, the accumulation of TERRA can directly inhibit the binding of the telomerase enzyme, which leads to rapid telomere attrition and cellular senescence (Redon et al., 2010). In telomerase deficient *Saccharomyces cerevisiae* and human cancer cells, the accumulation of these non-coding RNA repeats is required to maintain the recombinogenic ability and prevents the onset of cell-cycle arrest in ALT cancer cells (Arora et al., 2014; Balk et al., 2013; Flynn et al., 2015)

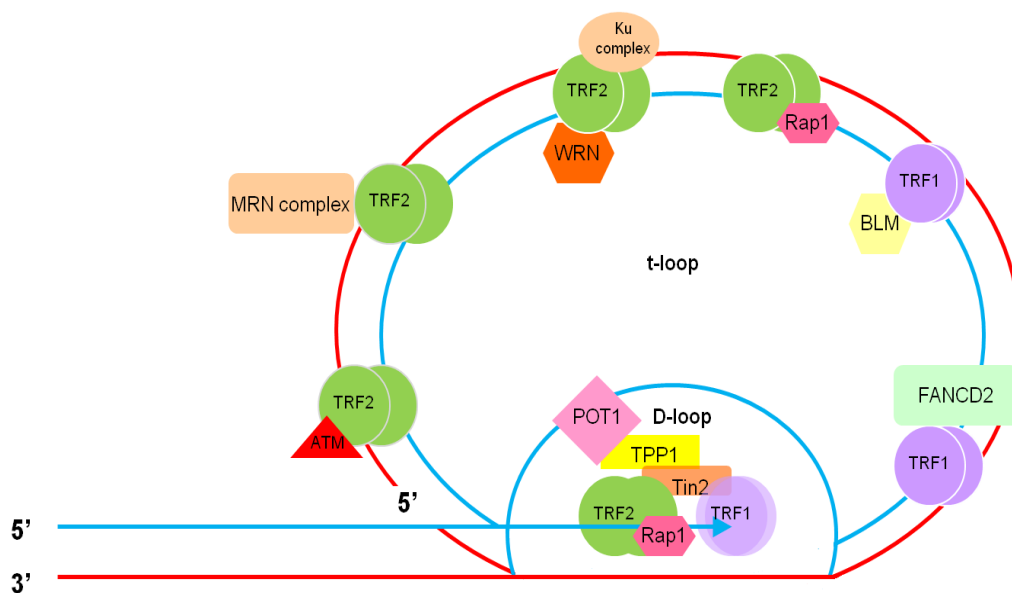
Aberrant accumulation of TERRA can affect the dynamics of telomere length and the genome stability and therefore the transcription of these telomeric RNA must be tightly

regulated. Besides the regulation by the Shelterin complex, such as the Rap1 subunit (Kabir et al., 2014; Martinez et al., 2010), the telomere length and the epigenetic state of the telomeres is also implicated in the transcription regulation of these non-coding telomere repeats (Arnoult et al., 2012). The telomeric region is governed by high levels of DNA methylation and repressive histone marks, including the trimethylation of Lysine 9 on histone H3 (H3K9me3) and Lysine 20 on histone H4 (H4K20me3). In cells from patients with Immunodeficiency, Centromere Instability and Facial Anomalies (ICF syndrome) where the methylation state at the subtelomeric region is lost, the level of TERRA RNA is substantially increased (Yehezkel et al., 2008). A similar de-regulation of these non-coding repeats was also detected following the removal of the two key histone methyltransferases (HMTase), the Suppressor of variegation homologs family (Suvar) that maintain the heterochromatic marks at telomeres (Schoeftner and Blasco, 2008). This further indicates the importance of the heterochromatic marks in the regulation of TERRA synthesis.

Page intentionally left blank

Figure 1.1 The telomere structure.

Telomere is the structure that caps the end of chromosomes. It is made up of long stretches of double-stranded (TTAGGG)_n repeats which terminate as a single stranded G-rich sequence at the 3' end. This G overhang invades into the duplex region of the telomeric tract, forming a displacement loop (D-loop) and a t-loop. The structural integrity of the telomere is maintained by a six component protein complex, the Shelterin (TRF1 and TRF2, TIN2, TPP1, Rap1 and POT1). Other molecular interacting proteins such as the MRN complex, RecQ-like family helicases Bloom and Werner's syndrome proteins, DNA damage signalling proteins ATM and ATR are involved in the regulation of t-loop structure formation during S-phase.



Page intentionally left blank

1.1.3 The epigenetic state of telomeres and its role in the maintenance of telomere length and genome stability

The telomere length usually ranges between 9-20kb. In normal somatic cells, the gradual shortening of the telomeres by 100-200bp after every cell cycle eventually leads to the onset of cellular senescence (reviewed in (Verdun and Karlseder, 2007)). For this reason, cancer cells have to maintain their length to attain unlimited proliferative capacity. The reactivation of the telomerase enzyme to facilitate the *de novo* addition of the telomere repeats is commonly used by 80% of human cancers (Shay and Bacchetti, 1997). In a subset of cancers that are mostly mesenchymal in origin, the homeostasis of the telomere length is maintained by a recombination based mechanism – the ALT pathway (Bryan et al., 1997; Dunham et al., 2000). These telomerase null cancer cells contain ALT associated PML nuclear bodies (APB) which fuel the process of T-SCE. The high frequency T-SCE contributes to the more heterogeneous and substantially longer telomere length in ALT cancer cells. Under normal physiological conditions, long telomeres are maintained by a trimming process to generate extra-chromosomal telomere repeats (ECTR) (Pickett et al., 2011). In ALT cells, these single-stranded circular telomeric by-products act as a substrate to fuel telomere extension through the rolling circling mechanism (Nabetani and Ishikawa, 2009). The detection of these single-stranded circular telomeric DNA by a PCR-based C-circle assay therefore offers another method for validating the ALT status of cancer cells (Henson et al., 2009).

In somatic cells, the telomere chromatin is enriched in heterochromatic histone modification marks, including trimethylation of Histone H3 Lysine 9 (H3K9me3) and Histone H4 Lysine 20 (H4K20me3). The presence of H3K9me3 helps to recruit repressive proteins such as the Heterochromatin protein 1 (HP1), as well as the histone

methyltransferases family. The binding of these Suppressor of variegation homologs proteins including Su(var)3-9H1 and Su(var)3-9H2, as well as the Su(var)4-20H1 and Su(var)4-20H2 to the telomere helps to promote further heterochromatinization of the telomere chromatin (Benetti et al., 2007; Garcia-Cao et al., 2004). In addition to these repressive histone marks, the adjacent subtelomeric region consists of cytosine residues that can be modified by DNA methyltransferases including Dnmt1, Dnmt3a and Dnmt3b (Gonzalo et al., 2006) (Figure 1.2). The mechanism involved in telomere heterochromatinization is conserved amongst eukaryotes, with the exception of *Saccharomyces cerevisiae*. In budding yeast, the establishment of a repressive chromatin state is maintained by transcriptional regulators at the sub-telomeric region involving the Silent Information Regulators (Sir) family protein of histone deacetylases, the Sir2-Sir3-Sir4 complex and the Shelterin subunit Rap1 and its associated factor Rif1 (reviewed in (Blasco, 2007)).

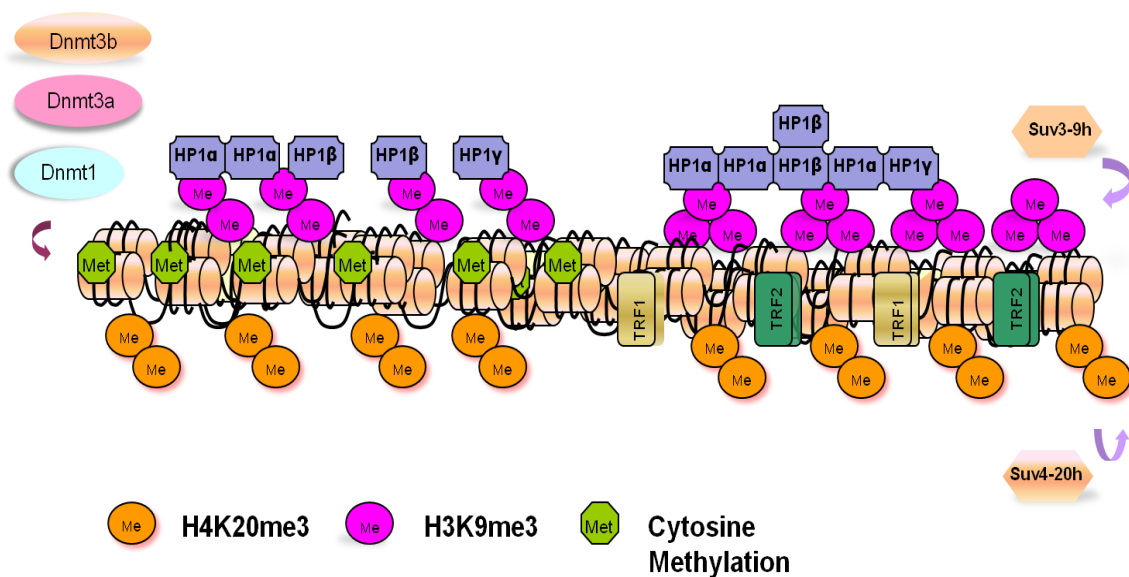
Aberrant telomere elongation due to the loss of H3K9me3 at the subtelomeric region can cause developmental defects during the early stage of embryogenesis (Dan et al., 2014). More importantly, the less repressive chromatin environment can confer cellular tumorigenic potential which predisposes cells to cancer development. For example, an increase in the level of telomere transcript and proliferative capacity was observed following the loss of Su(var)H4-20 during cellular re-programming of differentiated cells (Marion et al., 2011). Furthermore, an increase in the frequency of telomere DNA recombination or T-SCE, as well as the appearance of APB which are prominent features detected in ALT cancers are observed following the removal of the two histone HMTase for the maintenance of telomere epigenetic state, Su(var)h3-9 and Su(var)h4-20 (Benetti et al., 2007; Garcia-Cao et al., 2004). In addition, a number of studies have demonstrated the deregulation of telomere chromatin state and tumorigenic potential. It is also worth

noting that the chromatin in ALT cancers is also hypoacetylated and contains substantially less repressive histone marks such as H3K9me3 in comparison to its non-ALT counterparts (Episkopou et al., 2014). Furthermore, a higher level of TERRA is also detected in these telomerase deficient tumours (Arora et al., 2014). As the heterochromatic state directly impacts the transcription regulation of the telomeres (Arnoult et al., 2012), this emphasizes the important roles of epigenetic factors in the regulation of telomere integrity and genome stability.

Page intentionally left blank

Figure 1.2 The heterochromatic nature of telomere chromatin

The telomere chromatin is characterised by typical epigenetic repressive signature marks such as H3K9me3 and H4K20me3 (Blasco, 2007). The presence of these heterochromatic marks is essential to recruit chromatin modifiers such as the Heterochromatin protein 1 (HP1) protein family and the “suppression of variegation” methyltransferases Suv3-9H1 and Suv3-9H2 and Suv4-20H1 and Suv4-20H2 to further propagate the heterochromatic state. In addition to these histone marks, subtelomeric region contains methylable cytosine residues, which can be methylated by the DNA methyltransferases family (Dnmt1, Dnmt3a and Dnmt3b). Together, these marks promote the silent chromatin state at the subtelomeric region to ensure the telomeric position variegation effect (TPE).



Page intentionally left blank

1.1.4 The ALT pathway – a model to illustrate the association between the maintenance of telomere integrity and tumorigenesis

The prevalence of the ALT mechanism has been found in cancers that are of mesenchymal in origin. These include the pancreatic neuroendocrine tumours (PanNET), osteosarcomas and a range of paediatric brain tumours. In a subset of malignant pediatric brain tumours that harbour mutation on the checkpoint protein p53 binding protein (TP53), the activation of the ALT pathway was reported to be associated with better survival in these patients (Mangerel et al., 2014). Although somatic mutations on genes such as TP53 and the isocitrate dehydrogenase 1 enzyme (IDH1) have been identified in ALT tumors, the underlying factors that promote the induction of this recombination based mechanism remains unclear. ALT cancers have higher levels of genome instability, including high levels of DNA damage foci and an activated DNA damage response in the absence of exogenous insults (Lovejoy et al., 2012). There is growing evidence to suggest that the DNA damage arises from the replicative fragility of the telomeric region is a key factor which predisposes cells to the activation of the ALT pathway. In a recent study, the disruption to the chromatin assembly following the removal of H3 histone chaperone, Anti-Silencing Factor (ASF1) leads to ALT induction. Although ASF1 depletion leads to a global mis-regulation of histone supply, telomeres are particularly susceptible to this defect due to the inherent replicative stress that arises during the replication process. In the absence of continual histone supply to the damage sites, the activation of homologous recombination to repair the telomeric DNA can affect subsequent re-establishment of the epigenetic state at the telomeres, and therefore underlie the induction of the ALT pathway.

Several recent studies have also reported the inactivating mutation of the H3.3 histone chaperone, Alpha Thalassemia Mental Retardation X-linked protein (ATRX) in ALT tumours and >90% of immortalized cancer cell lines (Heaphy et al., 2011a; Jiao et al., 2011; Lovejoy et al., 2012; Schwartzentruber et al., 2012) (see Table 1.1). The deposition of H3.3 by ATRX and its partner, the Death domain associated protein 6 (DAXX) is important for maintaining telomere integrity (Lewis et al., 2010; Wong et al., 2010; Wong et al., 2009). Recent studies have also proposed that ATRX mediated H3.3 deposition is required to promote re-chromatinization of repaired DNA associated at stalled replication sites (Clynes and Gibbons, 2013; Clynes et al., 2013; Huh et al., 2012; Leung et al., 2013; Watson et al., 2013). In these studies, it is shown that the loss of ATRX protein correlates with a substantial increase in the frequency of damage on replicating telomeres, indicating the importance of ATRX in maintaining telomere integrity (Huh et al., 2012; Leung et al., 2013; Watson et al., 2013). However, the precise roles of ATRX and H3.3 deposition in the regulation telomere DNA replication and the mechanism underlying ALT induction in cancers cells carrying ATRX mutation remain largely unclear. Recent studies by Reddel's group have shown that ATRX deficiency in somatic cell hybrids was insufficient to activate the ALT mechanism (Bower et al., 2012). Furthermore, the restoration of ATRX expression in ALT cancer cells resulted in the reduction of ALT activity (Napier et al., 2015). Further investigations are required to elucidate how inactivation of ATRX can affect H3.3 deposition at the telomeres and compromise the downstream propagation and re-establishment of the epigenetic state on the newly synthesized DNA (Clynes and Gibbons, 2013; Sarkies et al., 2010).

Although it is unclear how ATRX mutation induces ALT activity, it is evident that ALT cells suffer a change in the epigenetic state at the telomeres and these chromatin changes could provide a favourable environment for the propagation of ALT activity. ATRX is

known to play an important role in regulating transcription at heterochromatin (Gibbons et al., 2000; Goldberg et al., 2010). In ALT cancers, loss of ATRX is implicated with the de-regulation of TERRA transcription and binding to telomeres. The aberrant binding of TERRA at the telomeres promotes the downstream recruitment of DDR proteins required for maintaining the ALT pathway (Flynn et al., 2015). It is known that telomere transcripts can form secondary structures that could impede both the replication and transcription machinery (Aguilera and Garcia-Muse, 2012); however, the physiological impact of this to the chromatin integrity remains not clear. In telomerase positive cancers, a study has revealed that the over-expression of TERRA can alter the genome-wide expression profile (Hirashima and Seimiya, 2015). Besides the maintenance of T-SCE in ALT cancers, it remains to be determined whether these TERRA transcripts are involved in altering the gene expression profile during the initiation stage of ALT pathway to allow the propagation of this mechanism.

Table 1.1 Prevalence of ALT activity and ATRX mutation in various cancer subtypes

Types	H3F3A mutation	% of H3F3A mutation	% of ALT activity	% of ATRX mutations	References
Pancreatic neuroendocrine tumours (PanNET)			61%	43%	(Jiao et al., 2011)
					(Heaphy et al., 2011a)
			11%	7.1%	(Heaphy et al., 2011a; Heaphy et al., 2011b)
Adult Glioblastoma Multiforme					(Scheel et al., 2001)
Osteosarcoma			40%	N/A	
Pediatric brain tumours					
Choroid plexus carcinoma			22.6 %	N/A	(Heaphy et al., 2011a; Heaphy et al., 2011b)
					(Schwartzentruber et al., 2012)
Neuroblastoma			9%	5/70 ¹	
Oligodendroglioma			20%	7.7	
Glioblastoma multiforme (grade IV high-grade glioma)			44%	35%	
Diffuse intrinsic pontine glioma			19-25%	14.3	(Wu et al., 2012)
	H3F3A K27M	60-71%	3/6 (50%)	30%	(Dorris et al., 2014; Khuong-Quang et al., 2012; Schwartzentruber et al., 2012; Sturm et al., 2012)
Non-brainstem High grade glioblastoma	G34R or G34V	0%	56%	100%	
	K27M	13-19%			
	G34V	9-14%	2/2 (100%)		

¹ 5 out of 70 tumour samples have targeted ATRX deletion, resulting in low ATRX mRNA levels

Recent studies have also identified inactivating mutation on histone variant H3.3 in human cancers (Khuong-Quang et al., 2012; Schwartzentruber et al., 2012; Sturm et al., 2012; Wu et al., 2012). In particular, ATRX mutation is found to be closely linked to the mutation of Glycine 34 residue on H3.3 gene in ALT cancers (Schwartzentruber et al., 2012; Sturm et al., 2012) and see section 1.4 below for further discussion). It remains unknown how H3.3 G34 mutation acts together with ATRX inactivation to promote tumourigenesis. Furthermore, how each of these mutations affects H3.3 PTM and nuclear distribution is also unclear. Considering the importance of chromatin state in maintaining telomere biology and genome stability, one of the aims of this study was to examine changes in H3.3 PTM in ALT cancers, and how these changes contribute to the maintenance of chromatin state and cell proliferation in ALT cancers.

1.2 The role of histone post-translational modifications to the maintenance of genome stability

In eukaryotes, a 146bp DNA is wrapped around histone octamers to form the basic assembly unit, the nucleosome. These nucleosomes are connected by a linker protein, Histone H1 to form a higher order chromatin structure. The canonical nucleosome is made up of one H3-H4 tetramer and two H2A-H2B dimers. The N-terminal tail of individual histones can be subjected to different types of post-translational modifications (PTM), including methylation, phosphorylation, acetylation, ubiquitination and glycosylation (Kouzarides, 2007) (Table 1.2). Some of these modifications are known to be cell-cycle regulated, such as the glycosylation on the Threonine 32 residue of histone H3 which is observed during the G2 phase (Fong et al., 2012). The impact of these modifications on different histones generally impose similar effects on chromatin regulation, for example, the acetylation on Lysine residues of histones H3 and H4

promotes chromatin relaxation that increases the accessibility by transcriptional machinery (reviewed in (Zentner and Henikoff, 2013)); however, the effect of the PTM on different residues within the same histone family can also have opposing effects. This is best illustrated by the methylation on Lysine 4 and Lysine 9 on histone H3 which marks the active and repressive gene domains, respectively. Furthermore, each modification can affect the PTM on neighbouring residues in a process known as histone cross-talk, and thereby affects the downstream recruitment of effector or 'reader' proteins to the chromatin. This suggests that histone modifications can have distinct effects depending on the context of the chromatin environment. Considering the association between an altered epigenetic environment and cancer development, this thesis will examine the function of this 'histone code' in the context of different cellular processes.

Table 1.2 Major Histone modifications on canonical histone H3

Histone residue	Post-translational Modification	Enzyme	Function
H3 Threonine 3	Phosphorylation	Haspin	Regulates centromeric organization during mitosis
H3 Lysine 4	Methylation	Histone methyltransferases (MLL)	Associated with active gene domain
H3 Lysine 9	Methylation	Suv39H1 and Suv39H2; PRDM3 and PRDM16; SetDB1	Establishment and maintenance of heterochromatin integrity; involved in DNA damage
H3 Serine 10	Phosphorylation	Aurora kinase B and MSK1 and 2 at interphase; Aurora kinase A and B at mitosis	Gene transcription; chromosome condensation
H3 Threonine 11	Phosphorylation	CHK1 at interphase; Dlk/ZIP during mitosis	Transcription regulation during DNA damage; centromeric organization at mitosis

H3 Lysine 27	Methylation	Polycomb protein	Gene regulation and maintenance of repressive chromatin state
H3 Serine 28	Phosphorylation	MSK1 and Aurora B	Gene activation at interphase; modulates the dissociation of Polycomb protein from the chromatin at mitosis during cellular reprogramming
H3 Lysine 36	Methylation	SETD2	Active chromatin mark; Transcription elongation; also implicated in DSB repair

1.2.1 The function of histone phosphorylation and methylation in the regulation of gene transcription and chromatin organization

The genome is generally distinguished into separate chromatin domains by key epigenetic signatures. At the euchromatin, the presence of histone acetylation, accompanied by the trimethylation of H3K4, H3K36 and H3K79 correlates with an active chromatin state; whereas the maintenance of the heterochromatic state is promoted by the existence of H3K9 and H3K27 trimethylation (Zentner and Henikoff, 2013). In addition to lysine methylation, phosphorylation on the serine residues of canonical histone H3 is involved in the regulation of gene transcription. Considering the proximity of both S10 and S28 residues to the repressive chromatin marks K9 and K27, modification of these serine residues can regulate the binding of other proteins to its neighbouring partners (Fischle et al., 2005; Fischle et al., 2003). This forms the basis of the methyl/phospho switch, which plays an important role in the establishment of the chromatin signature on gene loci upon cellular differentiation (Sabbattini et al., 2014). The co-existence of active/repressive histone marks on the same loci is rare; however, such a poised bivalent state is often found on the promoters of genic regions involved in cellular pluripotency and development (Bernstein et al., 2006).

The Polycomb Protein Complex (PRC2) regulates the methylation of Lysine 27 on histone H3. The modification of H3K27 is known to play a crucial role in the regulation of gene expression and the propagation of epigenetic memory in pluripotent stem cells. The formation of the di- or tri-methylation on H3K27 allows the spreading of PRC2 to ensure the proper propagation for gene silencing (Margueron and Reinberg, 2010). During cellular reprogramming, the recruitment of PRC2 to active gene loci enriched with H3K36me3 marks can lead to gene silencing (Cai et al., 2013). Furthermore, the

dynamics of PRC2 binding is influenced by the modification of neighbouring histone marks on the nucleosomes. This includes the symmetric localisation of two active histone marks, such as H3K4me3 and H3K36me3 (Voigt et al., 2012), as well as the phosphorylation of the serine residues including S10 and S28. At interphase, phosphorylation on the S28 residue by mitogen and stress activated kinase (MSK1) can inhibit the binding of PRC2 to the repressive H3K27me3 mark, which results in gene activation (Gehani et al., 2010). Similarly, phosphorylation of Serine 28 also impacts the binding dynamics of the Polycomb complex to the neighbouring K27me3 mark during mitosis. The extent of Polycomb localisation on mitotic chromatin is reported to play a key role in the establishment of epigenetic memory during cellular reprogramming (Fonseca et al., 2012).

Besides the H3K27me3/S28ph mark, the double modifications on H3K9/S10 also play a key role in the regulation and maintenance of gene transcription (Sawicka and Seiser, 2012). The H3K9me3 is a histone mark that recruits the binding of Heterochromatin Protein 1 family (HP1) and histone methyltransferases to the heterochromatin. In *Drosophila*, phosphorylation of the Serine 10 residue by JIL-1 kinase prevents the spreading of the heterochromatic mark such as H3K9me3 into active genic region (Wang et al., 2011). In mammals, Aurora B kinase mediated H3S10 phosphorylation during mitosis is known to prevent the binding the HP1 proteins to its neighbouring Lysine 9 residue. In addition, H3K9me3/S10ph is also present on gene loci regulated by the Polycomb complex in differentiated cells. The existence of this double modification mark prevents the association of PolIII enzyme to ensure the establishment of the repressed state following differentiation (Sabbattini et al., 2007; Sabbattini et al., 2014). These examples demonstrate that the importance of the serine phosphorylation in

controlling gene expression, through the cellular interpretation of the histone modifications on H3K9 and H3K27.

Besides the regulation of gene transcription, histone modifications are associated with chromatin organization during mitosis. These include modifications on Threonine 3 and Threonine 11 by Haspin and Dlk/ZIP kinases that facilitate the organization of the centromeric chromatin, as well as the global increase in Serine 10 and Serine 28 phosphorylation on the chromosome arms by Aurora B kinase (Dai et al., 2005; Goto et al., 2002; Hendzel et al., 1997; Preuss et al., 2003; Wei et al., 1999). The increase in the level of the H3S10ph mark facilitates a cascade of protein exchange such as the recruitment of histone deacetylase for H4K16 and the transient displacement of HP1 from its binding to the neighbouring H3K9me3 mark (Fischle et al., 2005; Hirota et al., 2005). This ensures the chromosome is properly condensed before the segregation into daughter cells.

1.2.2 The role of histone modifications in DNA damage signalling and repair

Genome stability is constantly challenged by a combination of external (e.g. UV and drug induced DNA damage) and internal insults (stalling of DNA replication fork). Loss of genomic integrity can lead to chromosome rearrangements and predisposition to cancer development. The continual surveillance by a network of DNA damage signalling proteins ensures these damage sites are repaired before further cell-cycle progression. The presence of double-stranded breaks (DSB) is detected by sensory proteins including the Mre11-Rad50-Nbs1 (MRN complex) and the DNA-PK components, Ku 70/80 complex. This leads to the downstream activation of the PI3-kinase like kinases family such as ATM and DNA dependent protein kinase (DNA-PK), which phosphorylates histone H2AX at the Serine 139 residue (γ H2AX). The localisation and spreading of this

prominent DNA damage mark can facilitate the downstream recruitment of effector proteins, such as the Checkpoint kinases family (CHK1 and CHK2) to the DNA damage foci (Shiloh, 2003). In addition to remodelling the damaged DNA template for more efficient binding of the DDR proteins, the activation of these DNA repair factors is involved in the transcription regulation of cell-cycle associated genes. It is known that the methyl/phospho switch is important in the regulation of gene expression under normal cellular condition, as discussed in section 1.2.1. In the presence of DNA damage, the phosphorylation on histone H3 can also affect the acetylation state of neighbouring residues. For example, activation of CHK1 during DNA damage leads to decreased H3 Threonine 11 phosphorylation, resulting in reduced recruitment of GCN5, a histone acetyltransferase which promotes acetylation of H3K9 (Shimada et al., 2008). As histone acetylation is directly linked to transcription activation, a reduction in the distribution of these histone marks on the promoter therefore promotes repression of genes associated with cell-cycle progression. Recently, the presence of repressive histone marks has been reported to play an important role in DDR signalling. As chromatin compaction can hamper the accessibility of the chromatin to DNA repair proteins (Cann and Delleire, 2011), it seems counterintuitive that repressive histone marks is pivotal for the proper activation of the DDR signalling pathway. Indeed, the transient formation of H3K9me3 by the KAP-1/Suv39H1/HP1 complex at sites of DNA damage, even at euchromatic genomic regions is necessary for stabilising DSB (Ayrapetov et al., 2014). This histone mark recruits another histone acetyltransferase TIP60 which promotes the relaxation of the chromatin. The concurrent activation of the ATM kinase subsequently helps to remove the H3K9me3 mark to allow the binding of the DNA repair factors.

The choice of DNA damage repair mechanism is crucial in the re-establishment of the epigenetic state. Although the activation of the DNA repair mechanism is cell-cycle

dependent, the presence of several histone marks surrounding the damaged chromatin can indirectly determine the pathway to be activated. In euchromatic regions, the trimethylation of the H3K36 active histone mark by its methyltransferase SETD2 promotes the activation of homologous recombination pathway (Pfister et al., 2014). It is known that any perturbations to the coding sequence can alter gene regulation, such as the induction of oncogenes. This template dependent mechanism therefore ensures that no errors can be introduced during the course of the repair. The accumulation of other histone marks such as the H3K79me2 and H4K20me2, as well as the ubiquitination of H2A Lysine 15 (Fradet-Turcotte et al., 2013) are known to promote the recruitment of an important DDR effector, p53-binding protein (53BP1). The 53BP1 protein is a key determinant of DNA repair kinetics. Although the presence of 53BP1 has been shown to be a repressor of the HDR pathway, its association can alter the chromatin dynamics and mobility surrounding the DSB foci (Dimitrova et al., 2008). This enhances the closer proximity of the neighbouring DNA at the DSB foci to promote the repair by the error-prone end-joining mechanism.

During interphase, the activation of the various different cell-cycle checkpoints in response to DNA lesions from interphase ensures these damaged sites are repaired before further propagation. In most cancer cells, the loss of cell-cycle checkpoint function allows these unrepaired lesions to be transmitted into the following cell cycle. Nevertheless, mitotic cells are equipped with the spindle assembly checkpoint (SAC), which functions to delay mitotic progression until accurate chromosome segregation can be guaranteed. Another checkpoint, the mitotic exit DNA damage checkpoint, ensures the damaged cells can be eliminated through the process of mitotic catastrophe (Huang et al., 2005). It is known that the mitotic phase is considerably short in comparison to other stages of the cell cycle. Furthermore, the activation of the DDR signalling at mitosis

results in an increase in chromosome mis-segregation and telomere fusion (Bakhoun et al., 2014; Orthwein et al., 2014). Nevertheless, the presence of DNA damage can slightly delay the mitotic progression (Mikhailov et al., 2002). This helps to promote the phosphorylation of Serine 139 on H2AX, as well as the activation of both CHK2 and ATM, all of which are activators of the DDR signalling pathway (Giunta et al., 2010; Stephan et al., 2009). As binding of 53BP1 can lead to DDR induction which can compromise genome stability (Giunta et al., 2010; Lukas et al., 2011), 53BP1 is phosphorylated to limit its binding onto the mitotic chromatin until the subsequent G1 phase (Lee et al., 2014). In this case, any DNA lesions acquired during mitosis can only be marked for subsequent repair upon cell-cycle exit. In conclusion, the histone code plays a key role in regulating the integrity of chromatin functions. More importantly, epigenetic modification by histone variants is also implicated in the maintenance of chromatin structure and dynamics. The following session will emphasize on the role of histone variant H3.3, which has been identified to be altered in cancers that utilize the ALT pathway.

1.3 The role of histone variants in the maintenance of chromatin integrity

The epigenetic modifications on canonical histones play an important role in the regulation of genome stability. In addition, eukaryotic chromatin contains highly conserved histone variants which further contribute to the complexity of the histone code (see Table 1.3). These histone variants are mostly found in the H2A and H3 histone family, with very few isoforms currently identified for histones H2B and H4. The dynamic deposition and the cell-cycle independent expression of these histone variants indicate their distinct chromatin regulatory function at gene domains. Histone variants are known to play an important role in the regulation of gene transcription. For example, incorporation of H2A.Z can alter chromatin organization to facilitate the accessibility of the transcription machinery at the promoter of an active gene region (Jin and Felsenfeld, 2007). Conversely, deposition of macroH2A at heterochromatic regions and alpha-globin genes is associated with transcription repression (Ratnakumar et al., 2012). During DNA synthesis, the active H2A.Bbd variant is also transiently recruited to the newly synthesised chromatin (Sansoni et al., 2014). During embryonic development, some of these histone variants play a specific role in the re-establishment of the chromatin environment. The testis specific H2A.Lap1 histone variant, a homologue of H2A.Bbd, is involved in transcriptional regulation and the re-establishment of the epigenetic environment during spermatogenesis (Soboleva et al., 2012).

The histone H3 family consists of six variant members: the replication dependent H3.1 and H3.2, the replication-independent H3.3, centromere specific Cen-H3/ CENP-A, as well as the testis specific H3.3C and H3.3t (Loyola and Almouzni, 2007). The dynamic incorporation of these histone variants to specific chromatin regions is determined by their histone chaperone (reviewed in (Szenker et al., 2011)). For example, the cell-cycle dependent deposition of the CENP-A protein at the centromere during late

telophase/early G1 phase is driven by the HJURP protein (Dunleavy et al., 2009; Foltz et al., 2009); whereas the loading of H3.3 histone variant at active gene loci is mediated by the HIRA or the ATRX/DAXX complex at telomeres and pericentric heterochromatin (Drane et al., 2010; Elsaesser and Allis, 2010; Goldberg et al., 2010; Lewis et al., 2010; Wong et al., 2010). The aberrant expression or localisation of these histone variants have been shown to promote tumourigenesis and genome instability, such as the mitotic defects associated with the over-expression of the CENP-A protein in colorectal cancers (Tomonaga et al., 2003). Furthermore, DAXX mediated ectopic CENP-A localisation to the chromosome arms provides protection to the chromatin from DNA damage (Lacoste et al., 2014). More recently, the deregulation of histone variant H3.3 and its chaperone ATRX has also been identified in a range of ALT positive cancers (Heaphy et al., 2011a; Jiao et al., 2011; Schwartzenruber et al., 2012) Together, these findings provide the first evidence to support the role of aberrant chromatin integrity and cancer tumorigenesis. Considering the importance of H3.3 in the maintenance of chromatin integrity, the following section will discuss the function of histone H3.3 in the context of its role in various cellular processes.

Table 1.3 Histone variants and their cellular function

Histone family	Histone variant	Localisation	Function
Histone H2A	H2A.Z	Promoter region of active genes	Transcription
	H2A.Bbd	Active genic region	Transcription regulation;
		Newly synthesized DNA Sites of DNA damage foci	DNA replication and DNA damage repair
	H2A.Lap1	Testis-specific Transcription start sites	Transcription regulation
	γ H2AX	A DNA damage mark	DNA damage signalling
Histone H3			
	H3.1 and H3.2	Replicating DNA	Assembly of nucleosomes on newly synthesised DNA
	H3.3	Transcription start sites Heterochromatic regions such as telomeres	Transcription regulation; Epigenetic bookmarking maintenance of chromatin integrity
	H3.3C and H3.3Y	Testis specific	Unknown
	Cen-H3/ CENP-A	Centromere	Organization of Centromeric chromatin;

required for normal
mitotic progression

1.3.1 Replication independent role of H3.3

During DNA synthesis, the presence of the replication fork causes DNA unwinding and the transient displacement of the nucleosomes. As (H3-H4) tetramers play a key role in the re-establishment of the epigenetic landscape, it is important that these parental histones are accurately transferred. The splitting of the H3/H4 tetramers into dimers has been suggested to promote the even distribution of parental histones into the daughter DNA. The hybrid intermediates assembled on the post-replicative DNA will therefore comprise the 'old' and the newly synthesized dimers. The semi-conservative propagation of the nucleosomes therefore allows the epigenetic chromatin signature to be re-established post DNA replication; however, this has been challenged by a study that utilized the SILAC approach to examine the propagation of nucleosomes during DNA replication (Xu et al., 2010). In particular, the bulk of the (H3.1-H4) enriched fraction was deposited as an intact tetramer onto the post-replicative DNA. This conservative propagation of (H3.1-H4) during replication was further substantiated in *S. cerevisiae*, where the displaced tetramers are transferred to the nascent DNA by the replisome and the H2A-H2B histone chaperone Facilitates Chromatin Transcription complex (FACT) (Foltman et al., 2013). Although the bulk of histones are distributed asymmetrically onto the daughter DNA, the presence of the existing tetramers can act as a docking site to recruit histone binding proteins or modifiers such as the HP1 protein family. This allows the post-translational modifications to be copied onto the newly incorporated nucleosomes.

Although histone variants H3.3 and H3.1 differ only by only five amino acids, the distinct assembly pathway indicates these two histones have distinct cellular functions. Immunoprecipitation combined with mass spectrometry analysis indicated these pre-deposited H3.1 and H3.3 form two distinct cellular complexes. The histone chaperone

Chromatin Assembly Factor 1 (CAF-1) was found exclusively in the H3.1 complex, whereas the Histone Chaperone Regulator A (the HIRA complex) was identified in the H3.3 fraction (Tagami et al., 2004). As discussed earlier, newly synthesized H3.1 are deposited on the nascent DNA during replication. In contrast, H3.3 is deposited on active gene loci in a replication independent manner (Ahmad and Henikoff, 2002). The transcription activating function of H3.3 is associated with its dynamic turnover gene regulatory elements such as the promoter and enhancers, which are enriched with active chromatin modification marks (Kraushaar et al., 2013; Schwartz and Ahmad, 2005). Furthermore, recent studies have also suggested an important function of H3.3 in response to DNA damage. This includes the reassembly of repaired DNA chromatin at replicative stalled sites (Clynes and Gibbons, 2013), as well as the transcriptional restart following DNA damage (Adam et al., 2013). Together, these studies have shown a more diverse function of H3.3 in the regulation of chromatin integrity.

1.3.2 The role of H3.3 in the establishment of epigenetic reprogramming during embryonic development

During embryogenesis, the H3.3 variant plays an important role in global chromatin reorganization and epigenetic reformatting of the parental genomes. In mammals, H3.3 is encoded by both the *H3F3A* and *H3F3B* genes; however, the bulk of H3.3 is derived from the *H3F3B* allele. It is known that H3.3 plays a crucial role throughout the process of spermatogenesis. For example, the dynamic replacement of histones on the chromatin with protamines requires the presence of H3.3 during the maturation of spermatids. In the *H3f3B* knock-out mouse model, the absence of H3.3 expression affects the maintenance of the epigenetic landscape and disrupted the regulation of gene transcription associated with spermatogenesis. As a result, the males are infertile due to the abnormal development of the testis (Yuen et al., 2014). In comparison to the oocytes, the level of

H3.3 is found to be significantly higher in the male derivatives of the primordial germ cells, the pro-spermatogonia (Tang et al., 2014). As this enrichment of H3.3 coincides with the global re-establishment of the DNA methylation, this suggests H3.3 is likely to be associated with the reorganization of the chromatin states during epigenetic reprogramming in these cells.

In addition to the development of the gametes, H3.3 is required to facilitate the different cellular processes that occur upon the fertilisation process. The distribution of histone PTM signatures and the level of H3.3 are found to be asymmetric between the parental genomes at the early stage of the zygote formation in mammals (van der Heijden et al., 2005). In the male pronucleus, the nucleosome assembly on the paternal chromatin upon the replacement of the protamines is dependent on the maternal derived H3.3 that is deposited by the Hira complex (Lin et al., 2014). In *Drosophila*, this process is also co-regulated by a chromatin remodeller Chd1 (Konev et al., 2007). The incorporation of histone H3.3 facilitates the decondensation of the paternal chromatin, which precedes the first DNA synthesis (Lin et al., 2013). The loading of H3.3 is also essential to facilitate DNA replication, as well as ribosomal and pericentromeric satellite repeats transcription for embryogenesis (Lin et al., 2014; Santenard et al., 2010). In mammals, the removal of HIRA affects the deposition of H3.3 on the embryonic regulated genes in the oocyte, which can compromise the subsequent cell-cleavage process to the two-cell stage (Lin et al., 2014). However, the loss of Hira does not appear to affect the zygote development in *Drosophila*, although the subsequent epigenetic reprogramming in the differentiation process of *Arabidopsis* is shown to be impaired (Nie et al., 2014). Nevertheless, the importance of H3.3 in the establishment of the epigenetic state during embryonic development is conserved across different species.

1.3.3 The function of H3.3 in the dynamics of chromatin organization and the maintenance of chromatin integrity

In addition to the histone PTM signatures, the binding of an insulator element such as CCCTC-binding factor (CTCF) creates a boundary that separates the active and repressive chromatin domains. The co-localisation of H3.3 at the CTCF enriched sites suggests the dynamic incorporation of this histone variant underlies the formation of the boundary to prevent the spreading of the repressive marks, such as the trimethylation of H3K27 into neighbouring active domains (Weth et al., 2014). It is known that incorporation of H3.3 at different genomic regions is specified by the deposition pathways. In active gene domains, the targeting of H3.3 by the HIRA complex to regulate transcription activity is dependent on the enrichment of the Polymerase II enzyme. During the repair of DNA damage, this specific interaction is involved in facilitating the dynamics of chromatin assembly by the histone acetyltransferase (HAT1). The acetylation of H4 residues, coupled with the incorporation of H3.3 enhances chromatin remodelling and promotes subsequent recruitment of DNA damage proteins which favours the repair by homologous recombination (Yang et al., 2013). Furthermore, the HIRA mediated H3.3 deposition has also been shown to facilitate the restart of the transcription machinery after DNA damage repair (Adam et al., 2013). Besides the known replication independent role of H3.3 deposition, the transient disruption of nucleosome assembly at DNA replicative sites requires the loading of H3.3 by HIRA to protect the chromatin. In this case, this interaction helps to limit the occurrence of nucleosomal free DNA that can lead to the activation of DDR (Ray-Gallet et al., 2011; Schneiderman et al., 2012). In addition to the chromatin re-organization in proliferative cells, the accumulation of H3.3 histones is involved in the maintenance of chromatin dynamics in cells undergoing senescence. In non-replicating cells, the HIRA complex is

a major component involved in the formation of senescence associated heterochromatic foci (SAHF), which are enriched with repressive histone marks (Jiang et al., 2011). The precursors to these foci are small nuclear bodies known as the PML-NB. These domains can vary in the number, size and even in shape depending on the cell type and the stages of the cell cycle. In senescent cells, newly synthesized H3.3 histones are deposited at the active gene loci to maintain the extensive chromatin remodelling event (Corpet et al., 2014).

Through the action of HIRA, H3.3 is enriched in active gene loci or transcribed regions and at these sites, H3.3 is often associated with active chromatin marks including H3K4 methylation. However, H3.3 is also found at heterochromatic regions such as telomere and pericentric heterochromatin, where ATRX partners with DAXX to promote H3.3 deposition. At these heterochromatic regions, the loading of H3.3 is reported to contribute to chromatin integrity by ensuring the faithful propagation and re-establishment of epigenetic profile. This is best exemplified the importance of H3.3 deposition by ATRX and DAXX to maintain the telomere epigenetic state unique to the pluripotent mouse embryonic stem cells (mESC) (Wong et al., 2010; Wong et al., 2009). Besides the telomeres, H3.3 also contributes to the maintenance of the chromatin assembly at other repetitive loci. In both mouse and human cells, the recruitment of H3.3 by DAXX into PML-NB is essential to the organization and transcriptional regulation of the pericentromeric satellite repeats (Morozov et al., 2012).

Furthermore, H3.3 can also be deposited by the oncogenic protein Dek (Sawatsubashi et al., 2012). Although Dek is a non-histone chromosome associated protein, it plays an essential role in the maintenance of heterochromatin integrity. In *Drosophila*, the binding of Dek can enhance the recruitment of CBX3 (the homologue of human HP1 protein) to the H3K9me3 mark to facilitate the establishment of the repressive state (Kappes et al.,

2011). Furthermore, the association of DAXX and the histone deacetylase II complex with the chromatin is modulated by their interaction with Dek, which is known to possess a DNA binding capability (Hollenbach et al., 2002). In mESC, Dek acts as a gatekeeper to regulate the dynamics and distribution of H3.3 deposition to the chromatin by other histone chaperones. Loss of this protein affects the loading of H3.3 to the telomeres by ATRX/DAXX complex and led to the re-localisation of this histone variant to other genomic regions such as the chromosome arms. As a result, this leads to a telomere damage phenotype reminiscent to the removal of ATRX protein (Ivanauskiene et al., 2014). Together, these studies reveal an important function of H3.3 in the maintenance of heterochromatin stability and integrity.

The important role of ATRX in the transcription regulation of repetitive regions was first uncovered in patients with the Alpha Thalassemia Mental Retardation X-linked (ATR-X syndrome) (Gibbons et al., 2000). The ATRX protein belongs to the SWI/SNF protein family involved in chromatin remodelling. Its association with the heterochromatin is dependent on the ATRX-DNMT3-DNMT3L (ADD) domain at the N-terminal which recognizes the trimethylation on Lysine 9 and the unmethylated Lysine 4 on histone H3 (Dhayalan et al., 2011; Eustermann et al., 2011). ATRX has been reported to be involved in gene regulation at specific loci, such as the promoter region of alpha globin gene and more recently, the intergenic region of neurodevelopmental genes (Law et al., 2010; Levy et al., 2014).

ATRX is also vital to the repetitive chromatin region. For example, inactivation of ATRX affects the methylation state on both the ribosomal repeats and the sub-telomeric repetitive elements, which promotes an aberrant transcriptional regulation of these heterochromatic repeats in ATR-X patients (Gibbons et al., 2000). Similarly, the increase in the level of telomeric RNA (TERRA) was also reported in ATRX null mESC which

showed loss of H3.3 deposition at the telomeric region (Goldberg et al., 2010). Recently, ATRX is also shown to be recruited by the presence of H3K9me3/S10ph to regulate centromere transcription in stimulated neuronal cells (Noh et al., 2014). Collectively, this indicates a general transcription deregulation of the repetitive regions in the absence of ATRX protein.

The binding of ATRX to G-rich tandem repeats has previously been reported to regulate gene transcription (Law et al., 2010). Recent study has also indicated the association of ATRX with RNA during the establishment of X-chromosome inactivation. In this study, the interaction between the chromatin remodeller and the X-inactivating specific transcript RNA (Xist) helps to facilitate the binding of the Polycomb complex to promote the establishment and propagation of H3K27me3 for gene silencing (Sarma et al., 2014). Besides the maintenance of the X-chromosome inactivation, the regulation of H3K27me3 by PRC2 at the genome-wide level is also affected in the absence of ATRX. It remains unclear whether the reduction of H3K27me3 at the heterochromatin region is directly linked to the inactivation of ATRX considering its role in the propagation of H3K9me3. In a recent report, an increase in the level of H3K27me3 at the pericentric satellite repeats was detected following the loss of the repressive chromatin state in the Suv39 deficient mouse ES cells. It remains to be determined whether such redundant mechanisms exist in the maintenance of telomere heterochromatin.

Recent studies have also suggested that ATRX has an important role at these G4-rich loci during DNA synthesis. Following the removal of ATRX, a substantial increase in replication stress and telomere dysfunction was reported to be further exacerbated in the presence of G4-stabilizing drugs (Clynes and Gibbons, 2013; Huh et al., 2012; Leung et al., 2013; Watson et al., 2013). Although ATRX binding targets are shown to have a higher tendency to form G4 structures (Law et al., 2010), no direct evidence has been

shown to confirm such an interaction exists between ATRX and these secondary structures *in vivo*. Furthermore, the precise role of ATRX in ensuring chromatin integrity at G4 enriched repetitive loci remains unknown. It is possible that the incorporation of H3.3 by ATRX could promote dynamic nucleosome remodelling that facilitates the restoration of the chromatin integrity.

1.4 The role of histone modifications on H3.3 in the regulation of genome stability and cancer development

In recent studies, several groups have reported the recurrent mutations on specific residues on *H3F3A* gene in pediatric brain tumours. These studies have not only highlighted the importance of histone variants in controlling chromatin function, but also demonstrated how the de-regulation of their post-translational modifications can result in cancer development (Khuong-Quang et al., 2012; Schwartzenuber et al., 2012; Sturm et al., 2012; Wu et al., 2012). The two specific mutations on Lysine 27 and Glycine 34 define subgroups of brain malignancies that arise from different anatomical location. For example, the mutation of H3.3 Lysine 27 to Methionine is found in diffuse intrinsic pontine gliomas (DIPG) that arises from the brainstem, whereas the substitution of Glycine 34 is only detected in high-grade gliomas (HGG) (Khuong-Quang et al., 2012; Schwartzenuber et al., 2012; Sturm et al., 2012; Wu et al., 2012). Interestingly, the frequency of ATRX inactivation is also different between these cancers that harbour these two recurrent mutations on the H3.3 (Khuong-Quang et al., 2012; Mangerel et al., 2014; Schwartzenuber et al., 2012; Wu et al., 2012). Although ATRX inactivation found in gliomas is usually associated with poor prognosis, in other brain tumours subtypes such as the astrocytomas, a better outcome is observed in the absence of the ATRX (Wiestler et al., 2013). Furthermore, loss of ATRX confers a better prognosis in patients with tumours harbouring the Glycine 34 substitution compared to the Lysine 27

counterparts. Therefore, it remains to be determined whether the frequency of ATRX inactivation directly contributes to the altered methylation and gene expression profile between the K27 and G34-mutants (Sturm et al., 2012).

As discussed earlier, histone cross-talk plays a key role in the regulation of the chromatin epigenetic profile. The recent identification of recurrent mutations on critical residues of *H3F3A* allele in paediatric brain tumours has illustrated this effect. For example, the substitution of Glycine 34 to Valine or Arginine has been reported to alter the genome-wide distribution of the H3 Lysine 36 trimethylation mark (Bjerke et al., 2013). In DIPG, the substitution of the Lysine to Methionine on residue 27 which is frequently observed on the *H3F3A* or *HIST1B* (encoding H3.1) genes was reported to disrupt the binding dynamics and the methyltransferase activity of the Polycomb complex. Importantly, this has led to the global reduction in the level of H3K27me3 in this type of brain cancer cells (Lewis et al., 2013). Considering the transcription repressive role of H3K27me3, the dominant effect of H3.3K27 substitution has led to the global reduction and redistribution of this histone mark, which drives the aberrant gene expression profile in these brain tumour cells (Bender et al., 2013). Nevertheless, the mechanism that promotes tumorigenesis in H3.3K27 mutant tumours remains unclear.

H3.3 differs from canonical replication dependent H3.1 by five residues, including the Serine 31 at the N-terminal and the cluster of four amino acids at the C-terminal globular region. In plants, the C-terminal tail of H3.3 is involved in the transcription of ribosomal DNA by regulating the dynamics of nucleosome assembly (Shi et al., 2011). In eukaryotes, the Serine 31 is a highly conserved residue as the corresponding position in H3.1/2 is an alanine. During mitosis, the phosphorylation of the Serine 31 residue (H3.3S31ph) is found enriched at the pericentric heterochromatic region in somatic cells and at the telomeres of pluripotent mouse ES cells (Hake et al., 2005; Wong et al., 2009).

This association indicates an important regulatory role of H3.3S31ph at heterochromatic region. Unlike the Serine 10 and Serine 28 residues on canonical histone H3, the function and the kinase responsible for the phosphorylation of H3.3 Serine 31 remains unknown. In a recent report, the binding of a H3.3 K36me3 reader protein, ZMYND11 has been shown to require the Serine 31 residue (Wen et al., 2014). Considering the transcription regulation of ZMYND11 in the expression of oncogenes, this suggests that any perturbation to the phosphorylation state of Serine 31 can potentially affect the PTM state on other residues and binding of ZMYND11, thus, affecting the transcription regulation of genes including those associated with tumorigenesis. As the ATRX-H3.3 axis is found to be highly mutated in ALT cancers, this thesis will examine the distribution of H3.3S31ph and the impact of ATRX deficiency to distribution of H3.3S31ph in ALT cancers.

Chapter 2

PML-NBs provide a platform for the assembly of H3.3 and ATRX to maintain telomere chromatin in pluripotent mouse Embryonic Stem cells

2.1 Overview

The telomere structure is essential to protect the chromosome end from damage and aberrant DNA recombination. In normal cells, the shortening of the telomere length limits their proliferative capacity. To overcome this, most cancer cells maintain the telomere length by re-expressing the telomerase enzyme. In a subset of tumours, a recombination based mechanism known as the ALT pathway is being used for telomere elongation. These telomerase null cancer cells have a heterogeneous range of telomere length attributed to extensive T-SCE. Besides this, these cells are characterized by the presence of a distinct type of ALT-associated PML-NB (APB) (Yeager et al., 1999). In addition to the presence of Promyelocytic leukemia protein (PML) scaffold, these structures also contain telomere associated proteins (e.g. TERF1 and TERF2) (Yu et al., 2010), telomeric DNA as well as DNA repair and homologous recombination proteins such as the Mre11-Rad50-Nbs1 (MRN complex). As the removal of PML protein and one of these components within the APBs including the MRE11 and NBS1 inhibits the assembly of the APB and suppresses the occurrences of telomere sister chromatid exchange (T-SCE) (Jiang et al., 2005), the presence or assembly of these APBs have been proposed to be essential for continual telomere elongation and cell survival of ALT cancer cells.

The PML-associated nuclear bodies (PML-NB) are specialized nuclear domain structures involved in the regulation of various cellular processes (reviewed in (Bernardi and Pandolfi, 2007)). These include the epigenetic regulation of heterochromatin, activation of apoptosis, DNA damage signaling (Yeung et al., 2012), tumour suppression, as well as the activation of anti-viral defense mechanism. The PML protein family consists of seven isoforms; each of these proteins has a conserved N-terminal TRIM or a Ring

domain, B domain and a Coil-Coiled domain (RBCC) motif, which allows the oligomerization of PML to form the PML-NB structure. The differential splicing of the exons at the C-terminal region contributes to the diverse function of individual isoform (Bernardi and Pandolfi, 2007) . In addition, the presence of the Sumoylation Interacting Motif (SIM) is essential for the recruitment of interacting partners, such as Sp100, Death domain associated protein 6 (DAXX), Alpha Thalassemia Mental Retardation X-linked (ATRX), Heterochromatin Protein 1 (HP1) and the Bloom helicase to these domain bodies (Bischof et al., 2001; Chang et al., 2011; Dellaire et al., 2006a; Ishov et al., 1999). During S-phase, the number of PML-NBs increases significantly by a fission mechanism and disassembles at mitosis. The PML proteins attach onto the nuclear matrix throughout the mitotic stage where they re-aggregate to reform the bodies as cells enter G1 phase (Dellaire et al., 2006b).

In somatic cells, the telomere chromatin is characterized by repressive histone marks including high levels of the trimethylation on H3K9 and H4K20 (Blasco, 2007; Garcia-Cao et al., 2004). The maintenance of these heterochromatic marks is an important regulator of the telomere length by suppressing telomere exchange (Benetti et al., 2007). Interestingly, the level of these repressive histone marks at telomeres is remarkable lower than those in the pluripotent mouse embryonic stem cells (mESC). Besides this, the histone variant H3.3 which is mostly found in active gene loci, is also enriched at the telomeric region of mESC (Wong et al., 2009). The deposition of H3.3 is facilitated by ATRX and its interacting partner, DAXX (Drane et al., 2010; Lewis et al., 2010). The association of H3.3 and DAXX/ATRX with the telomere is significantly reduced following the induction of cellular differentiation in mESCs. Furthermore, the removal of either H3.3 or ATRX by RNAi depletion induces a telomere dysfunction indicating their

presence at telomeres is required to maintain the unique telomeric chromatin integrity specifically at the pluripotent state (Wong et al., 2010; Wong et al., 2009).

In this study, we have identified similar PML nuclear bodies that associate with the telomeres in a cell-cycle dependent manner in pluripotent mESC. The assembly of these PML-NBs is impaired in the absence of the PML protein. Importantly, loss of these PML-NBs affects the binding of H3.3 and ATRX to this heterochromatic region and results in an increase in the DNA damage marker, the 53BP1 at the telomeric foci (TIF). The increase in the frequency of TIF indicates dysfunctional telomeres upon the disassembly of the PML-NB. We have also examined the level of telomere exchange in mESC and found no significant difference in the absence of PML-NBs. Furthermore, the depletion of the DNA damage signalling proteins that are critical to the assembly of APB does not affect the formation of telomere associated PML-NBs in these pluripotent ES cells. Together, these data suggests that the PML-NB found in mESC is functionally distinct from the APB found in telomerase null ALT cancer cells. These telomere associated PML-NBs serve to provide a platform to facilitate the loading of H3.3 by ATRX and DAXX, which is important to maintain the unique telomere chromatin in the undifferentiated cellular state.

2.2 Materials and method

2.2.1 Cell lines

ES129.1 mESCs were cultured in Dulbecco's Modified Eagle Medium (DMEM) supplemented with 12% heat-inactivated FCS (v/v), 1000 units/ml leukemic inhibitory factor, 0.1 mM β -mercaptoethanol and non-essential amino acids. Mouse embryonic fibroblasts NIH3T3 cells and human fibrosarcoma cell line HT1080 were grown in

Dulbecco's Modified Eagle Medium (DMEM) with 10% heat-inactivated FCS (v/v) and 1% Penicillin/Streptomycin (v/v).

2.2.2 Antibodies

Primary antibodies used were mouse monoclonal antibodies against Pml (Millipore), Nbs1, 53BP1; rabbit polyclonal antibodies against Mre11a, DAXX, ATRX (H-300, Santa Cruz) and phosphorylated H3.3 Serine 31 (Abcam). For secondary antibodies used in immunofluorescence analysis, Alexa Fluor 488 donkey anti-rabbit IgG, Alexa Fluor 488 donkey anti-mouse IgG, Alexa Fluor 594 donkey anti-rabbit IgG, Alexa Fluor 594 donkey anti-mouse IgG (Molecular Probes, Life Technologies) were used at a final concentration of 2 μ g/mL. For immunoblotting, goat anti-mouse IgG (H+L) HRP was used at a dilution of 1:5000; goat anti-rabbit IgG (H+L) (Life Technologies) was used at a dilution of 1:20,000.

2.2.3 Cell-cycle analysis

Cells were arrested with 2.5 mM thymidine (Sigma-Aldrich) for 16 h prior to release from the G1 block by washing 3 times in PBS and released in the presence of 2.5 μ M of deoxyctidine. For FACS analysis, cells were harvested, washed in ice-cold PBS and blocked in 1% BSA (w/v) before fixing in absolute ethanol overnight. Cells were spun and resuspended in 1% BSA (w/v) in PBS. The cell pellet was collected by centrifugation before washing with ice-cold PBS. Cell population was stained with Propidium iodide (50 μ g/mL) and RNase (10 μ g/mL) in PBS and analyzed on a FACS LSR II Analyzer (BD Biosciences) with ModFit software (Verity).

2.2.4 Immunofluorescence analysis and Telomere-FISH analysis

Cells were treated with microtubule disrupting agent, Colcemid (Life Technologies) at a final concentration of 0.1 $\mu\text{g/ml}$ and 40 ng/ml , respectively, for 1 h before being harvested for immunofluorescence analysis. Cells were subjected to hypotonic treatment in 0.075 M KCl, cytopun on slides at 1,000 rpm and incubated in KCM buffer (120 mM KCl, 20 mM NaCl, 10 mM Tris-HCl pH7.5, 0.5 mM EDTA, 0.1% (v/v) Triton X-100). Cells were extracted with 0.5% (v/v) Triton X-100 in KCM for 5 mins and blocked in KCM buffer containing 1% (w/v) BSA before incubation with relevant primary and secondary antibodies at 37°C for 1 h. After each round of antibody incubation, slides were washed three times in KCM buffer. Slides were then fixed in KCM with 4% (v/v) formaldehyde and mounted with Vectashield (Vector Lab) supplemented with DAPI at 250 ng/ml . Images were collected using a fluorescence microscope linked to a CCD camera system. Microscopy analyses were processed using the Axio Vision (Carl Zeiss Microscopy). For telomere fluorescence in-situ hybridization (FISH) analysis, slides were prepared according to the manufacturer's instructions (Dako). Briefly, slides were fixed in 4% formaldehyde followed by dehydration in a series of cold ethanol and hybridization with the telomere PNA Probe/Cy3 under denaturing conditions at 80°C. The slides were rinsed in wash buffer followed by a series of cold ethanol dehydration.

2.2.5 siRNA transfection and real time PCR analysis

siRNA oligonucleotides against mouse PML, MRE11 and NBS1 were transfected with Lipofectamine 2000 (Invitrogen). A set of low-GC rich Scramble siRNA was used as a control for all experiments. Cells were trypsinized with 0.25% Trypsin-EDTA and plated out in Complete DMEM media supplemented with 12% heat-inactivated FBS. The lipid-DNA complex was prepared at a ratio of 2:1. For each reaction, 100 nM of siRNA

oligonucleotides were used (Table 2.1). The cells were harvested and examined after 48 h of transfection. RNA was prepared according to the manufacturer's protocol (Roche) and treated with DNase using the Promega RQ1 reagent (Promega). cDNA was synthesised with oligo d(T)₁₂₋₁₈ (Life Technologies) using the cDNA Reverse Transcriptase kit (Life Technologies). The cDNA amount equivalent to 7.5 ng of RNA was amplified with 250 nM of the respective primers (Table 2.2) and quantitated with the Sybr Green PCR Master Mix using the ABI PRISM 7900HT (Life Technologies). All data analyses were calculated using the comparative cycle threshold method (C_T). The ΔC_T was calculated by subtracting from the average C_T values of the housekeeping gene β -Actin. The difference in the mRNA level was expressed as $2^{-\Delta\Delta C_T}$.

Table 2.1 siRNA sequence for PML, MRE11 and NBS1 depletion in ES129.1 cells

Sequence	
PML siRNA	5' CCU CAA GAU UGA CAA UGA AUU 3' (antisense)
oligo set 1	5' CUU UGA CCU CAA GAU UGA CAA UGA AAC CCA 3' (sense)
PML siRNA	5' CGG UGA ACC GGG AAA GCA AUU 3' (antisense)
oligo set 2	5' UUG CUU UCC CGG UUC ACC GCG 3' (sense)
MRE11 siRNA	5' GAG GCU UUG AAC CUU UCA AUU 3' (antisense)
oligo set 1	5' UUG AAA GGU UCA AAG CCU CUU 3' (sense)
MRE11 siRNA	5' GGGCACAACAUCUAGCAAUU 3' (antisense)
oligo set 2	5' UUU GCU AGA UGU UGU GCC CUU 3' (sense)
NBS1 siRNA	5' GCC CUU GGU UGU UUG UUC UUU 3' (antisense)
oligo set 1	5' AGA ACA AAC AAC CAA GGG CUU 3' (sense)
NBS1 siRNA	5' CCA GAA AUC UAU GUG UAA AUU 3' (antisense)
oligo set 2	5' UUU ACA CAU AGA UUU CUG GUU 3' (sense)

Table 2.2 Primers used for quantitative PCR analysis for PML, MRE11 and NBS1 siRNA

Sequence	
PML oligo set 1	5' GAC TAT GAA CAC AGC CAA AGC C 3' (forward) 5' GCC TTG CAG ATG GGG CAC TGC 3' (reverse)
PML oligo set 2	5' GCC TGG AGC ACA CCC TGT ACC 3' (forward) 5' GGA GCT TGT GGC CAA CCT GTC 3' (reverse)
MRE11 oligo set 1	5' CCA ATT CCA GGG CTG ATC AA 3' (forward) 5' CTC TGG GAC ATC CGT TTG CT 3' (reverse)
MRE11 oligo set 2	5' GTT CTG GCT AAC CAC CCA AA 3' (forward) 5' CCA CCC GTA GTC GGA TAA GA 3' (reverse)
NBS1 oligo set 1	5' CCT GCC GGA CCC TCA CT 3' (forward) 5' CCA GGG TCG CAT TCT GAG A 3' (reverse)
NBS1 oligo set 2	5' GGA GTA CGT TGT TGG GAG GA 3' (forward) 5' CTG TCT TCA ACG TGC AGG AA 3' (reverse)
NBS1 oligo set 3	5' TAA ATG CCA AGC AGC ACA AG 3' (forward) 5' ACA TCA ACA ACG CAG GTT CC 3' (reverse)
Actin oligo set 1	5' TCC CTG GAG AAG AGC TAC GA 3' (forward) 5' AGC ACT GTG TTG GCG TAC AG 3' (reverse)
Actin oligo set 2	5' CAT GTT TGA GAC CTT CAA CA 3' (forward) 5' GTG AGG ATC TTC ATG AGG TA 3' (reverse)

2.2.6 CO-FISH assay

Cells were incubated in fresh medium containing 10 μ g/ml of BrdU for 16-20 h, followed by the addition of Colcemid for 2 h to enrich for mitotic cells. Cells were harvested and resuspended in 0.075 M KCl of hypotonic buffer for 10 min at room temperature before fixing in ice-cold Methanol: Acetic Acid (3:1). The cell suspension were washed twice in fixative and spin at 1,500 rpm for 5 mins. Cells were dropped onto slides and air-dry overnight. The slides were washed in PBS for 5 min, treated with 0.5 mg/ml RNase for 10 min at 37°C and stained with Hoechst 33258 for 15 min. The slides were then covered in 2xSSC and exposed to 365 nm UV light for 1 h. To digest the BrdU containing DNA strands, the slides were treated with 10 U/ μ l of Exonuclease III for at 37°C for 30 min, followed by dehydration in an ice-cold ethanol series. The FISH hybridization was performed with the Telomere PNA/Probe in a non-denaturing condition according to the manufacturer's instructions (Dako).

2.2.7 Cell extracts and Western Blot analysis

Cells were lysed in cold RIPA buffer (150 mM NaCl, 50 mM Tris-HCl at pH 7.5, 0.25% sodium deoxycholate, 0.1% NP40, 0.05% SDS, 1 mM NaF, 1mM sodium orthovanadate, and protease inhibitor), followed by a 10-sec pulse sonication. The lysate was collected after a 15-min centrifugation at 12,000 rpm and boiled in SDS/PAGE sample buffer prior to SDS-PAGE and Western blotting. All proteins were detected using the SuperSignal West Pico Chemiluminescence HRP substrate detection kit (Thermo Scientific).

2.3 Results

2.3.1 PML-NB is associated with the telomeres in pluripotent mESC during S-phase

The dynamics of H3.3 incorporation to different genomic regions is specified by the histone deposition pathways. At the telomeric region, the loading of H3.3 is known to be mediated by the ATRX and its partner DAXX (Lewis et al., 2010; Wong et al., 2010); however, the platform that promotes and the mechanism which controls the nucleosomal assembly process remain unclear. In light of recent studies which showed that the interaction between H3.3 and its chaperones occurs within PML-NB (Delbarre et al., 2013), we hypothesized that these nuclear bodies act as an organizing centre for H3.3 prior to its loading onto the telomere chromatin. The targeting of DAXX and ATRX protein into the PML-NB has previously been observed in both mouse and somatic cells. In pluripotent ES129.1 mESCs, we have also observed the localization of ATRX and DAXX proteins within these PML-NBs by immunofluorescence staining (Figure 2.1 A-B). Considering the importance of ATRX and DAXX in the maintenance of the telomeric structural integrity in mES cells (Wong et al., 2010), we next examined the telomeric association of these PML-NBs in these pluripotent cells. In ES129.1 cells, immunofluorescence analysis showed overlapping signals between the PML protein and the telomere marker TERF-1 (Figure 2.1C). Importantly, this co-localization pattern was barely detectable in the non-pluripotent mouse embryonic fibroblasts NIH3T3 cells or human somatic HT1080 cells (Figure 2.1 D-E), with the exception of the ALT cancer W138-VA13/2RA cells (Figure 2.1 F). The co-localisation of telomeric proteins within the large PML-NBs or APB has been well documented. This data showing the co-localisation of telomere/TERF-1 with PML-NB suggests that the association of the PML-

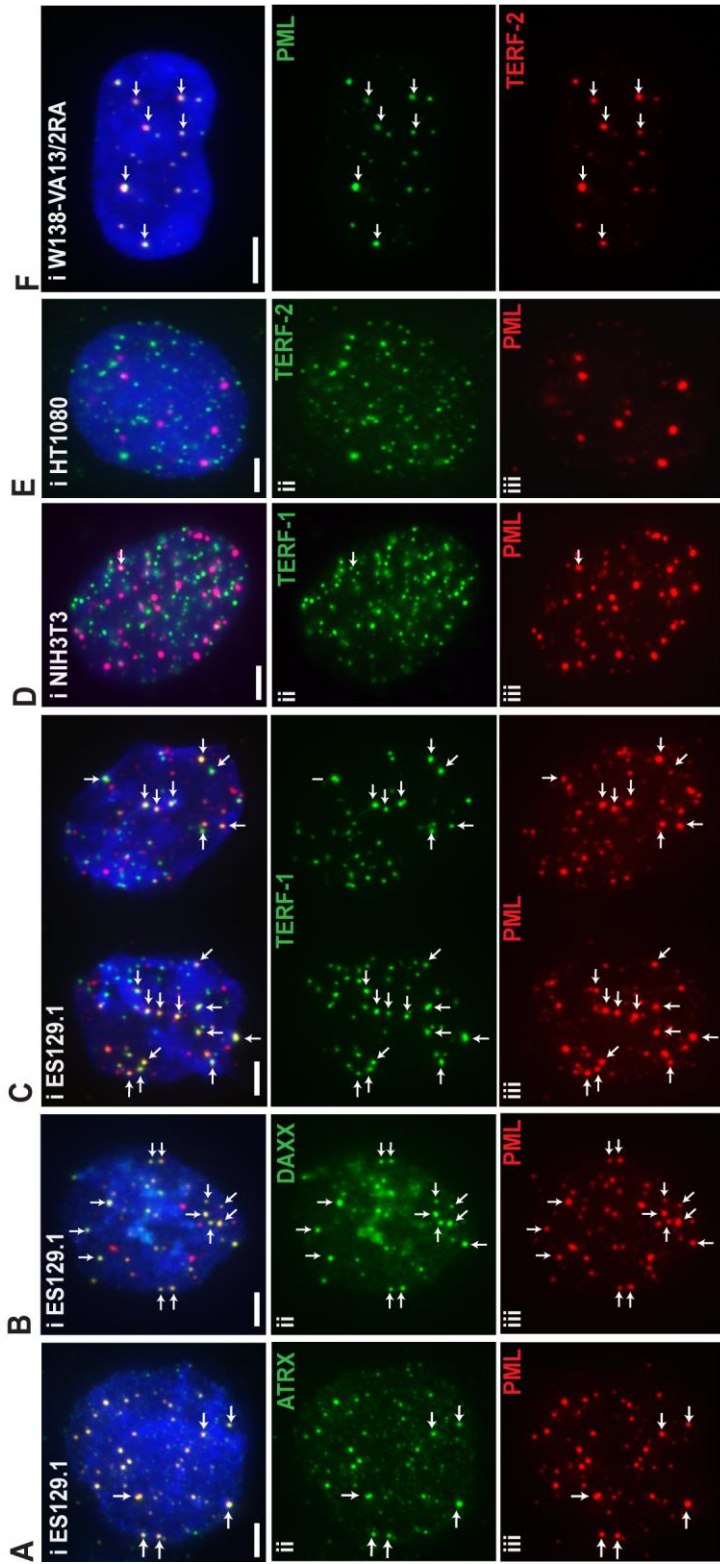
NB with the telomere heterochromatin is closely linked to the undifferentiated or pluripotent cellular state of mESCs (Figure 2.1C-E).

The increase in PML-NB assembly during S phase suggests these structures may be involved in DNA replication associated activities (Dellaire et al., 2006b). To investigate whether the assembly of these nuclear bodies plays a similar role in facilitating DNA replication at the telomeres, we performed immunofluorescence staining with telomere-FISH analysis. ES129.1 mESCs were synchronized by the addition of thymidine at the G1 phase and released in the presence of deoxycytidine. The kinetics of the cell-cycle progression was monitored by FACS analysis (Supplementary Figure 1). Following the release from the G1 phase, majority of the cell population had progressed through the S-phase by 4 h. At 6 h, the cells entered mitosis and exit into the next G1 phase at 8 h post release (Supplementary Figure 1). The number of PML/TERF1 co-localizing foci in a G1 cell was mostly less than 5 (<5 foci) (Figure 2.1 G) . At 0 h, the percentage of cells with <5 foci was 80%. In line with the cell-cycle progression, a significant reduction in the percentage of cells with <5 foci was noted at 4-6 h. This was accompanied by a substantial increase in the number of PML/TERF1 foci (≥ 5 foci) when the cells progressed through the replicative stage (Figure 2.1G). Consistent with the disassembly of PML-NB during mitosis (Dellaire et al., 2006b), the percentage of cells with ≥ 5 telomere associated PML-NB foci had reduced significantly (Figure 2.1 G). Together, this indicates the assembly of the PML at the telomere is closely linked to the replicative phase of the telomeres.

Page intentionally left blank

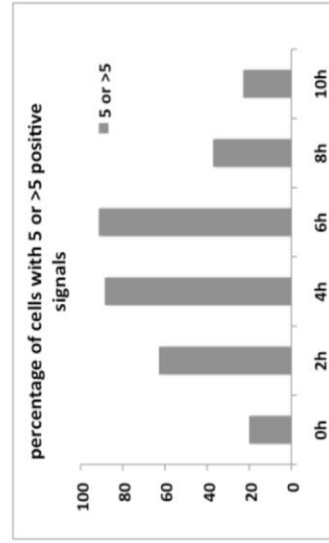
Figure 2.1 The localization of PML-NB at the telomere is dependent on the cellular pluripotent state

Immunofluorescence analysis with antibodies against **(A)** ATRX or **(B)** DAXX (green) and PML protein (red) confirmed the co-localization of these proteins to the PML-NB in mouse ES129.1 cells. **(C)** Antibodies against the Shelterin subunit TERF-1 (green) and PML protein (red) showed the co-localization of the PML-NB at the telomeres in mouse ES129.1 cells. No overlapping signal was observed in the **(D)** non-pluripotent NIH3T3 cells or **(E)** the human somatic HT1080 cells where the telomere was marked by the Shelterin subunit TERF-2. This indicates the absence of the PML-NB assembled specifically at the telomeric region in the differentiated cellular state. **(F)** In ALT cells W138-VA13/2RA, an increase in the overlapping signals was detected between TERF2 (green) and the PML protein (red). **(G)** Immunofluorescence analysis with telomere-FISH analysis was performed ES129.1 cells were synchronized from the G1 boundary by the addition of thymidine block. The frequency of the overlapping foci between PML and TERF1 was determined at different time points after the G1 release. The number of co-localizing foci in a G1 cells was less than 5. As the cells progressed into S-phase, there was an increase in percentage of cells with ≥ 5 co-staining. This suggests the assembly of PML at the telomeres occurs predominantly during the replication timing. Representative images of 50 interphase cells. Scale bar= 5 μ m.



G

Time period after G1/S release	0h	2h	4h	6h	8h	10h
Number of cells with <5 positive signals	28	13	4	3	22	27
Percentage with <5 positive signals (%)	80.00	37.14	11.43	8.57	62.856	77.14
Number of cells with 5 and >5 positive signals	7	22	31	32	13	8
Percentage with 5 and >5 positive signals (%)	20.00	62.86	88.57	91.43	37.14	22.86



Page intentionally left blank

2.3.2 Loss of PML-NB assembly leads the induction of telomere dysfunction

The ATRX/DAXX/H3.3 complex is deposited to the telomere during the replication process (Wong et al., 2010; Wong et al., 2009). The increase in the frequency of PML co-localizing with the telomeres during S-phase (Figure 2.1 G) suggests that the assembly of these nuclear structures facilitates the deposition of this complex to maintain the telomere chromatin integrity. To examine this, the PML scaffold had been removed from ES129.1 cells by siRNA mediated knock-down of PML expression for 48 h. The levels of reduction in the PML mRNA and protein were confirmed by immunoblotting and quantitative PCR analyses, respectively (Figure 2.2 A). Immunofluorescence staining was also performed to examine the loss of the PML-NB foci (Figure 2.2 B). In ES129.1 cells, the disassembly of these nuclear bodies did not cause a significant perturbation to the cell-cycle distribution (Figure 2.2 C).

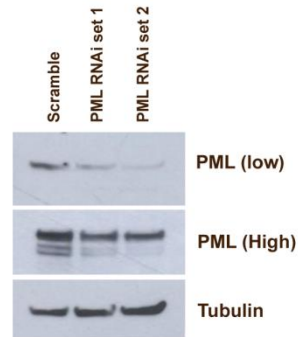
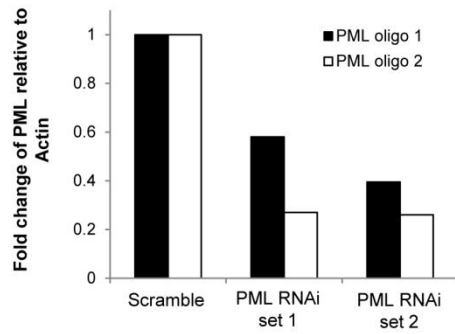
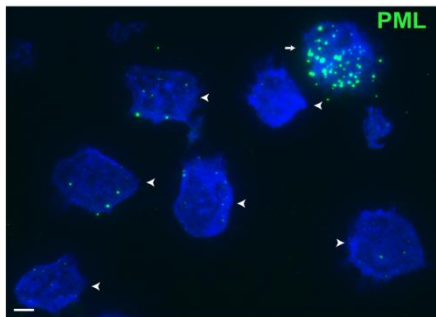
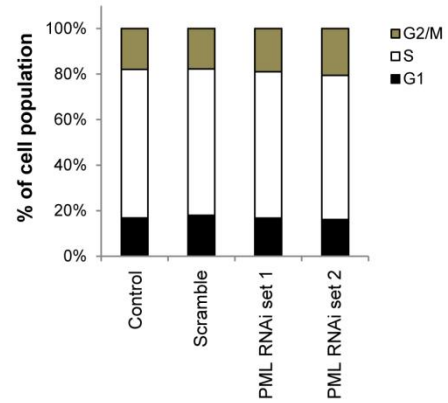
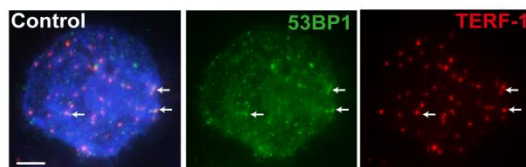
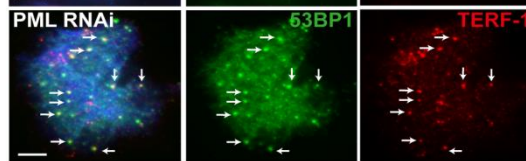
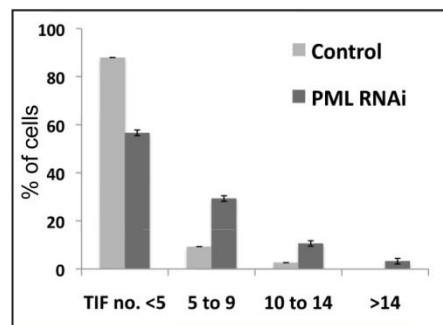
In our previous study, the deposition of the H3.3/ATRX complex is shown to play an important role in the maintenance of telomere integrity in pluripotent mESCs (Wong et al., 2010; Wong et al., 2009). Following the loss of the ATRX or H3.3 by RNAi mediated knockdown, there is a significant increase in the frequency of telomere damage induced foci. This is evident by the increase binding of DNA damage marker to the telomeric region (Wong et al., 2010; Wong et al., 2009). To examine the impact on the loss of PML-NB to the maintenance of telomere integrity, immunofluorescence analysis against the DNA damage marker, 53BP1 was performed to investigate the level of telomeric damage induce foci (TIF). In the control transfected cells, 53BP1 level at the telomere was very low in ES129.1 cells (Figure 2.2D,F). When the PML expression was depleted by siRNA mediated knock-down for 48 h, the percentage of cells with ≥ 5 53BP1/telomere foci had increased from 10-14% to 38-46% (Figure 2.2 E-F). This

further indicates that these PML-NBs are important to regulate the telomere chromatin integrity in the pluripotent mESC.

Page intentionally left blank

Figure 2.2 Loss of PML-NB assembly induces telomere damage in ES129.1 cells

(A) RNA was harvested from PML siRNA mediated knock-down ES129.1 cells after 48 h. The remaining PML mRNA was determined by quantitative PCR analysis. Immunoblotting with the PML antibody was also performed to examine the amount of the PML protein level (low). The different PML isoforms were shown in the longer exposure of the immunoblot. The tubulin level was used as a loading control (B) Immunostaining against the PML protein (green) was performed to illustrate the effect on the loss of the PML scaffold protein to the assembly of PML-NB (arrowhead). (C) The cell-cycle distribution of the PML siRNA transfected ES129.1 cells was examined by FACS analysis. No obvious perturbation to the cell-cycle progression was observed. (D) After 48 h of PML siRNA transfection, immunofluorescence analysis was performed with antibodies against DNA damage marker, 53BP1 (green) and TERF-1 (red) to examine the frequency of telomeric damage induced foci (TIF). In the control siRNA transfected cells, majority of the interphase cells has less than 5 53BP1/TERF-1 overlapping signals. Following the disassembly of the PML-NB, a significant increase in the percentage of cells with more than ≥ 5 foci was observed. (E) The data were grouped into 4 different category based on the number of TIF (<5, 5-9, 10-14, >14) and plotted against the % of cells examined for each subgroup. Representative graph for three independent experiments are shown. Scale = 5 μ m.

A**B****C****D****E****F**

Page intentionally left blank

2.3.3 The disassembly of PML-NB affects the loading of H3.3 and ATRX to the telomere in mES cells.

Considering the targeting of the ATRX to the PML-NB in ES129.1 (Figure 2.1 A), we examined the nuclear distribution of the ATRX protein by immunofluorescence analysis. Indeed, majority of the ATRX foci is lost upon the loss of these PML-NBs (Figure 2.3 A). To investigate the effect on the loss of these PML nuclear structures to the ATRX binding at the telomeres, immunostaining with ATRX coupled with telomere-FISH was performed on cells that were blocked at the G1 phase and were released for 4 h to enrich for S-phase cells (Figure 2.3 B-C). In the scramble control RNAi transfected population, the percentage of cells with ATRX at the telomeres (≥ 5 ATRX foci) was 83%. In comparison, only 43% of the cell population has ≥ 5 telomere associated ATRX foci. (Figure 2.3 D). This indicates the disassembly of the PML-NB leads to the delocalization of the ATRX protein and affects the binding of the ATRX protein to the telomeric region during telomere replication timing.

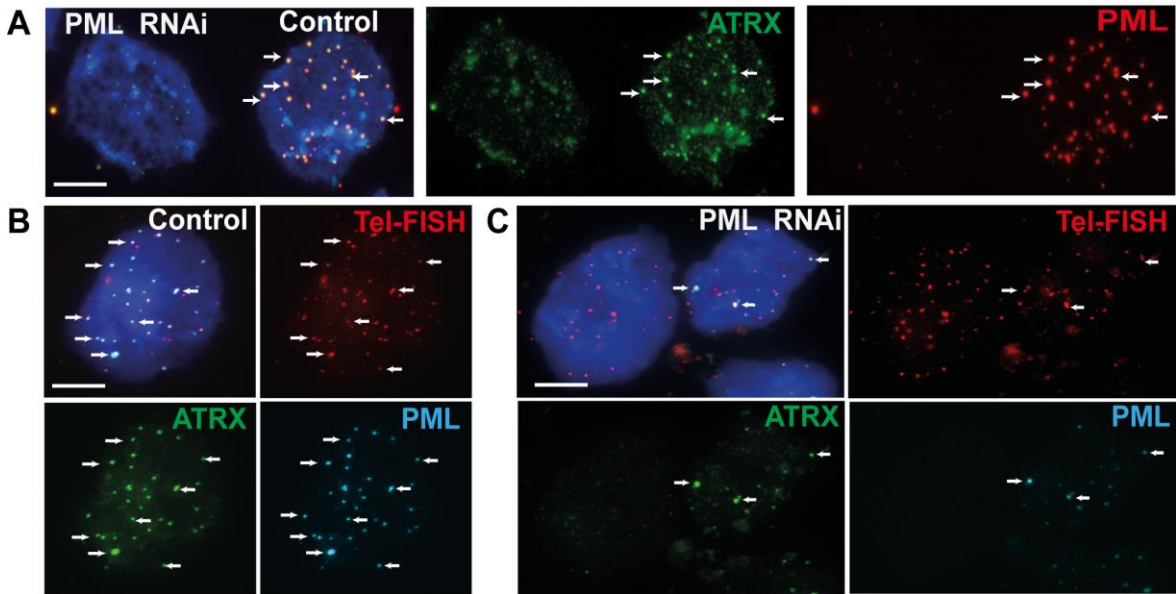
ATRX protein plays an important role in the regulation of H3.3 nucleosomes assembly at the telomeres (Wong et al., 2010). To determine whether the deposition of the H3.3 to the telomere is affected in the absence of the PML protein, we assessed the distribution of the phosphorylation on H3.3S31 (H3.3S31ph). H3.3S31ph is a unique mark that is only observed on mitotic chromosomes (Hake et al., 2005). In mESCs, this phosphorylated histone mark is present on the telomere heterochromatin (Wong et al., 2009). Immunofluorescence analysis against ATRX and H3.3S31ph was performed on PML siRNA transfected ES129.1 cells after 48 h. Cells were treated with Colcemid for 1 h to enrich for mitotic cells. In the control cell population, the ATRX localized at the pericentric region, whereas H3.3S31ph remained enriched at the telomere heterochromatin (Figure 2.3 E). The depletion of the PML protein resulted in a loss of the

telomere enrichment of H3.3 S31ph on metaphase chromosomes (Figure 2.3 F). Besides this, there is an increase in the level of immunostaining of ATRX at the pericentric region, which is consistent with the de-localization of the protein in the absence of PML-NB assembly (Figure 2.3 F arrowhead). Our data suggests that the loss of the PML-NB formation affects the maintenance of the telomere chromatin integrity, likely as a consequence of an impaired the binding of ATRX and thus loading of H3.3 at telomeres.

Page intentionally left blank

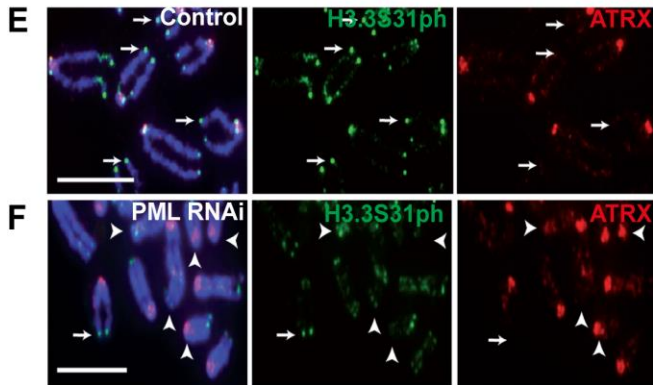
Figure 2.3 The disassembly of PML-NB affects the deposition of ATRX and H3.3 to the telomere in ES129.1 cells

Immunofluorescence analysis with antibodies against ATRX (green) and PML (red) was performed on PML siRNA transfected cells after 48 h. **(A)** In the interphase cell where the PML protein was not depleted, overlapping signals between the ATRX protein and the PML bodies was detected. The ATRX protein is de-localized from the PML-NB following its disassembly upon the depletion of the PML protein scaffold (red). After 24 h of PML siRNA mediated knock-down, ES129.1 cells were blocked at G1 phase by the addition of thymidine for 16 h. Cells were released for 4 h to enrich for S-phase cell population. Immunostaining analyses with antibodies against ATRX (green) and PML (cyan) were performed, followed by telomere-FISH analysis (red). **(B)** In the control siRNA transfected cell population, overlapping staining signals of ATRX/PML/telomeres were detected (arrow). **(C)** The loss of the PML-NB assembly led to the de-localization of the ATRX at the telomeric region (left). **(D)** The number of ATRX/telomere overlapping foci was grouped into different subgroups: <5, 5-9, 10-14, >14. The data was plotted against the % of cells counted for each category. In the control siRNA transfected population, the % of cells with > 5 co-localizing foci is 80%. Following the disassembly of the PML-NB at the telomeres, the % of cells with >5 co-localizing foci has reduced to 43%. **(E)** Immunofluorescence analyses with H3.3S31ph (green) and ATRX (red) were also performed. In the control ES129.1 cells, the H3.3S31ph was enriched at the telomere heterochromatin (arrow) during mitosis, whereas ATRX was found in the pericentric satellite repeats. **(F)** The siRNA depletion of the PML protein led to a loss of H3.3S31ph level at the telomeres (arrowhead). Scale = 5 μ m.



D

		n=1		n=2		n=3	
		Control	PML RNAi	Control	PML RNAi	Control	PML RNAi
number of ATRX/TRF-1 foci	<4	17.14	57.14	14.29	60	20	54.29
	5-9	54.29	25.71	60	25.71	54.3	31.43
	10-14	17.14	14.29	20	11.43	17.1	8.57
	>14	11.43	2.86	5.71	2.86	8.57	5.71
total % cells with ≥ 5 foci		82.86	42.86	85.71	40	80	45.71
average % of cells with ≥ 5 foci		control = 82.9%		PML RNAi = 42.9%			



Page intentionally left blank

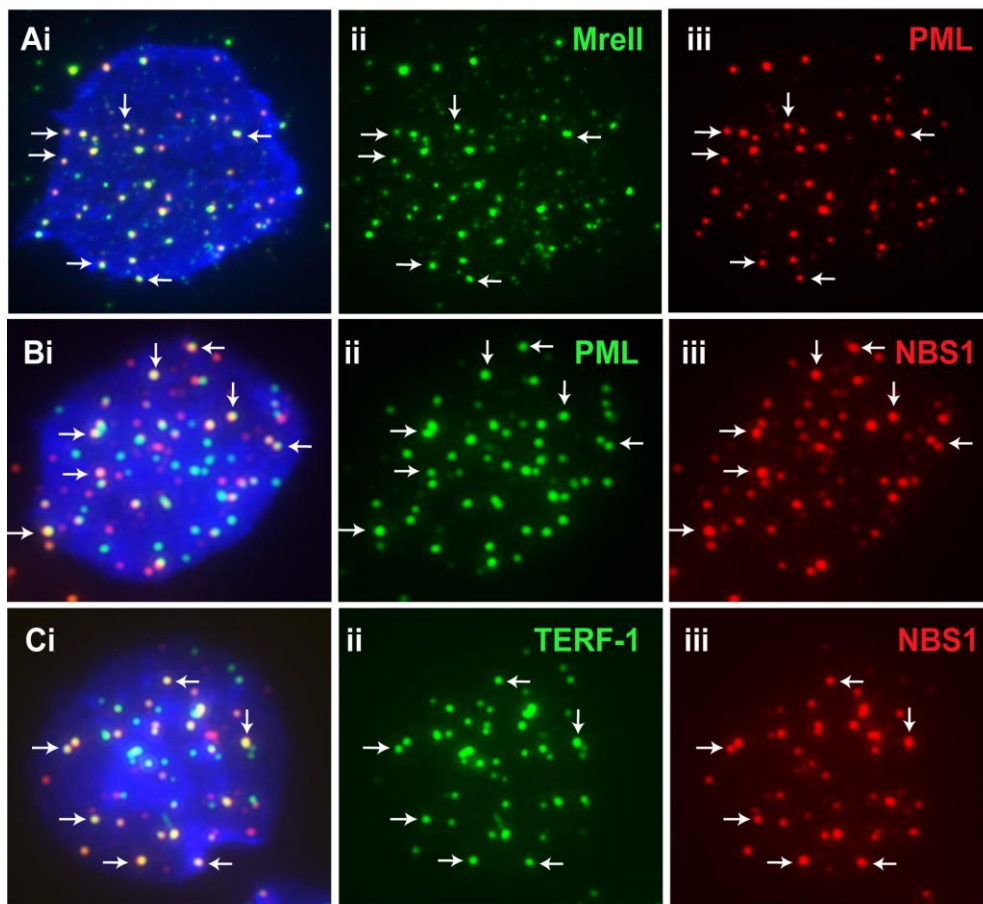
2.3.4 The telomere associated PML-NB is functionally different from the ALT associated PML-NB (APB) in ALT positive cancer cells

To our knowledge, the assembly of the PML-NBs at the telomeric region mESC has only been observed in the ALT positive cancer cells (Figure 2.1 F). In ALT cancer cells, the ALT associated PML-NB (APB) facilitates the maintenance of telomere integrity and is required for cell survival (Wu et al., 2003; Zhong et al., 2007). Considering the functional similarity between these nuclear bodies in the maintenance of telomere chromatin, we first examined the interacting partners present within these telomere associated PML-NBs in ES129.1 cells. Besides the DAXX and ATRX proteins (Figure 2.1 A-B), we detected the localization of DDR signaling proteins, including the MRE11 and NBS1 proteins at the telomere associated PML-NBs (Figure 2.4). This is consistent with the function of these DNA damage signaling proteins in facilitating telomere replication (Verdun et al., 2005). In ALT cancer cells, the presence of the MRE11 and NBS1 proteins plays a key role to the assembly of the APB and the maintenance of ALT activity (Jiang et al., 2005; Wu et al., 2003; Zhong et al., 2007). To determine whether the localization of the PML at the telomeres was affected by the loss of these DDR signalling proteins, we depleted the MRE11 protein in ES129.1 cells by siRNA specific oligonucleotides for 48 h (Figure 2.5 A-B). There was no significant impact to the cell-cycle distribution in the absence of the MRE11 protein (Figure 2.5 C). To examine the dynamics of telomere associated PML-NBs specifically at S-phase, the MRE11 was depleted by siRNA mediated knockdown for 24 h before being blocked at the G1/S boundary by the addition of thymidine for 16 h. Immunofluorescence analysis was performed on the cell population which has progressed through to the S-phase at 4 and 6 h. There was no significant difference in the percentage of cells with ≥ 5 telomeres associated PML-NB when MRE11 was removed (Figure 2.5 D-E). Similar observation

was also made with the siRNA mediated knockdown of NBS1 in ES129.1 cells (Figure 2.6). In contrast to the APB, loss of neither MRE11 nor NBS1 did not result in any significant impact on the assembly of the PML bodies and the localization of telomeres to these nuclear bodies in mESCs.

Figure 2.4 Localization of DDR signalling proteins to the telomeres and PML-NB in ES129.1 cells

(A) Immunofluorescence analysis was performed on ES129.1 cells to examine the distribution of the MRN complex. Overlapping signals between MRE11 (green) and PML (red) were observed in pluripotent ES cells (arrows) (B) Likewise, co-localized foci of PML (green) and NBS1 (another component of MRN complex) is observed in ES129.1 cells. (C) Immunostaining of the telomere marker TERF-1 (green) and NBS1 protein (red) at telomeres is also detected.



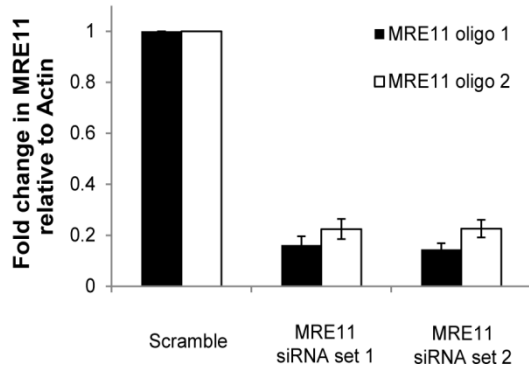
Page intentionally left blank

Page intentionally left blank

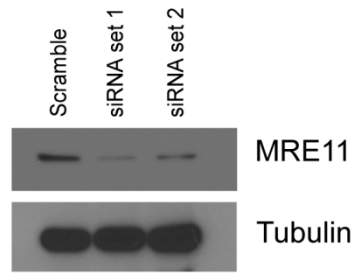
Figure 2.5 The removal of MRE11 protein does not affect the assembly of PML-NB at the telomere in ES129.1 cells

ES129.1 cells were transfected with scramble control siRNA and two different sets of MRE11 siRNA oligonucleotides for 48 h. (A) RNA were harvested to examine the remaining level of MRE11 mRNA. (B) Immunoblotting with the MRE11 antibody was performed on lysates collected from siRNA knockdown ES129.1 cells. (C) FACS analysis was performed to examine the cell-cycle distribution. No perturbation to the cell-cycle progression was observed upon the removal of the MRE11 protein. (D) Immunofluorescence analysis was performed on ES129.1 cells transfected with MRE11 siRNA oligonucleotides for 24 h prior to blocking of cells at the G1 phase by the addition of thymidine for 16 h. Cells were released for 4 and 6 h to enrich for S-phase cell populations. The number of PML/TRF1 overlapping signals was categorized into different subgroups: (<5, 5-9, 10-14, >14); the data was present according to the percentage (%) of cells for individual category. No significant difference the percentage (%) of cell population for each subgroup was observed between the control and MRE11 siRNA transfected cells. Representative data for three independent experiments (a total of 50 interphase cells counted per experiment) are shown.

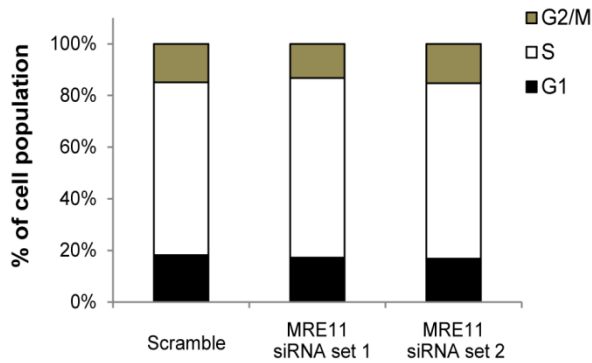
A



B



C



	G1	S	G2/M
Scramble	18	67	15
MRE11 siRNA set 1	17	70	13
MRE11 siRNA set 2	17	68	15

D

		Scramble control siRNA	MRE11 siRNA set 1	MRE11 siRNA set 2
Number of co-localising PML and TERF-1 foci (% of cells)	<5	33.90	41.35	39.45
	5 to 9	44.92	37.50	43.12
	10 to 14	18.64	18.27	16.51
	>14	2.54	2.88	0.92
% of cell with ≥ 5 foci		66.10	58.65	60.55

E

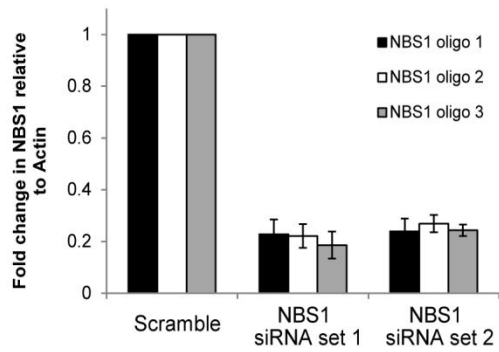
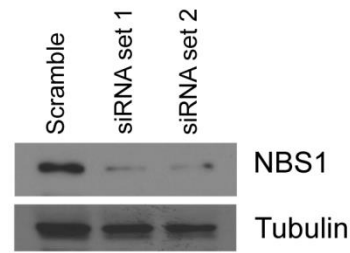
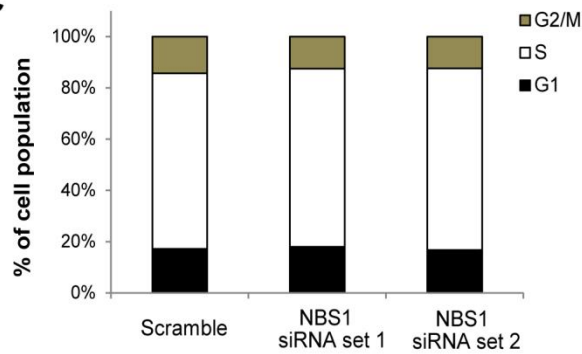
		Scramble control siRNA	MRE11 siRNA set 1	MRE11 siRNA set 2
Number of co-localising PML and TERF-1 foci (% of cells)	<5	32.00	15.12	24.17
	5 to 9	42.00	41.86	45.83
	10 to 14	17.00	23.26	21.67
	>20	9.00	19.77	8.33
% of cell with ≥ 5 foci		68.00	84.88	75.83

Page intentionally left blank

Page intentionally left blank

Figure 2.6 Loss of the NBS1 protein does not affect the assembly of PML-NB at the telomere in ES129.1 cells

ES129.1 cells were transfected with two different sets of NBS1 siRNA oligonucleotides for 48 h. (A) RNA were harvested to examine the remaining level of NBS1 mRNA. (B) Immunoblotting against the NBS1 protein was performed on lysates collected from siRNA knockdown cells after 48 h. (C) FACS analysis was performed to determine the cell-cycle distribution. No significant impact to the cell-cycle progression was observed upon the removal of the NBS1 protein. (D) Immunofluorescence analysis was performed on ES129.1 cells that were transfected with NBS1 siRNA oligonucleotides for 24 h prior to blocking of cells at the G1 phase by the addition of thymidine for 16 h. Cells were released for 4 and 6 h to enrich for S-phase cell populations. The number of PML/TRF1 overlapping signals was categorized into different subgroups: (<5, 5-9, 10-14, >14); the data was presented according to the % of cells for individual category. No significant difference the percentage (%) of cell population for each subgroup was observed between the control and NBS1 siRNA transfected cells. Representative data for three independent experiments (a total of 50 interphase cells counted for each experiment) are shown.

A**B****C**

% of cell population			
	G1	S	G2/M
Scramble	17	69	14
NBS1 siRNA set 1	18	69	13
NBS1 siRNA set 2	17	71	12

D

		Scramble control siRNA	NBS1 siRNA set 1	NBS1 siRNA set 2
Number of co-localising PML and TERF-1 foci (% of cells)	<5	24.71	29.46	32.00
	5 to 9	60.00	43.75	49.00
	10 to 14	10.59	21.43	13.00
	>14	4.71	5.36	6.00
% of cell with ≥ 5 foci		75.29	70.54	68.00

E

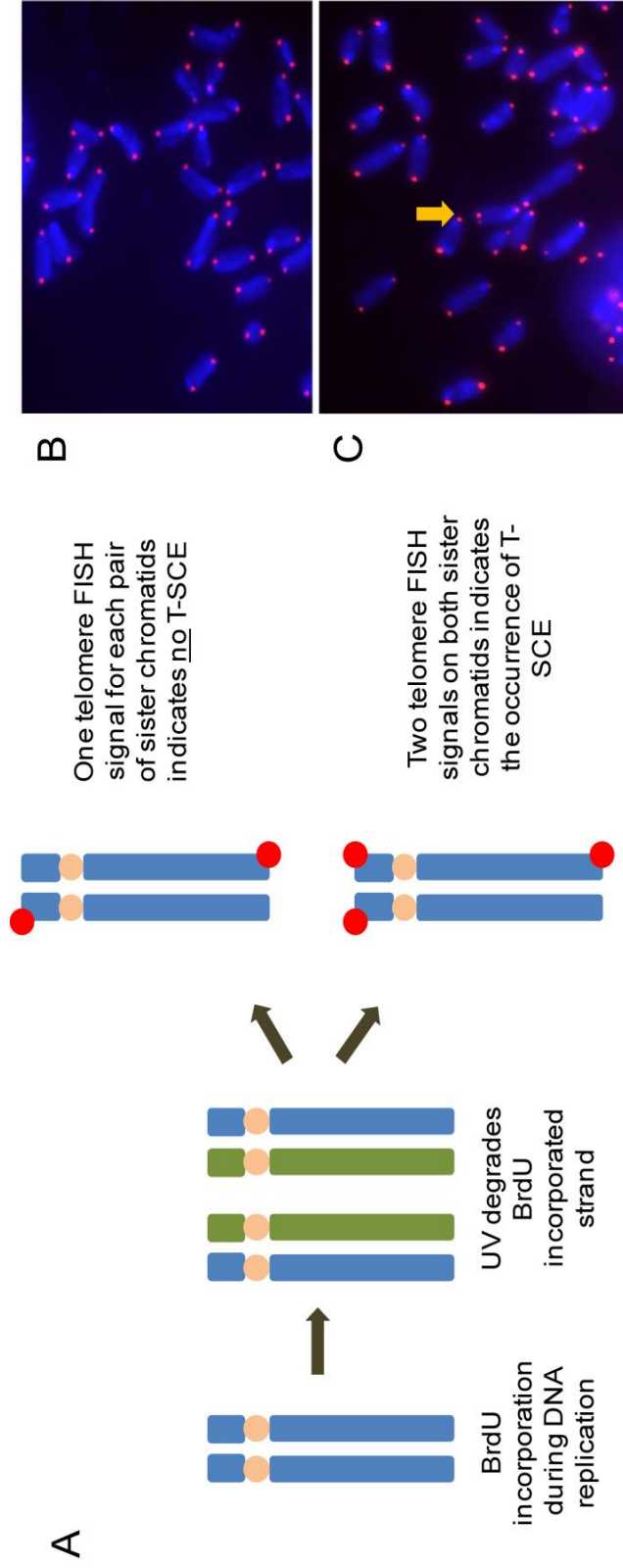
		Scramble control siRNA	NBS1 siRNA set 1	NBS1 siRNA set 2
Number of co-localising PML and TERF-1 foci (% of cells)	<5	29.59	15.84	20.24
	5 to 9	41.84	51.49	52.38
	10 to 14	18.37	16.83	19.05
	>14	10.20	15.84	8.33
% of cell with ≥ 5 foci		70.41	84.16	79.76

Page intentionally left blank

The maintenance of the telomere length in ALT cancer cells is facilitated by the high rate of T-SCE that occurs within the APB (Draskovic et al., 2009). Considering the link between the PML protein and telomere recombination, the rate of T-SCE and the loss of PML-NB in ES129.1 cells can be determined by a commonly used CO-FISH assay (Figure 2.7 A). In the absence of T-SCE, only one telomere-FISH signal is expected to be observed on each pair of sister chromatids (Figure 2.7 B). The occurrence of T-SCE is indicated by the presence of the telomere FISH signals on both sister chromatids (Figure 2.7 C). Based on our findings, there was no significant increase in the rate of T-SCE between the scramble control and PML siRNA transfected ES129.1 cells (Figure 2.7 D). Together, this indicates the PML-NB assembled at the telomeres in mESC has a different function in the maintenance of telomere integrity compared to the APB in telomerase null cancer cells.

Figure 2.7 No increase in the frequency of T-SCE in PML RNAi-depleted mES cells

(A) Schematic diagram to illustrate the principle of telomere CO-FISH analysis to examine the frequency of T-SCE. (B) In the absence of telomere exchange, only one telomere signal is observed on each chromosome. (C) The occurrence of T-SCE is denoted by the presence of a double telomere FISH signal on a pair of sister telomeres. (D) Telomere FISH analysis was performed on PML RNAi-depleted ES129.1 cells. A summary of the frequency of T-SCE for three independent experiments was shown. No significant difference in the frequency of telomere exchange was noted following the depletion of PML protein, and disassembly of PML-NBs.



D

	N=1		N=2		N=3	
	Ctrl	PML RNAi	Ctrl	PML RNAi	Ctrl	PML RNAi
Number of chromosome spreads with T-SCE	10/600	13/600	17/600	20/600	14/600	21/600
Percentage of T-SCE	1.7%	2.2%	2.8%	3.3%	2.3%	3.5%

Page intentionally left blank

2.4 Discussion

The PML-NBs are often regarded as domain structures that are randomly distributed to facilitate the regulation of cellular processes. Recently, these nuclear bodies have been shown to be actively recruited to specific gene loci, including the Major Histocompatibility Class I (MHCI) gene clusters and the Cytomegalovirus promoter on transgene array (Newhart et al., 2012; Ulbricht et al., 2012). In this study, we have demonstrated a specific association of the repetitive telomeric DNA with PML-NBs and identified a novel function of these nuclear bodies in maintaining telomeric chromatin integrity in mES cells. These telomeric DNA associated PML-NBs in mES cells are functionally different to the APBs observed in human ALT cancer cells. Firstly, the association of these PML-NBs with the telomeric repeats is closely linked to the pluripotent state of the cells because it is not observed in non-pluripotent mouse and human somatic cell lines. Secondly, we also show evidence that these PML-NBs serve as a platform for H3.3 deposition by its histone chaperone ATRX to maintain the telomere integrity in mES cells. In ALT cells, the frequent loss-of-function of ATRX/DAXX (H3.3 chaperone) indicates that the APB is unlikely to be involved H3.3 deposition at the telomeric region. We also show that the removal of DNA damage repair proteins (including MRE11 and NBS1) does not affect the assembly of the PML-NBs and their association with the telomeres in mESs. In addition, neither the depletion of PML expression nor loss of PML body assembly results in a change in the rate of T-SCE in these cells. Conversely, in ALT cells, the formation of APB in ALT cancer cells requires the presence of MRE11 and NBS1 (Jiang et al., 2005; Wu et al., 2003), and these bodies are essential for T-SCE. Altogether, PML-NBs play distinct roles in the regulation of telomere chromatin and structural integrity in these cell types.

Among the components found associated with the PML-NB, the H3K9 methyltransferase Setdb1 is the only protein that has been shown to regulate the assembly of these nuclear bodies (Cho et al., 2011). It remains to be determined whether the epigenetic chromatin state at telomeres contributes to the localization of telomeres within PML bodies or recruitment of PML-NBs to the telomeres; however, the 'less heterochromatic' chromatin environment in mES cells could favor the targeting of the PML-NB to the telomeric region. Supporting this argument is the localization of the APB to the telomeres in telomerase null cancer cells, which are characterized by a less repressive chromatin environment (Episkopou et al., 2014). Furthermore, an increase in the frequency of APB enriched at the telomeric region was observed in cells that are deficient in DNA and histone methyltransferases, suggesting the change in the telomere epigenetic state regulates the recruitment of PML-NB to genomic loci (Gonzalo et al., 2006).

The interaction between PML-NB and the repetitive heterochromatin has been suggested to play a role in the re-establishment of the chromatin state. This is evident by the co-localization of the pericentric satellite DNA within PML nuclear bodies in patients with the Immunodeficiency, Centromeric instability and Facial dysmorphism (ICF syndrome) (Luciani et al., 2006). The presence of these PML-NBs facilitates the targeting of chromatin modifiers such as the Bloom helicase, Topoisomerase II and Heterochromatin protein (HP1) to promote the remodeling of the hypomethylated chromatin (Luciani et al., 2006). In this case, these nuclear bodies provide an environment for the repressive chromatin state to be re-established. Besides the known function of PML-NB to promote the epigenetic establishment, these nuclear bodies can act as an intermediate body or triage centre to facilitate the organization and assembly of H3.3 octamer complex by its chaperones prior to its deposition onto the chromatin (Delbarre et al., 2013; Ivanauskiene et al., 2014). As the incorporation of H3.3 plays a role in the maintenance of epigenetic

stability at repetitive loci (Morozov et al., 2012), it is reasonable to suggest that the epigenetic chromatin re-establishment is perturbed as the binding of the ATRX/H3.3 binding to the telomeres is affected due to the disassembly of the PML-NB. This is evident by an increase in the levels of heterochromatic marks such as the trimethylation of H3K9 and H4K20 (data not shown). Furthermore, a significant increase in the frequency of telomere damage induced foci (TIF) which is indicative of telomere dysfunction was also noted. In light of this, the assembly of these nuclear bodies in mESCs has therefore provided a platform for the establishment of a chromatin environment which is compatible to the pluripotent status of mESCs.

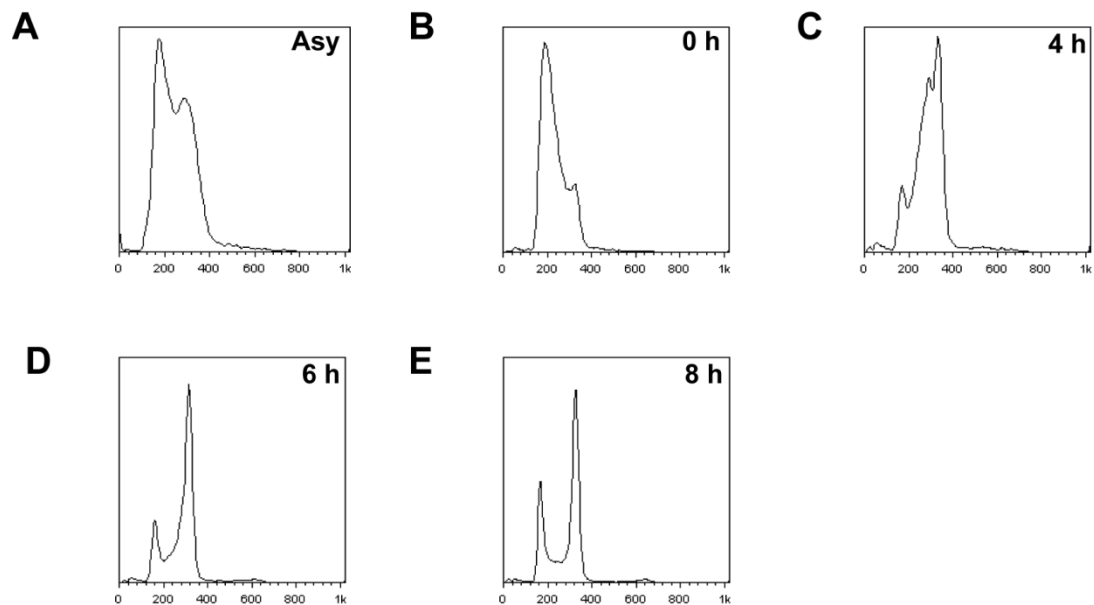
Recently, the ATRX protein is required to promote the nucleosomes reassembly after the stalling of the replicative machinery during DNA synthesis (Huh et al., 2012; Leung et al., 2013). Besides the ATRX/DAXX/H3.3 complex, we have also detected the presence of the MRE11 and NBS1 proteins that are known to play an important role during telomere replication (Verdun et al., 2005). Consistent with the increase in the number of PML-NB binding to the telomere during S-phase, we propose that the assembly of these bodies creates an environment to allow the remodeling of the telomere chromatin by the MRN complex. In addition, the deposition of H3.3 at telomeres by ATRX/DAXX complex within these PML-NBs also facilitates the re-chromatinization of the telomeric DNA and re-establishment of a proper chromatin state. This may be achieved by recruiting other chromatin modifiers that are also important for directing heterochromatin assembly, such as the HP1 protein which is known to bind ATRX. Taken together, these DDR signaling proteins, H3.3, ATRX, DAXX, HP1 and possibly others work in a concerted effort within the PML-NBs to ensure that the epigenetic state is properly propagated onto the newly synthesized telomeric DNA, and this is essential for maintaining the pluripotent status of ESCs.

Our findings have therefore highlighted the importance of PML-NBs in the maintenance of cell pluripotency, in this case, providing a novel role of PML-NBs in the maintenance of telomere chromatin by regulating ATRX/DAXX/H3.3 function. We have shown that the recruitment of ATRX and H3.3 is dependent on the assembly of the nuclear bodies at the telomeric region and loss of the H3.3/ATRX/DAXX complex alters the chromatin state through an increase in the overall repressive chromatin marks. Considering the possible impact of the change in epigenetic state in regulating TERRA transcription and control of telomere length (Arnoult et al., 2012), it will be interesting to determine as future studies the effects of the long term loss of PML-NB to the overall maintenance of telomere chromatin integrity and function. These may include telomere lengthening, protein binding and structural organization, in order to better understand the role of PML-NBs in controlling telomere renewal.

Supplementary information

Supplementary Figure 1 The synchronization of ES129.1 cells by a single thymidine treatment protocol

Cells were blocked at the G1 phase by the treatment of thymidine for 16 h followed by the release into media containing deoxycytidine. The kinetics of the cell-cycle progression was shown. (A) A FACS plot showing the asynchronous cell-cycle distribution of ES129.1 cells. (B) An enrichment of cells at the G1 phase was shown at the 0 h before its release from the thymidine block. (C) A substantial population of cells has entered S-phase at 4 h. (D-E) At 6 h, cells progressed into the G2/M boundary; by 8 h, the G2/M population began its exit into the next G1 phase.



Chapter 3

CHK1-driven histone H3.3 serine 31 phosphorylation maintains chromatin dynamics and cell survival in human ALT cancer cells

3.1 Overview

The regulation of histones and its post-translational modification (PTM) profile is important to the maintenance of chromatin structure and dynamics. In addition to the canonical histone family, histone variants also play a role in regulating chromatin integrity and have been implicated in cancer development. This is evident by the recurrent mutations of the histone variant H3.3 and its specific residues, including Lysine 27 and Glycine 34 in a range of pediatric brain tumours which utilize the Alternative Lengthening of the Telomeres (ALT) pathway (Khuong-Quang et al., 2012; Schwartzenuber et al., 2012; Sturm et al., 2012; Wu et al., 2012). As discussed earlier, the deposition of histone variant H3.3 is known to be independent of DNA replication. Histone H3.3 consists of a Serine 31 residue which is evolutionarily conserved and unique to H3.3, as the corresponding position in H3.1 and H3.2 is an Alanine which cannot be post-translationally modified. Unlike the phosphorylation of Serine 10 and Serine 28 residue by the Aurora kinase family during mitosis (Crosio et al., 2002), the kinase that mediates the phosphorylation of H3.3 Serine 31 is not known.

Telomerase-null ALT cancer cells are characterized by extensive levels of genome instability, indicated by severe chromosomal fragmentation, frequent micronucleation, a high basal level of DNA damage foci, and elevated DNA damage response (DDR) signaling in the absence of exogenous damage (Gagos et al., 2008; Lovejoy et al., 2012). The Checkpoint kinase 1 (CHK1) is a serine/threonine kinase involved in DDR signaling (Zhang and Hunter, 2014). Previous studies have shown that CHK1 mediates the phosphorylation on Serine 10 and Threonine 11 residue on canonical H3 to regulate gene transcription upon the detection of DNA damage (Metzger et al., 2008; Shimada et al., 2008). Interestingly, CHK1 kinase has also been reported to be important role in

promoting cell survival of a pediatric glioma cell line which harbours specific mutation on the Glycine 34 residue of H3.3 (Bjerke et al., 2013).

Besides the mutation on H3.3, the Alpha Thalassemia Mental Retardation X-linked (*ATRX*) gene has been reported to be inactivated in 90% of *in vitro* immortalized ALT cell lines (Lovejoy et al., 2012), while loss of wild type *ATRX* expression in somatic cell hybrids correlates with the activation of ALT mechanism (Bower et al., 2012). Furthermore, mutations in *ATRX* have been detected at a very high rate in ALT tumours, including pancreatic neuroendocrine tumours, neuroblastomas, and medulloblastomas (Jiao et al., 2010; Kannan et al., 2012; Levy et al., 2014; Nguyen et al., 2013; Schwartzenuber et al., 2012), suggesting that *ATRX* acts as a suppressor of the ALT pathway. *ATRX* associates with *DAXX* to function as a histone chaperone complex that deposits histone variant H3.3 to telomeres and pericentric heterochromatin (Chang et al., 2013; Drane et al., 2010; Goldberg et al., 2010; Law et al., 2010; Lewis et al., 2010; Wong et al., 2010; Wong et al., 2009). Recent studies also suggest that it is important for the resolution of stalled replication forks and re-chromatinization of repaired DNA upon recovery from stalled replication (Clynes and Gibbons, 2013; Clynes et al., 2013; Giraud-Panis et al., 2013; Huh et al., 2012; Leung et al., 2013; Watson et al., 2013). In these studies, it is shown that *ATRX*-deficient ALT cells show elevated DDR signaling, evidenced by high levels of phosphorylated histone variant H2AX on Ser139 (γ H2AX), a DNA damage marker, and activation of the DNA damage proteins ATM and CHK2 (Huh et al., 2012; Lovejoy et al., 2012; Watson et al., 2013).

Although it is clear that loss of *ATRX* function results in a failure to deposit H3.3 in heterochromatin (Bower et al., 2012; Jiao et al., 2010; Lovejoy et al., 2012; Mikhailov et al., 2002; Schwartzenuber et al., 2012), whether this leads to further aberrant H3.3 loading and/or PTMs in other genomic regions is unknown. Considering the frequent

inactivation of ATRX in the ALT cancer cells, this study aims to investigate the distribution of H3.3 through the examination of the serine 31 phosphorylation (H3.3S31ph) staining pattern in ATRX-deficient ALT cancer cells. In mammalian cells, H3.3S31ph is a chromatin mark found at the heterochromatin during mitosis (Hake et al., 2005). In somatic cells, H3.3S31ph is enriched at pericentric satellite DNA repeats of metaphase chromosomes (Hake et al., 2005), while in pluripotent mouse embryonic stem (ES) cells, it localizes at telomeres (Wong et al., 2009). Here, an extremely high level and extensive spreading of H3.3S31ph across the entire chromosome arms was detected in mitotic human ALT cancer cell lines. This observation is in sharp contrast to the previously reported heterochromatic localization of H3.3S31ph in both human and mouse telomerase positive cells (Hake et al., 2005; Wong et al., 2009). The aberrant pattern of H3.3S31ph noted in these cells is shown to be driven by the high endogenous levels of activated CHK1 kinase, attributable to the persistent DNA damage and genome instability. In addition, either substitution of the Serine residue with an Alanine or inhibition of CHK1 activity in ALT cancer cell lines during mitosis results in increased level of γ H2AX on chromosome arms, and reduced cell viability. Collectively, this suggests a role for CHK1-mediated H3.3S31ph in DNA damage signaling, chromatin maintenance and cell survival in these ALT cancer cells.

3.2 Materials and Methods

3.2.1 Cell cultures

Telomerase positive cell lines HT1080 (fibrosarcoma), A549 (lung adenocarcinoma), HT29 (colorectal cancer), HeLa (cervical cancer) and ALT positive cell lines Saos-2 (osteosarcoma), U2OS (osteosarcoma), G292 (osteosarcoma), KMST6 (immortalized fibroblast), SUSM1 (immortalized fibroblast), SKLU1 (lung adenocarcinoma), GM847

(SV40-transformed fibroblasts) and W138-VA13/2RA, (SV40-transformed fibroblasts) were cultured in RPMI1640 supplemented with 10% FCS + 1% (v/v) Penicillin/Streptomycin. Mouse ES129.1 monochromosomal cell hybrid ESmar10 cells were cultured in DMEM with 12% heat-inactivated FCS (v/v) and 1000 units/ml leukemic inhibitory factor, 0.1 mM β -mercaptoethanol, non-essential amino acids and 100 μ g/ml Zeocin (Chueh et al., 2005; Thompson et al., 2012; Wong et al., 2005).

3.2.2 Antibodies and inhibitors

Primary antibodies used were rabbit antibodies against ATRX (H-300 Santa Cruz), H3.3 (96C10, Millipore), H3.3 Serine 31ph (Abcam; Active Motif), CHK1 Ser317 (D12H3, Cell Signalling Technology), CHK2 Thr68 (Cell Signalling Technology), CHK1 (2G1D2, Novus Biologicals) and CHK2 (clone 7, Millipore); mouse monoclonal antibodies against γ H2AX Ser139 (Millipore) and Myc-Tag (4A6, Millipore); rat monoclonal antibody against β -Tubulin (Abcam) and human anti centromere CREST serum.

For secondary antibodies used in immunofluorescence analysis, Alexa Fluor 488 donkey anti-rabbit IgG, Alexa Fluor 488 donkey anti-mouse IgG, Alexa Fluor 594 donkey anti-rabbit IgG, Alexa Fluor 594 donkey anti-mouse IgG, Alexa Fluor 594 goat anti-human IgG (Molecular Probes, Life Technologies) were used at a final concentration of 2 μ g/mL. For immunoblotting, goat anti-mouse IgG (H+L) HRP and goat anti-rat IgG HRP was used at a dilution of 1:5000; goat anti-rabbit IgG (H+L) (Life Technologies) was used at a dilution of 1:20,000.

CHK1 inhibitor UCN-01 and SB218078 (Millipore) was used at a concentration of 1 μ M and 5 μ M respectively. For cell counting at G1 phase, cells were blocked with 2.5 mM of thymidine.

3.2.3 Cell-cycle analysis

Cells were arrested with 9 μM of RO-3306 (Sigma-Aldrich) for 17 h prior to release from the G2/M block by washing 3 times in PBS. For FACS analysis, cells were harvested, washed in ice-cold PBS and blocked in 1% BSA (w/v) before fixing in absolute ethanol overnight. Cells were spun and resuspended in 1% BSA (w/v) in PBS. The cell pellet was collected by centrifugation before washing with ice-cold PBS. Cell population was stained with Propidium iodide (50 $\mu\text{g}/\text{mL}$) and RNase (10 $\mu\text{g}/\text{mL}$) in PBS and analyzed on a FACS Calibur Analyzer (BD Biosciences) with ModFit software (Verity).

3.2.4 RNAi transfection and quantitative RT-PCR

Small interfering RNA (siRNA) oligonucleotides specific to CHK1 and ATRX protein (Table 3.1) were transfected using the Lipofectamine 3000 (Invitrogen). A set of low-GC rich Scramble RNAi oligos was used as a control for all experiments. Briefly, cells were trypsinised and plated out in media without the addition of Penicillin/Streptomycin. The lipid and DNA complex was prepared in Optimem-I solution at a ratio of 2:1. The final concentration of the RNAi used was 100 nM. After 48 h of transfection with CHK1 siRNA, the RNA was prepared according to the manufacturer's protocol (Roche) and treated with DNase using the Promega RQ1 reagent (Promega). cDNA was synthesised with oligo d(T)₁₅ (Promega) using the cDNA Reverse Transcriptase kit (Life Technologies). The cDNA amount equivalent to 7.5 ng of RNA was amplified with 250 nM of primers and quantitated with the FastStart DNA Green Sybr using the LightCycler (Roche). All data analyses were calculated using the comparative cycle threshold method (C_T). The ΔC_T was calculated by subtracting from the average C_T values of the

housekeeping gene β -Actin. The difference in the CHK1 mRNA level was expressed as $2^{-\Delta\Delta CT}$.

Table 3.1 siRNA sequence for CHK1 depletion in human ALT cancer cells

Sequence	
CHK1 siRNA oligo	5' CCC UCA UAC AUU GAU AAA UTT 3' (antisense) 5' AUU UAU CAA UGU AUG AGG GTT 3' (sense)
ATRX siRNA oligo set 1	5' GGA AGU UCC ACA AGA UAA AGA 3' (antisense) 5' UUU AUC UUG UGG AAC UUC CUG 3' (sense)
ATRX siRNA oligo set 2	5' GAC AGA AGA UAA AGA UAA ACC 3' (antisense) 5' UUU AUC UUU AUC UUC UGU CUU 3' (sense)

Table 3.2 Primers used for CHK1 quantitative RT-PCR

Sequence	
CHK1 oligo set 1	5' GCC TGA AAG AGA CTT GTG AGA AGT TGG G 3' 5' TCC ATC ACC CTT AGA AAG CCG GAA 3'
CHK1 oligo set 2	5' GTG AGA AGT TGG GCT ATC AAT GG 3' 5' GAA CTC CAA TCC ATC ACC CTT AG 3'
Actin	5' GGC ATC CTC ACC CTG AAG TA 3' 5' GGG GTG TTG AAG GTC TCA AA 3'

3.2.5 Cell extracts and Western blot analysis

Cells were lysed in cold RIPA buffer (150 mM NaCl, 50 mM Tris-HCl at pH 7.5, 0.25% sodium deoxycholate, 0.1% NP40, 0.05% SDS, 1 mM NaF, 1mM sodium orthovanadate, and protease inhibitor) with Benzonase at a concentration of 0.05 units/ul (Sigma), followed by a 10-sec pulse sonication. The lysate was collected after a 15-min centrifugation at 12,000 rpm and boiled in SDS/PAGE sample buffer prior to SDS-PAGE and Western blotting. Unless otherwise stated, the membranes were blocked in 1% (w/v) Bovine Albumin Serum with 1% (v/v) Sheep serum for 1 h at room temperature. All proteins were detected using the Immobilon HRP substrate detection kit (Merck/Millipore); the loading control was detected with the SuperSignal West Pico Chemiluminescent HRP substrate detection kit (Thermo Scientific). The intensity of protein bands was quantitated using the Image J software. The relative protein level was expressed as a ratio to the tubulin loading control.

3.2.6 Immunofluorescence analysis

Cells were treated with Colcemid (Life Technologies) or Nocodazole (Sigma) at a final concentration of 0.1 µg/ml and 40 ng/ml, respectively, for 45 to 60 m before being harvested for immunofluorescence analysis (Chan et al., 2012; O'Sullivan et al., 2014; Thompson et al., 2012; Uren et al., 2000). Cells were subjected to hypotonic treatment in 0.075 M KCl, cytopun on slides at 1,000 rpm and incubated in KCM buffer (120 mM KCl, 20 mM NaCl, 10 mM Tris-HCl pH 7.2, 0.5 mM EDTA, 0.1% (v/v) Triton X-100). Cells were extracted with 0.5% Triton X-100 in KCM for 5 mins and blocked in KCM buffer containing 1% BSA before incubation with relevant primary and secondary antibodies at 37°C for 1 h. After each round of antibody incubation, slides were washed three times in KCM buffer. Slides were then fixed in KCM with 4% (vol/vol)

formaldehyde and mounted with Vectashield (Vector Lab) supplemented with DAPI at 250 ng/ml. Images were collected using a Zeiss Imager M2 fluorescence microscope linked to an AxioCam MRm CCD camera system. Microscopy analyses were processed using the Zen software 2011 (Carl Zeiss Microscopy).

3.2.7 Immunoprecipitation and *in vitro* kinase assay

For immunoprecipitation, cells were lysed in ice-cold lysis buffer (50 mM HEPES pH8.0, 600 mM KCl, 0.5% NP-40, 0.1 mM DTT, complete protease inhibitor, 25 mM β -glycerophosphate, 50 mM NaF, 1 mM Na_2VO_4) for 5 min, followed by brief sonication. The lysates were pre-cleared with Protein-A beads prior to incubation with antibodies against CHK1 and protein A sepharose agarose beads overnight at 4°C with constant agitation. Beads were washed 3 times in ice-cold lysis buffer and twice in *in vitro* kinase assay buffer (60 mM HEPES pH7.4, 30 mM MgCl_2 , 30 mM MnCl_2 , 12 mM DTT, 5% glycerol, protease inhibitor cocktail, 0.2 mM ATP). The immunoprecipitated CHK1 was then incubated with 1 μg of H3.3 recombinant protein in kinase buffer, with or without the presence of CHK1 inhibitor SB218078 at 30°C for 1 h. The reaction was terminated by addition of 2x SDS-PAGE sample buffer. The samples were then subjected to SDS-PAGE and Western blot analysis.

For *in vitro* kinase reaction with recombinant GST-tagged CHK1 protein (Sapphire Biosciences), 0.5 μg of recombinant kinase was incubated with 1 μg recombinant H3.1 or H3.3 protein in the presence of Magnesium/ATP cocktail (Millipore) for 1 h at 37°C. The samples were then subjected to SDS-PAGE and Western blot analysis. All proteins were detected with the SuperSignal West Pico Chemiluminescent HRP substrate detection kit (Thermo Scientific).

3.2.8 Exome sequencing of *H3F3A* and *H3F3B* genes

Genomic DNA was prepared using the Roche PCR Template Purification kit (Roche). The amplification of the PCR was performed using the Phusion High Fidelity DNA polymerase (NEB), using 100 ng of DNA. The PCR product was gel purified according to the manufacturer's instruction using the Wizard SV gel and PCR Clean-up kit (Promega). For the sub-cloning analysis of *H3F3A* exon 2 from U2OS, a poly(A) overhang was added to the blunt-end PCR product with the Taq DNA polymerase prior to its ligation into the pGEM-T Easy vector (Promega). The ligated product was transformed into DH5 α and screening was performed with the Ampicillin/X-Gal/IPTG selection. All sequencing reactions were amplified with a PCR reaction using the Big Dye 3.1 (Life Technologies). The primers for amplification and sequencing of the respective gene were shown in Table 3.3 and Table 3.4.

Table 3.3 Primers used for PCR amplification

<i>H3F3A</i> gene	
Exon 1- Exon 2	5' CCTCCATTGTGTGTGATTGG 3' 5' TTCCTGTTATCCATCTTTTTGTT 3'
Exon 2 – Exon 3	5' GATTTTGGGTAGACGTAATCTTCA 3' 5' TGCAGCATCCATAAACCAAA 3'
Exon 4	5' GCATCTTGCCCAGTCATTTT 3' 5' CACGTCTCAGATATAAAGTGAC 3'

<i>H3F3B</i> gene	
Exon 1 – Exon 3	5' GGTTCATGACGCAGAGACG 3' 5' CCCTCCCCTAATGACTCAGG 3'
Exon 2 – Exon 4a	5' CTTATCTTCGGGGCGTCTTT3' 5' CCTTGAAAAAGCCACATTC3'
Exon 4b – Exon 4c	5' ACCATCATGCCCAAAGACAT 3' 5' CTGGCTCTCATGCTGTCTCA 3'
Exon 4d – Exon 4e	5' TGAGACAGCATGAGAGCCAG 3' 5' CCAGATGAATCAGAAGTCAGTG 3'

Table 3.4 Primers for sequencing *H3F3A* and *H3F3B* alleles

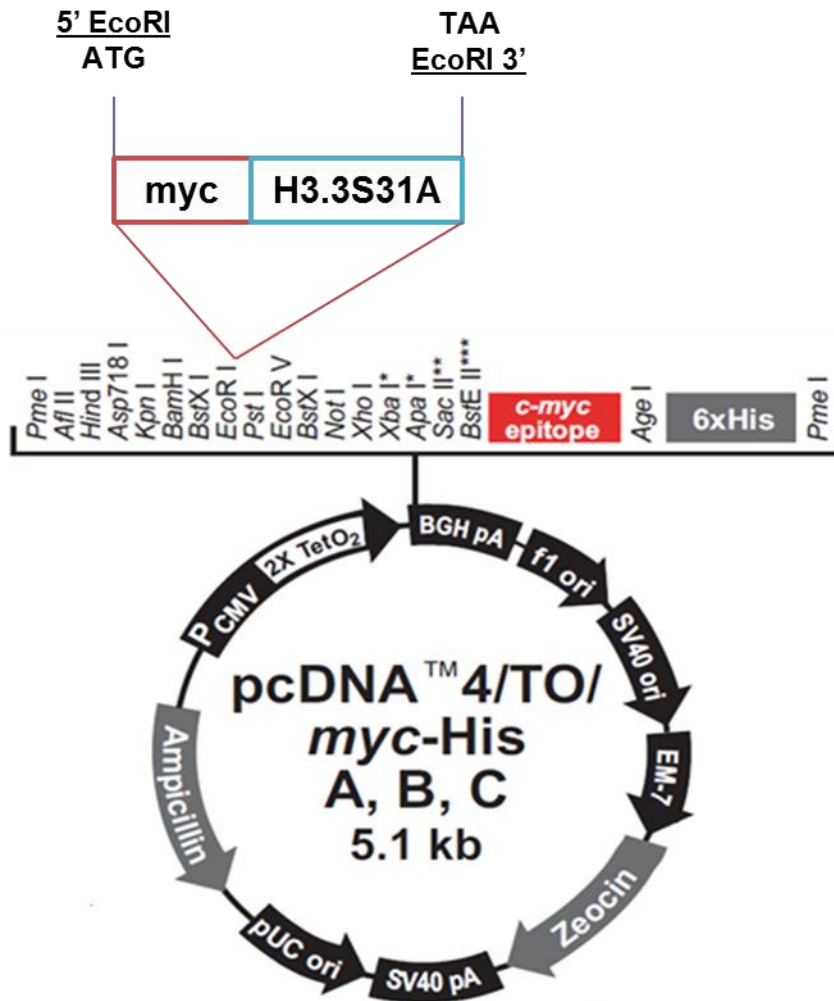
<i>H3F3A</i> gene	
Exon 1 – Exon 2	5' CCAGAGGGAACAGGGAAACT 3'
	5' GATTTTGGGTAGACGTAATCTTCA 3'
Exon 2 – Exon 3	5' TTTCTTTGAAGCTGCCCACT 3'
Exon 4	5' GCATCTTGCCCAGTCATTTT 3'
	5' TACCTTTTGACCCCATGGAA 3'
	5' TTGCGAGTGGAAAAATAGGG 3'
	5' CCGCTGAAACTTGTTCACTG 3'

<i>H3F3B</i> gene	
Exon 1	5' GGGTAAACCTACGAACGCCTA 3'
Exon 2 – Exon 4a	5' CTCCCTCACCAACCTCTG 3'
	5' ATGTCTTTGGGCATGATGGT 3'
	5' ACCATCATGCCCAAAGACAT 3'
Exon 4b – Exon 4c	5' TGCGCATTTATACCTTGCAT 3'
	5' TCCACCAAACAACACCTGAA 3'
	5' GCTCTCTGCTTGATTAAGATG 3'
	5' CCTTGAAAAAGCCCACATTC 3'
Exon 4d – Exon 4e	5' CTATGCTGTAGCGTGTCTG 3'
	5' TTTCTCCTTTGCCTCTGCTC 3'
	5' CCAGATGAATCAGAAGTCAGTG 3'

3.2.9 Over-expression of pcDNA4/TO/myc HisA N-terminal myc-tagged H3.3 S31A plasmid in ALT cancer cells

The myc-tagged wild type H3.3 was cloned in the pcDNA4/TO/myc-His A vector as previously described (Wong et al., 2010). The myc-tagged H3.3S31A gene fragment was synthesized from IDT gBlock Gene Fragments with the introduction of two EcoRI restriction sites at the both 5' and 3' ends. For generation of myc-H3.3 DNA plasmid, 100 ng of the gBlock Gene fragment was first digested with EcoRI, followed by ligation into the pGEM-T Easy vector (Promega). The mycH3.3 fragment was then digested with EcoRI and subsequently, cloned into the pcDNA4/TO/myc HisA vector (Life Technologies). The ligation reaction was performed at 25°C for 3 h with T4 DNA ligase according to the manufacturer's instruction (NEB). These plasmids were transformed into DH5 α and plated out under the selection of ampicillin (100 μ g/mL) at 37°C overnight. The positive bacterial clones carrying pcDNA4-myc-H3.3S31A were screened by performing NheI and ScaI restriction digest analysis. The positive clones were then further validated by sequencing analysis using the BDT BigDye 3.1 (Life Technologies) with the respective primers, *H3F3A* exon 2-4 forward 5' ATGGCTCGTACAAAGCAGAC 3' or *H3F3A* exon 2-4 reverse 5' TGTCTTCAAAAAGGCCAACC 3', in a PCR reaction. The PCR products from the sequencing reactions were sent to Micromon Sequencing Facility at Monash University, Clayton (Supplementary Figure 2) for sequence analysis. For each transfection reaction in a 12-well plate, 0.4 μ g of plasmid DNA were transfected using the Lipofectamine 3000 (Invitrogen). Briefly, cells were trypsinized and washed before plating out in RPMI media supplemented with 10% heat-inactivated FBS without the addition of Penicillin/Streptomycin. The lipid-DNA complex was prepared in Optimem-I solution at a ratio of 3:1 according to the manufacturer's protocol. Cells were re-transfected with the

plasmid (in a similar manner) after 48 h to ensure a longer period of expression of gene of interest and were harvested for analysis 48h after the second transfection.



3.3 Results

3.3.1 ALT cancer cells show intense and aberrant H3.3S31ph staining on chromosome arms at mitosis

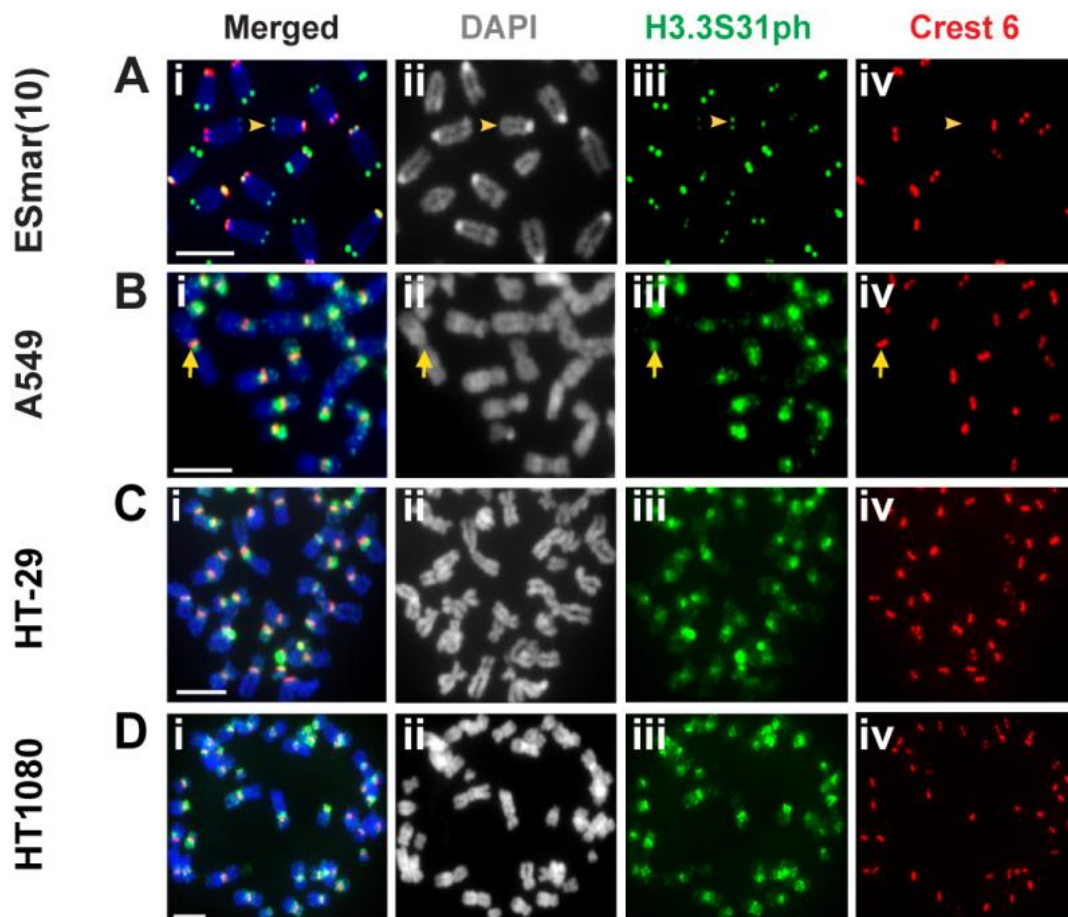
Considering the importance of ATRX/DAXX in H3.3 deposition and maintenance of heterochromatin at telomeres, it is not surprising that ALT cancer cells show severe telomere chromatin dysfunction in the absence of the ATRX protein. However, little is known on how the loss of ATRX could impact on H3.3 deposition and PTM profile in ALT cells. To investigate this, the distribution of H3.3S31ph was first examined in ALT cancer cell lines, as H3.3S31ph has been shown to serve as a reliable marker for heterochromatin in mammalian cells (Hake et al., 2005; Wong et al., 2009). Immunofluorescence analysis was performed using an antibody specific for H3.3S31ph. In telomerase-positive mouse ES cells show H3.3S31ph enrichment at telomeres of metaphase chromosomes (Wong et al., 2010; Wong et al., 2009) (Figure 3.1 A), whereas human telomerase-positive A549 lung adenocarcinoma cells (Figure 3.1 B), HT29 cells and HT1080 cells (Figure 3.1 C-D) display H3.3S31ph staining at pericentric satellite DNA repeats. In contrast, all ALT cancer cell lines with the exception of SKLU1 cells showed strong H3.3S31ph staining - not only on pericentric regions but also along the entire chromosome arms (Figure 3.2). Immunofluorescence images of GM847 cells were also taken with a lower exposure time period to show that level of H3.3S31ph at pericentric DNA repeats are higher than those on chromosome arms (Figure 3.2I; this differential enrichment in H3.3S31ph staining is detectable by reducing the H3.3S31ph image acquisition time by 4 fold).

The specificity of this H3.3 Serine 31ph antibody had previously been validated by peptide competition using immunofluorescence assay. In A549 cells, the H3.3 S31ph

signal was at the pericentric region was removed when the antibody was co-incubated with a H3.3 Serine 31 peptide for 30 min before its application on immunostaining (Figure 3.3 A-B). The high level of H3.3 S31ph staining on chromosome arms was not observed in the ALT cancer cell line W138-VA13/2RA when 100 ng of peptide was used (Figure 3.3 D-E). At a lower peptide concentration, the H3.3S31ph signal at the pericentric heterochromatin in A549 cells and on chromosome arms in the ALT positive cancer cells was detected, however the labeling intensity was lower compared to control cells without the presence of the H3.3S31ph peptide.

Figure 3.1 Localisation of H3.3S31ph at heterochromatic regions in non-ALT cancer cell lines

Immunofluorescence analysis was performed using antibodies against H3.3S31ph (green) and centromeres (human Crest antibody; red). **(A)** H3.3S31ph localized at the telomeric region in mouse ESmar10 cells (*arrowhead*). **(B-D)** In telomerase positive A549, HT-29 and HT1080 cells, H3.3S31ph was enriched at the pericentric heterochromatin (*arrow*). No enrichment was observed on chromosome arms. Representative images of 50 chromosome spreads are shown. Scale bar = 5 μ m.

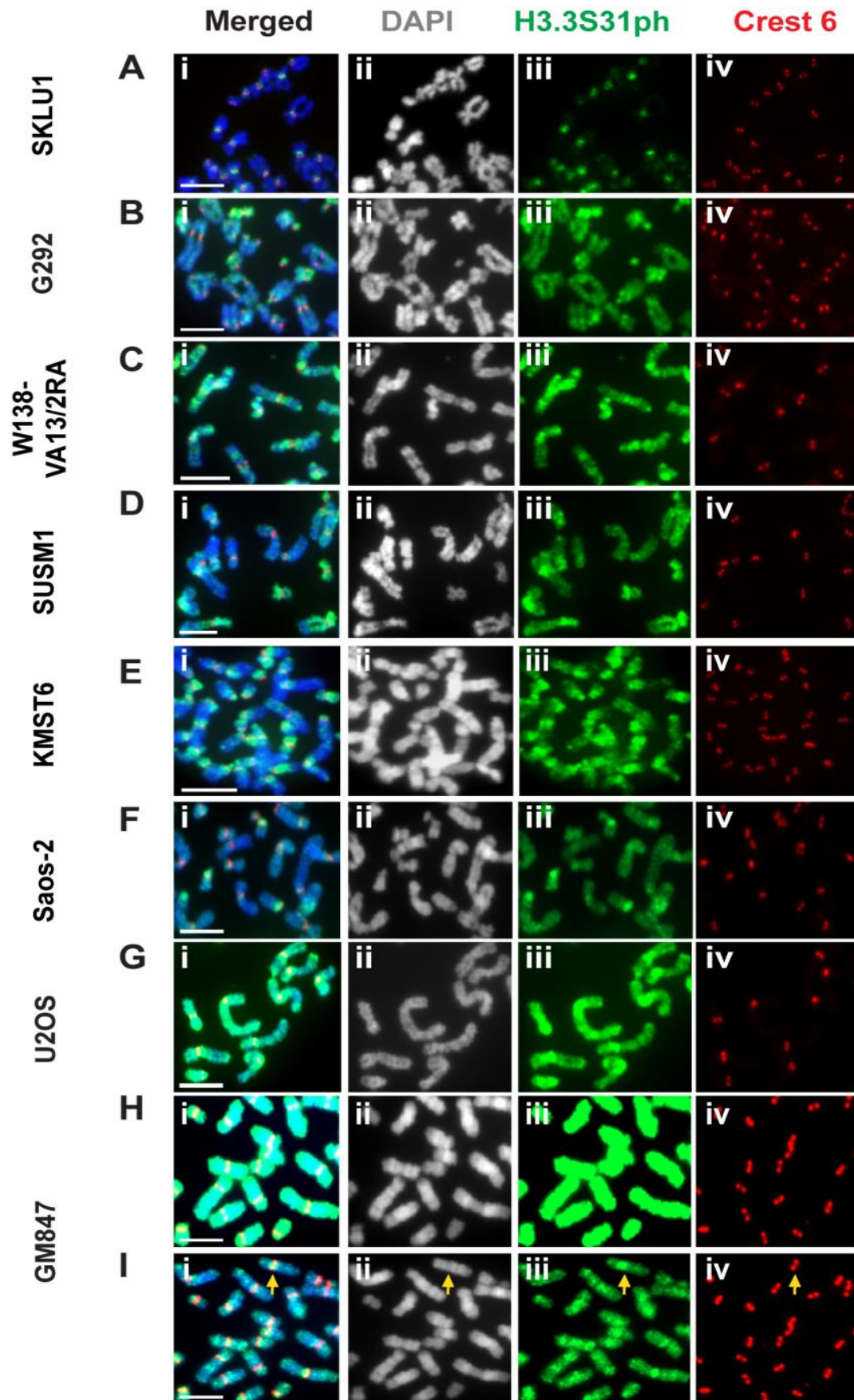


Page intentionally left blank

Page intentionally left blank

Figure 3.2 Aberrant localization of H3.3 S31ph on chromosome arms in ALT cancer cells

(A) In ALT positive SKLU1 cells, H3.3S31ph was enriched at the pericentric heterochromatin. No staining was observed on chromosome arms. (B) In ATRX-positive G292 human ALT cells, H3.3S31ph localized at both pericentric and across arm regions. (C-G) In human SV40 transformed fibroblast ALT cancer cells, W138-VA13/2RA, SUSM1, KMST6 cells and osteosarcoma ALT cancer cells Saos2 and U2OS, H3.3S31ph was found at extremely high level at both the pericentric satellite repeats and chromosome arms. (H-I) In GM847 human SV40 transformed fibroblast ALT cancer cells, a high level of H3.3S31ph was also detected on the pericentric repeats and chromosome arms. A lower exposure (I) indicated a slightly higher intensity of H3.3S31ph at the pericentric repeats (*arrow*). Representative images of 50 chromosome spreads are shown. Scale bar = 5 μ m.

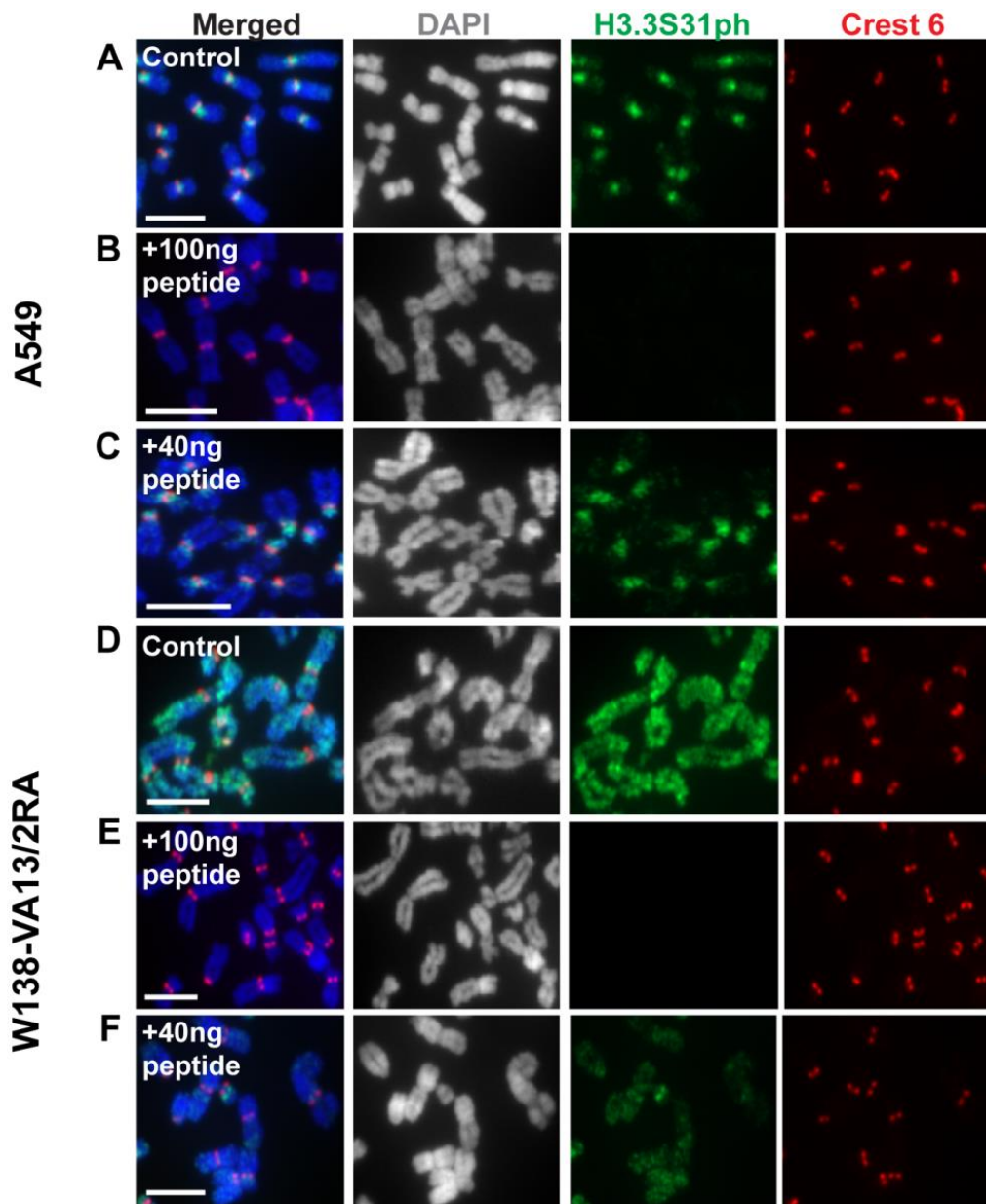


Page intentionally left blank

Page intentionally left blank

Figure 3.3 Specificity of the H3.3 Serine 31 ph antibody staining

The specificity of the H3.3S31ph antibody (green) was determined by co-incubating an H3.3 Serine 31 specific peptide with the antibody for 30 m before immunofluorescence analysis was performed. The centromeres were stained with Human Crest 6 antibody (red). **(A)** In A549 cells, H3.3S31ph was found at the pericentric region. **(B)** In the presence of a high concentration of the H3.3 Serine 31 peptide (100 ng), H3.3S31ph staining was not detectable. **(C)** The pericentric staining of H3.3S31ph was restored when a lesser concentration of the H3.3 Serine 31 peptide was used (40 ng). **(D-E)** Similarly, the high level of H3.3S31ph staining on chromosome arms in ALT positive W138-VA13/2RA cells was not observed when a 100 ng of the H3.3 Serine 31 peptide was used. **(F)** At a lesser peptide concentration, the staining of H3.3S31ph on the chromosome arms was detected, albeit at a lower intensity compared to the control. Representative images of 50 chromosome spreads were shown. Scale bar =5 μ m.



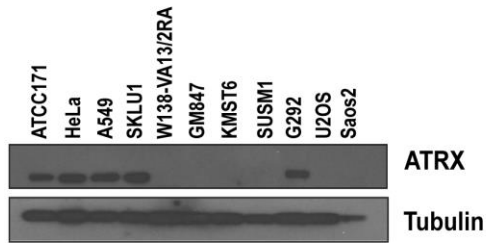
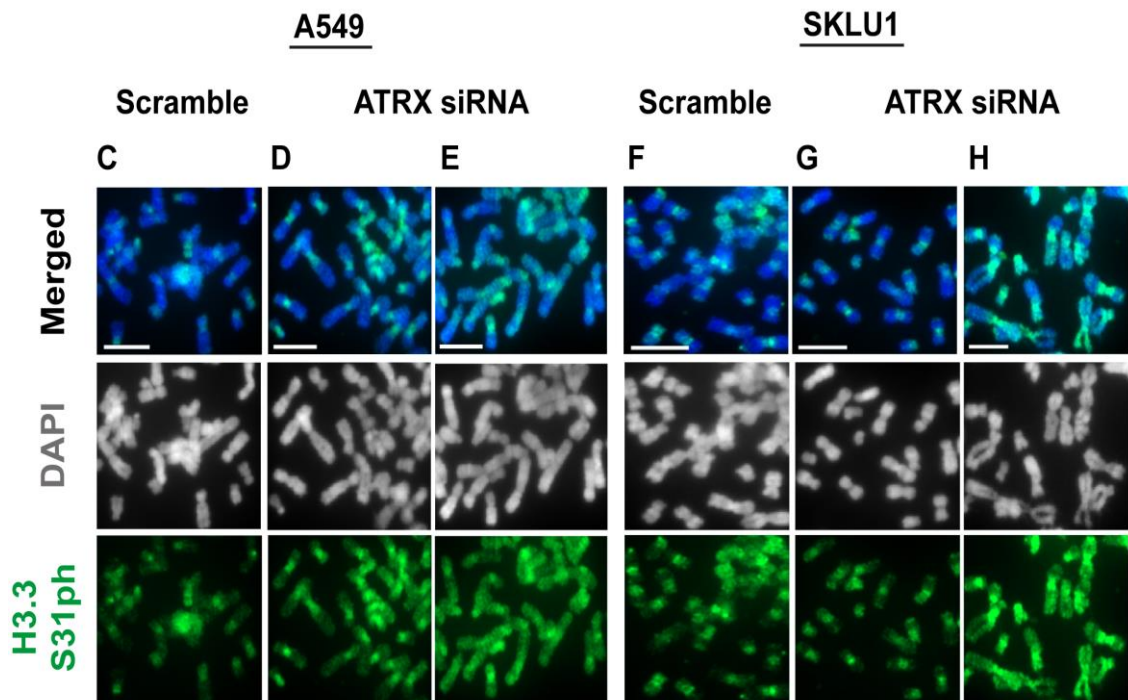
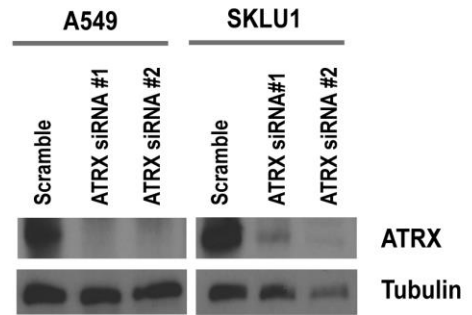
Page intentionally left blank

3.3.2 Loss of ATRX function does partially contribute to the aberrant H3.3S31ph staining on chromosome arms in ALT cancer cells

To our knowledge, these high level and aberrant distribution of H3.3S31ph on chromosome arms has not been previously described. We therefore hypothesize that it could serve as a hallmark of cancer cells that utilize the ALT pathway. To explore this, we extended our analyses to other ALT cell lines and determined whether aberrant H3.3S31ph staining correlated with loss of ATRX expression (Figure 3.4A). Among the ALT cell lines tested, all show high levels and spreading of H3.3S31ph on chromosome arms except for SKLU1 cells. A previous study had shown that SKLU1 ALT cell line showed a normal expression and cellular distribution of ATRX (Lovejoy et al., 2012). Although a positive ATRX protein band was also detected in G292 (Figure 3.4A), our immunostaining analysis showed an abnormal ATRX staining pattern in the G292 cells (data not shown), thus, in line with a previous study that showed that ATRX was defective in function in G292 cells (Lovejoy et al., 2012). To examine the role of the ATRX function and the aberrant H3.3S31ph distribution, the ATRX was depleted by siRNA for 48 h in both A549 and SKLU1 cells that have a normal pericentric localization of H3.3 S31ph. Following the loss of the ATRX protein, an increase labeling of H3.3S31ph was detected on chromosome arms in both cell lines (Figure 3.4 D-E, G-H). Nevertheless, the extent of this staining was less intense compared to ATRX null ALT cancer cells. This suggests the loss of ATRX is unlikely to be the sole factor that drives the intense H3.3 S31ph staining on chromosome arms.

Figure 3.4 Loss of ATRX expression correlates with the altered H3.3S31ph staining on chromosome arms in human ALT cancer cell lines.

(A) Cell lysates were prepared from ALT positive and negative cell lines and the ATRX expression was examined by immunoblotting. The ATRX protein was lost in all ALT cell lines, with the exception of SKLU1 and G292. Immunofluorescence analysis on the distribution of H3.3S31ph (green) was examined on ATRX siRNA transfected non-ALT A549 cells and ALT cancer SKLU1 cells after 48 h. In both A549 and SKLU1 transfected control cells, H3.3S31ph was found at the pericentric DNA repeats (**B, E**). After 48 h of ATRX depletion with siRNA depletion, the pericentric enrichment of H3.3S31ph labeling remained prominent in the majority of the chromosome spreads (**C,F**); however, there was also a slight increase (~2 fold) in the staining of H3.3S31ph on the chromosome arms (**D,G**). Representative image from 50 chromosome spreads. Scale bar =5 μ m.

A**B**

Page intentionally left blank

3.3.3 The altered H3.3 S31 phosphorylation staining pattern in ALT cancer cells is not caused by any underlying mutation in the H3.3 alleles or a differential expression of H3.3 at the protein level

Recently, the heterozygous mutation on Lysine 27 residue of *H3F3A*, the genes which encodes for H3.3, has been shown to result in a global reduction of the methylation state of this residue in glioblastoma (Lewis et al., 2013). Likewise, the aberrations on the H3.3 genes, particularly at the Serine 31 residue can also promote the altered phosphorylation dynamics in ALT cancer cells. The H3.3 protein is encoded by two different genes: *H3F3A* and *H3F3B*. Each of these genes consists of four exons, with the coding region located between exon 2 and exon 4. To examine this, primers were designed to amplify each of these four exons from the intronic regions and were subjected to sequencing analysis using internal primers. In all ALT cancer cell lines, no mutation at the Serine 31 residue on both *H3F3A* and *H3F3B* alleles was observed (Figure 3.5 A-B examples of sequencing chromatograms from Saos-2 and G292 cell lines). However, an aberration between the Glycine 34 and Valine 35 on the *H3F3A* allele was detected only in U2-OS cells (Figure 3.5C). To further investigate this, the PCR product corresponding to this region was amplified from the U2-OS cell line and was sub-cloned into a pGEM-T Easy vector for further sequencing analysis. From the six clones that were selected for analysis, the frequency of this abnormality was 33% (Figure 3.5D). This included a specific insertion of a Phenylalanine amino acid after Glycine 34, and a single base pair substitution which replaced the Valine on the residue 35 to Leucine. Nevertheless, this mutation has no effect on the expression of the H3.3 protein in the U2-OS cell line (Figure 3.6A).

Next, we also examined the overall H3.3 protein level in the ALT positive cells by immunoblotting analysis. As expected, no significant difference in the protein level was

observed between the ALT positive and negative cells in either the asynchronous or the mitotic enriched population (Figure 3.6 A-B). Furthermore, the pericentric localisation of the H3.3 Serine 31 phosphorylation does not alter following the over-expression of the myc-tagged H3.3 protein in non-ALT HeLa cells (Figure 3.6 D-E). In addition, there was no increase in the intensity of H3.3 S31ph on chromosome arms when the myc-tagged H3.3 protein was over-expressed in ALT positive U2OS and W138-VA13/2RA cancer cells (Figure 3.6 F-I). This indicates that the abundance of S31 phosphorylation on chromosome arms is unlikely due to an increase in H3.3 expression levels in the ALT cells. Together, our data show that in ALT cancer cells, H3.3S31ph is up-regulated and re-distributed; however, this re-distribution is not correlated with any underlying mutation at the Serine 31 position or an over-expression of H3.3 in these cells.

Page intentionally left blank

Figure 3.5 Exome sequencing of *H3F3A* allele for ALT cancer cells

The protein translation of the histone H3.3 is shown. The Serine 31 residue is located on the exon 2 of the *H3F3A* allele (underlined). **(B-D)** The chromatograms correspond to the positions between Lysine 27 and Lysine 36. No mutation was observed on the sequence surrounding Serine 31 residue (red box) in the ALT positive human osteosarcoma cell lines including Saos-2, G292 or the U2OS cells. **(D)** In the U2-OS cell line, aberrations were detected the sequence after the Glycine 34 residue (Blue box). **(E-F)** When the PCR product for this region was sub-cloned into the pGEM-T Easy vector for further sequencing analysis, a 3 base pair insertion and a substitution after position 34 was observed in 2 out of 6 the clones being selected.

A)

```
ATGGCTCGTACAAGCAGACTGCCCGCAAATCGACCGGTGTAAGCACCAGGAAGCAA
M A R T K Q T A R K S T G G K A P R K Q

CTGGCTACAAAAGCCGCTCGAAGAGTGGCCCTCTACTGGAGGGTGAAGAACTCAT
L A T K A A R K S A P S T G G V K K P H

CGTTACAGGCTGTACTGTGGCCCTCCGTGAAATAGACGTTATCAGAAGTCCACTGAA
R Y R P G T V A L R E I R R Y Q K S T E

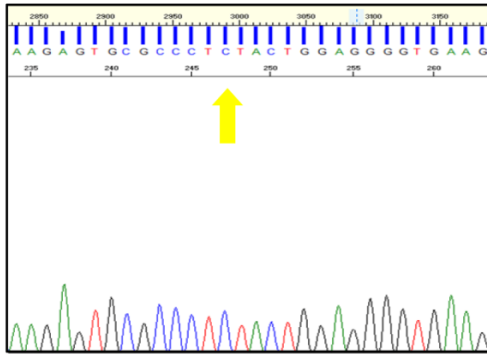
CTTCTGATTGCAAACTCCCTTCCAGCGTCTGGTGCAGAAATGCTCAGGACTTTAAA
L L I R K L P F Q R L V R E I A Q D F K

ACAGATCTGGCTTCCAGAGCGCAGCTATCGTGTCTTTCAGGAGGCAAGTGAGGCCTAT
T D L R F Q S A A I G A L Q E A S E A Y

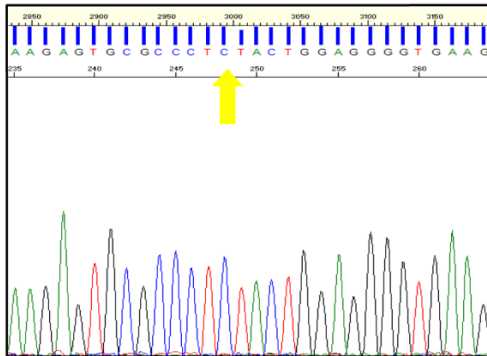
CTGGTTGCCCTTTTGAAGACCAACCTGTGTCTATCCATGCCAAACGTAAACAATT
L V G L F E D T N L C A I H A K R V T I

ATGCCAAAAGACATCCAGCTAGCACGCCGATACGTGGAGAACGTGCTTAA
M P K D I Q L A R R I R G E R A -
```

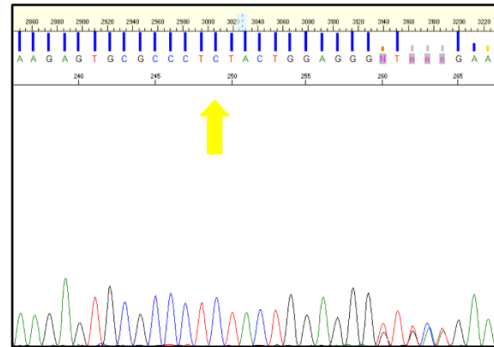
B) Saos2



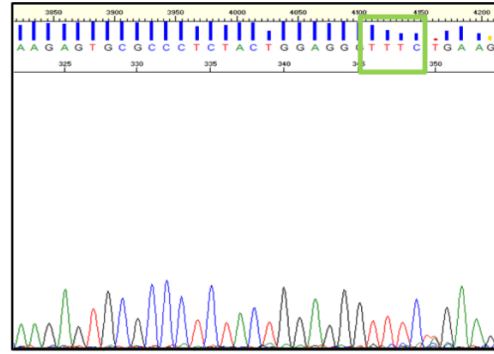
C) G292



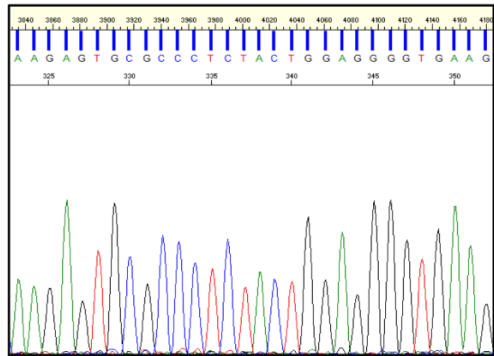
D) U2OS



E) U2OS with insertion



F) U2OS without insertion

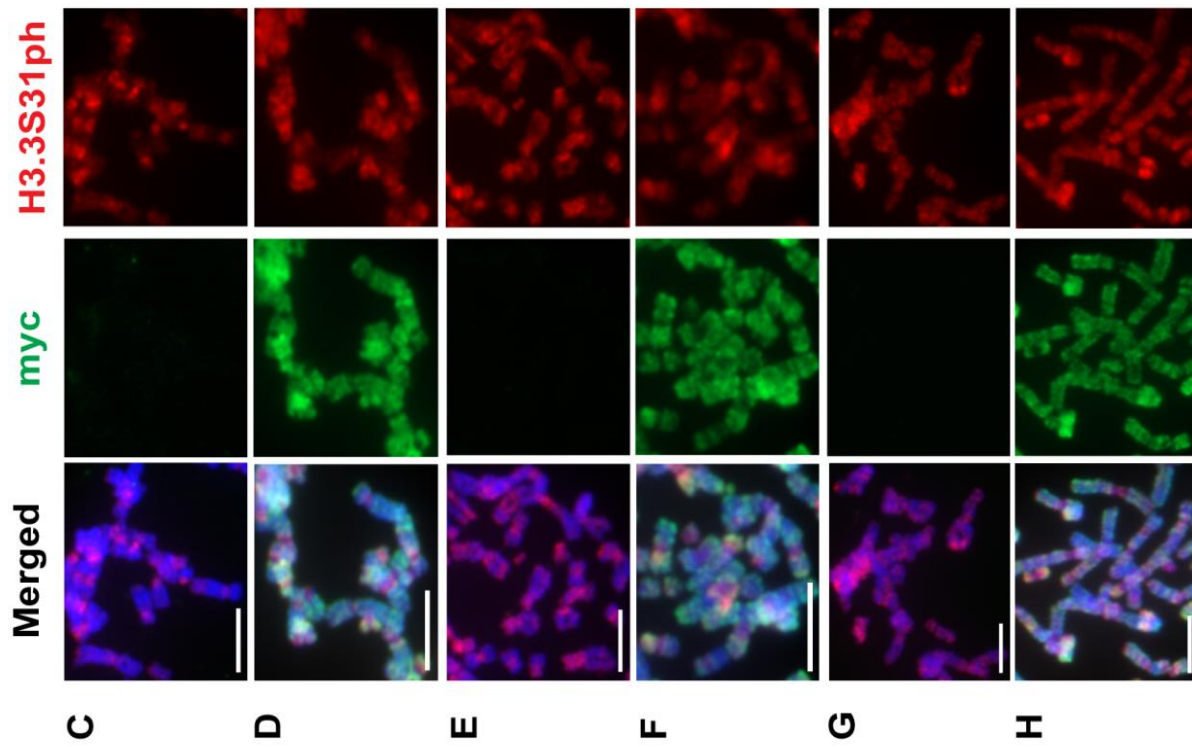


Page intentionally left blank

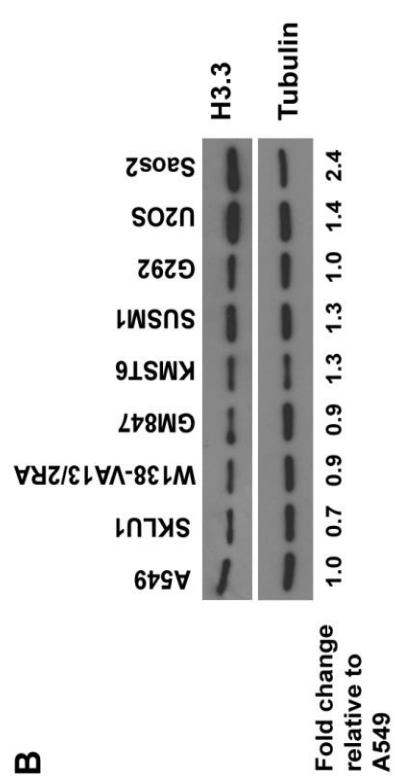
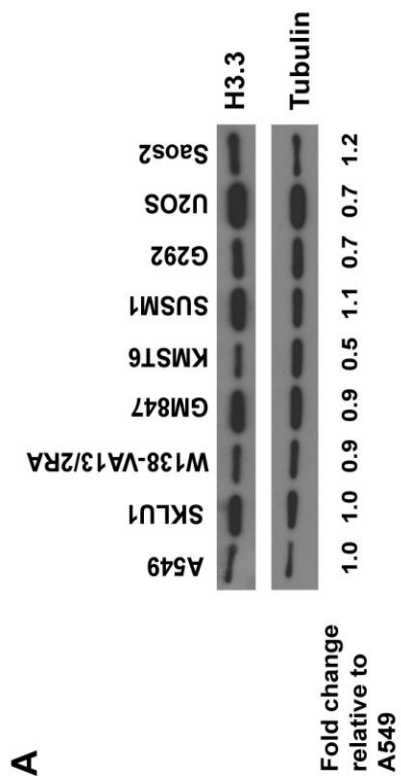
Page intentionally left blank

Figure 3.6 No association between H3.3 expression and altered H3.3 Serine 31ph dynamics in ALT cancer cells

(A) Lysates were prepared from asynchronous ALT positive and negative cell lines and the level of H3.3 protein was determined by immunoblotting. No significant difference in the H3.3 protein level was observed across all asynchronous cell lines examined. (B) Cells were arrested at the G2 boundary by the addition of RO-3306 for 16 h before being release into mitosis. Mitotic cells were enriched by the addition of Colcemid for 3 h. Immunoblotting with H3.3 showed no obvious difference in the level of H3.3 expression amongst ALT cells and non-ALT cell lines. Immunofluorescence analysis with antibodies against myc (green) and H3.3 S31ph (red) was performed on myc-tagged H3.3 transfected HeLa, U2OS and W139-VA13/2RA cells at 96 h following the transfection. (D) In non-ALT HeLa cells, the phosphorylation of H3.3S31 was detected at the pericentric heterochromatin (arrowhead) on mitotic chromosomes. (E) The distribution of this staining did not alter when myc-tagged H3.3 was expressed. In ALT positive U2OS cells (F-G) and W138-VA13/2RA (H-I), H3.3S31ph was found at the pericentric region and on chromosome arms. No significant increase in the level of H3.3S31ph staining on the arm regions was observed in the presence of myc-tagged H3.3 protein. Representative images of 50 chromosome spreads. Scale bar = 5µm.



HeLa U2-OS W138-VA13/2RA



Page intentionally left blank

3.3.4 A delay in mitotic progression contributes to the elevated and extensive

H3.3S31ph staining on metaphase chromosome arms in ALT cancer cells

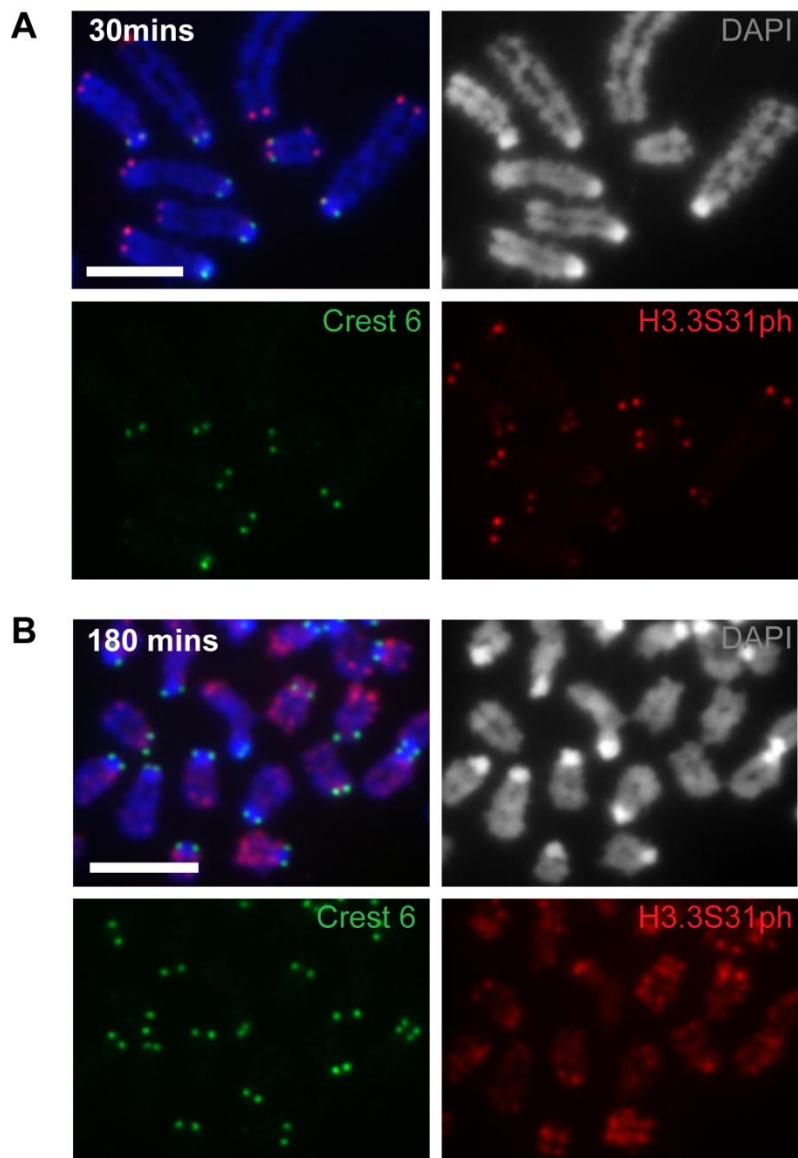
Given that H3.3S31 phosphorylation occurs during mitosis (Hake et al., 2005), it is possible that the aberrant H3.3S31ph pattern could be a result of prolonged mitotic progression in ALT cancer cells. Indeed, the de-localisation H3.3S31ph staining from the telomeres to chromosome arms was also noted when pluripotent mES cells were arrested in mitosis for 3 h by Colcemid treatment (Figure 3.7). Considering the continual presence of fragmented chromosomes and high levels of DNA damage in ALT cells (Figure 3.8), the delay in mitotic progression could lengthen the time available for a putative H3.3 kinase to promote phosphorylation of H3.3S31. In asynchronous ALT cancer cell populations, the FACS analysis revealed a higher percentage of G2/M cells (mitotic index) in both U2OS and GM847 ALT cancer cells compared to the ALT negative A549 cells (24% versus 15%; Figure 3.9A). To examine the kinetics of mitotic progression of ALT cells, A549, U2OS and GM847 cells were blocked at G2 by 17 h treatment with RO-3306 (a CDK1 inhibitor widely used to synchronize cells in G2/M phase (Vassilev et al., 2006)), followed by a release into mitosis and G1 phase. Upon release from G2/M arrest, the majority of A549 cells progressed through mitosis into G1 within 2 to 3 h, whereas U2OS and GM847 only exited mitosis 5 h after release from G2/M (Figure 3.9B). These data show that ALT cell lines suffer a marked delay in mitotic progression.

To examine whether this prolonged progression through mitosis contributed to the aberrant H3.3S31ph staining in ALT cells, cells were synchronized at the G2/M boundary with RO-3306. This was followed by a release and blocked at mitosis for different time periods with the presence of Colcemid. In A549 cells, the majority of the mitotic chromosome spreads showed specific staining of H3.3S31ph at pericentric satellite repeats after 15 min of Colcemid treatment upon G2/M release (Figure 3.9C).

After 2 h of Colcemid treatment, no significant increase in H3.3S31ph on pericentric regions or chromosome arms of A549 cells was detected (Figure 3.9D). In contrast, U2OS cells showed an intensive H3.3S31ph staining on both pericentric repeats and chromosome arms as early as 15 min after release from G2/M arrest (Figure 3.9E). Moreover, after 2 h in Colcemid, we noted a further increase in H3.3S31ph staining intensity on chromosome arms, and in the proportion of mitotic spreads (increased by 25%) with H3.3S31ph staining on chromosome arms (Figure 3.9F). These data suggest that a prolonged mitotic period may contribute to the increased intensity of H3.3S31ph on chromosome arms in these ALT cell lines; however, it is unlikely to be the primary cause for aberrant H3.3S31ph distribution in these cells. Consistent with this line of argumentation is the absence of high level of H3.3S31ph on chromosome arms in A549 cells even after 2 h of mitotic arrest (Figure 3.9D). Furthermore, the extensive H3.3S31ph signals observed on the arm regions in ALT cells even at the early stage of mitosis indicated that ALT cell mitotic chromosomes are subjected to rapid phosphorylation at H3.3S31 upon their entry into mitosis. Thus, it is likely that other factor(s) contributed to the aberrant H3.3S31 phosphorylation pattern in these ALT cancer cells.

Figure 3.7 Prolonged mitotic progression led to the de-localization of H3.3S31ph on chromosome arms in pluripotent mES cells

Immunofluorescence analysis with antibodies against CREST 6 (green) and H3.3S31ph (red) was performed on ES129.1 cells. (A) H3.3S31ph is only enriched at the telomeric region when cells were treated with Colcemid for 30 mins. No enrichment of H3.3S31ph on chromosome arms was observed. (B) When ESmar(10) cells were arrested for 3 h with Colcemid treatment, H3.3S31ph staining was detected at the telomeres and on chromosome arms. Representative images of 50 chromosome spreads were shown. Scale bar = 5 μ m.

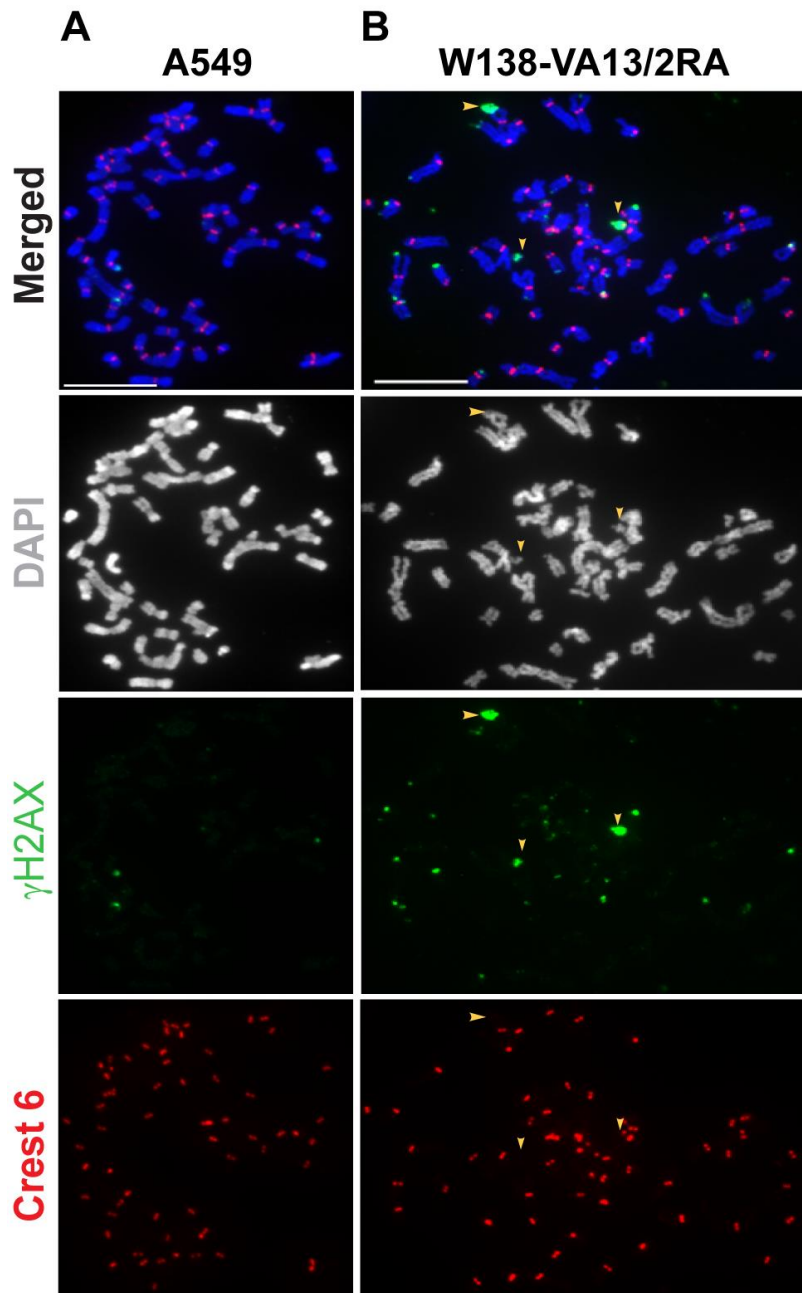


Page intentionally left blank

Page intentionally left blank

Figure 3.8 Human ALT cancer cell lines are burdened with severe genome instability.

(A) Immunofluorescence analysis was performed using antibodies against γ H2AX (marker of DNA damage; green) and centromeres (human CREST antiserum; red). (A) In ALT negative A549 cells, low levels of DNA damage mainly localized at the telomeres were observed. (B) In contrast, ALT positive W138-VA13/2RA cells showed increased staining of γ H2AX not only at telomeres, but also on fragmented DNA (arrowheads). Representative images of 50 chromosome spreads were shown. Scale bar = 10 μ m.

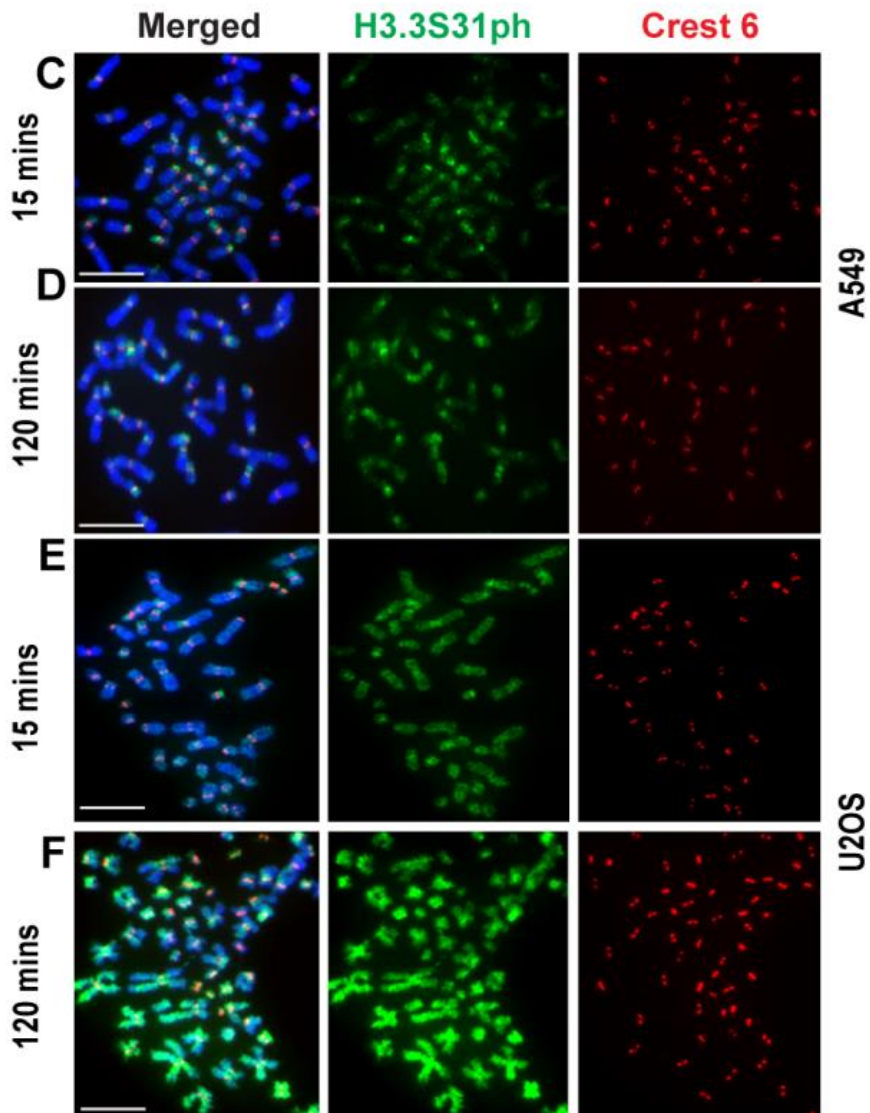
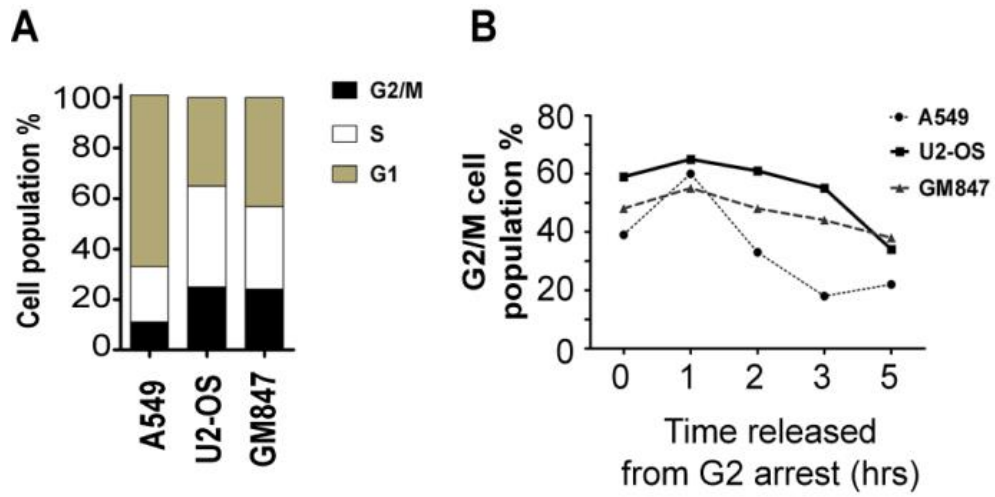


Page intentionally left blank

Page intentionally left blank

Figure 3.9 Association of prolonged mitotic progression with aberrant H3.3S31ph staining pattern in ALT cancer cell lines.

A) FACS analysis was performed to determine the cell-cycle profiles of A549, U2OS and GM847. The ALT cancer cell lines U2OS and GM847 showed higher percentages of G2/M cell population when compared to non-ALT A549 cells (24% versus 15%). **(B)** Human A549, U2OS and GM847 cells were arrested at G2/M boundary by treatment with RO-3306. FACS analysis was performed on these cells following their release into mitosis and G1. In A549, most cells exited mitosis by 3 h post release into mitosis. In contrast, U2OS and GM847 only exited mitosis 5 h post-release; at 3 h post-release, 45-55% of cells still remained at mitosis. Representative graphs of two independent experiments are shown. **(C-G)** Immunofluorescence analysis was performed on A549 and U2OS cells released from G2 arrest and subjected to subsequent Colcemid treatment (either 15 min or 2 h treatment). In A549 cells (C-D) subjected to Colcemid mitotic arrest, H3.3S31ph was enriched at pericentric DNA repeats, with no staining on chromosome arms. An additional 2 h mitotic arrest did not lead to significant increase in H3.3S31ph staining. In contrast, U2OS (F) ALT cancer cells showed high levels of H3.3S31ph staining at both the pericentric repeats and chromosome arms, even with only 15 min of Colcemid treatment. There was a further increase with the staining at chromosome arms after 2 h of mitotic arrest with Colcemid treatment (G). Representative images of 50 chromosome spreads are shown. Scale bar =10 μ m.



Page intentionally left blank

3.3.5 Up-regulated CHK1 kinase activity drives H3.3S31 phosphorylation in ALT cancer cells

As the level of H3.3 was unchanged, another attractive hypothesis is that an altered protein kinase activity could account for the aberrant H3.3S31ph level in ALT cancer cells. Unlike other canonical H3 residues, the kinase that promotes the phosphorylation of H3.3S31 remains unknown. The Checkpoint protein 1 (CHK1) is a serine/threonine kinase involved in DDR signalling. It has previously been shown to phosphorylate Ser10 and Threonine 11 on canonical H3 histone (Liokatis et al., 2012; Shimada et al., 2008). Considering the high levels of DNA damage and the elevated DDR signalling in ALT cancer cells (Lovejoy et al., 2012), CHK1 could be a candidate that drives the aberrant H3.3S31 phosphorylation in ALT cancer cells. From the Western blot analysis using an antibody against CHK1 Ser317 phosphorylation, a higher level of activated CHK1 was detected in ALT cells compared to non-ALT A549 cells even in the absence of an external DNA damaging insult (Figure 3.10A, supplementary table 1). This result is in agreement with increased CHK2 Thr68 phosphorylation (a mark of DDR signalling) in ALT cells (Figure 3.10A, supplementary table 2; see also (Lovejoy et al., 2012)). It is important to note that although ALT cells showed significantly elevated CHK1 and CHK2 activation, which is likely as a response to persistent DNA damage and genomic instability (Lovejoy et al., 2012). However, despite the increases in activities, these cell lines did not show elevated levels of total CHK1 and CHK2 (Figure 3.10B).

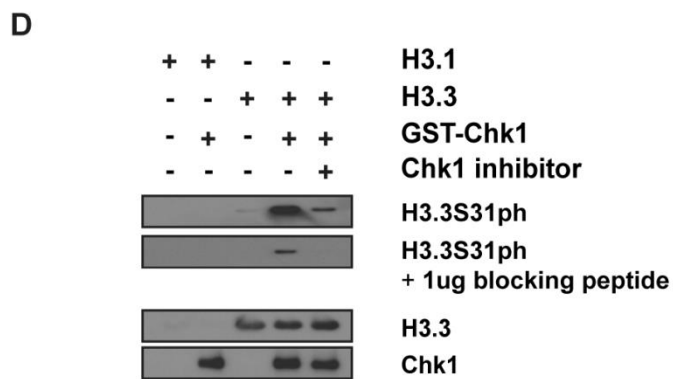
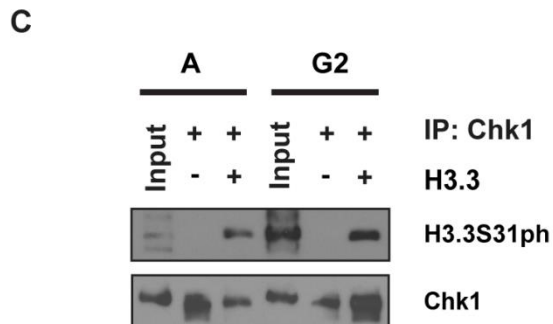
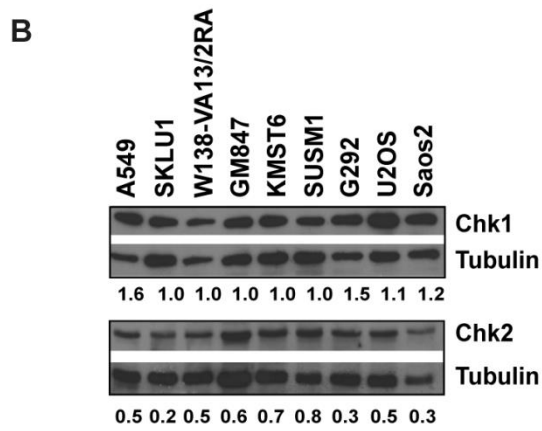
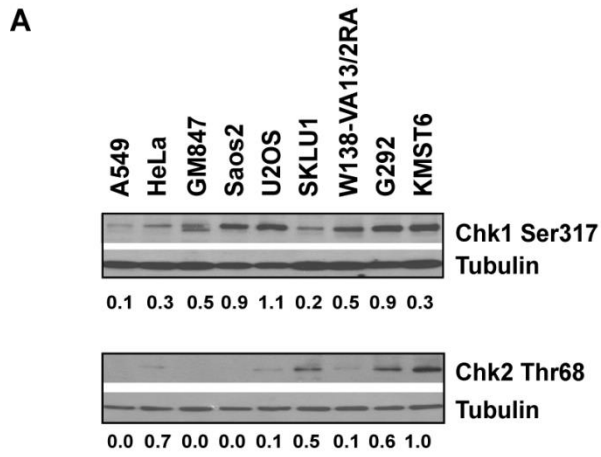
To determine the involvement of CHK1 in the phosphorylation of H3.3S31, endogenous CHK1 protein was purified from both asynchronous and from mitotic U2OS cell populations for *in vitro* kinase assays. The immunoprecipitated CHK1 was incubated with recombinant H3.3 in the presence of ATP and under a kinase assay condition. The phosphorylation of H3.3S31 by the immunoprecipitated CHK1 was examined by

Western blotting. The kinase reaction yielded a clear H3.3Ser31ph product, indicating that CHK1 activity can phosphorylate H3.3S31 *in vitro* (Figure 3.10C). The *in vitro* kinase assay was also performed using recombinant GST-tagged CHK1 protein which also resulted in a strong 17kDa H3.3S31ph product (Figure 3.10D lane 4). The intensity of the H3.3S31ph product was reduced when the immunoblot was co-incubated with an H3.3S31ph blocking peptide, providing evidence for the specificity of the antibody against phosphorylated H3.3S31. In addition, this 17kDa product was also not observed when H3.1 recombinant protein was used in the assay (lane 2). More importantly, the phosphorylation of H3.3S31 was abolished when the CHK1 inhibitor SB218078 was added to the *in vitro* kinase reaction (lane 5). Together, this data indicates the specific role of CHK1 in mediating the phosphorylation of H3.3S31.

Page intentionally left blank

Figure 3.10 CHK1 kinase mediates the phosphorylation of H3.3S31 in ALT cancer cell lines

(A) Cell lysates were prepared from asynchronous populations from ALT positive and negative cell lines. In comparison to telomerase positive HeLa and A549, the ALT cell lines U2OS, Saos-2, G292 and KMST6, showed elevated levels of CHK1 Ser317 phosphorylation (CHK1 Ser317). In some of these ALT cell lines, CHK2 Thr68 phosphorylation (CHK2 Thr68) levels were also higher (Lovejoy et al., 2012). (B) ALT cancer cell lines did not show significant difference in both CHK1 and CHK2 levels, when compared to HeLa and A549. The levels of tubulin were used as loading controls. Relative ratios of CHK1 S317 and CHK2 T68 were expressed against the tubulin loading control. (C) CHK1 protein was immunoprecipitated from either asynchronous or G2-enriched U2OS cells. The immunoprecipitated CHK1 was used in an *in vitro* kinase assay with the recombinant H3.3 protein, followed by Western blot analysis with an antibody against H3.3S31ph. A strong band corresponding to H3.3S31ph was detected when CHK1 was co-incubated with recombinant H3.3 protein. (D) *In vitro* kinase reaction was also performed using the recombinant GST-tagged CHK1 with the H3.1 or H3.3 protein, followed by Western blot analysis with the anti-H3.3S31ph antibody. A strong 17 kDa band was only observed when the CHK1 protein was incubated with the H3.3 protein. *Lane 1*: recombinant H3.1 protein alone; *lane 2*: 1 μ g recombinant H3.1 with 0.5 μ g GST-tagged CHK1; *lane 3*: recombinant H3.3 protein alone; *lane 4*: 1 μ g recombinant H3.3 with 0.5 μ g GST-tagged CHK1; *lane 5*: 1 μ g recombinant H3.3 with 0.5 μ g GST-tagged CHK1 and 1 μ M CHK1 inhibitor SB218078.



Page intentionally left blank

To investigate the role of CHK1 in mediating H3.3 S31 phosphorylation in ALT cancer cells, we also depleted the CHK1 with siRNA for 48 h. Following the loss of the CHK1 expression, there was an accumulation of the G1 population in the non-ALT A549 cells (Figure 3.10A). In U2OS ALT cancer cells, the block at the S-phase boundary suggested that further examination on the distribution of H3.3S31ph on mitotic chromatin is not possible as the entry into mitosis is inhibited (Figure 3.10B). This perturbation in the cell-cycle distribution of both cell lines is in line with the role of CHK1 as an important regulator of cell-cycle checkpoint and progression. Furthermore, we also noted an increase in the level of DNA damage marker, γ H2A.X in the interphase nuclei of ALT cells upon the loss of CHK1 protein expression (Figure 3.10 C and D). Therefore, to determine the effect of the loss of H3.3S31ph during mitosis, we switched to use specific inhibitors to block CHK1 activity, instead of siRNA knockdown of CHK1 expression, because this allowed us to specifically determine the impact of CHK1-inhibition/H3.3S31ph loss during mitosis.

We first performed Western blot analysis to assess the effect of the CHK1 inhibitor SB218078 on the level of H3.3S31ph. All cell lines examined showed an increase in H3.3S31ph after treatment with Nocodazole, a reversible microtubule toxin used to enrich for mitotic cells (Figure 3.11A, lane 2). We found that the CHK1 inhibitor SB218078 led to a reduction in H3.3S31ph in ALT cell lines including SKLU1, U2OS, Saos-2 and KMST6, but not in non-ALT A549 cells (lane 3). In addition, ALT cancer cells were treated with a CHK2 inhibitor but no change in H3.3S31ph level was detected (lane 4), suggesting that CHK2 was not involved in controlling H3.3S31 phosphorylation in ALT cells. These results argue, therefore, for an *in vivo* role of CHK1 in phosphorylating H3.3S31 in ALT cells. Next, immunofluorescence analysis was performed on cells that were synchronised at the G2/M boundary with RO-3306, and

released into mitosis either in the absence or presence of the CHK1 inhibitor SB218078. In A549 cells, CHK1 inhibition did not alter H3.3S31ph level in pericentric regions (Figure 3.11 B-C). In contrast, with the ALT cell line U2OS, CHK1 inhibition led to a significant reduction in H3.3S31ph staining on chromosome arms (Figure 3.11 D-E). Similar observations were made in other ALT cancer cell lines (Figure 3.11 F-G). Together, these findings showed a novel role of CHK1 as an H3.3S31 kinase. The up-regulated CHK1 kinase activity not only increases the level of H3.3S31ph, but also promotes aberrant distribution of H3.3 across chromosome arms in ALT cancer cells.

Page intentionally left blank

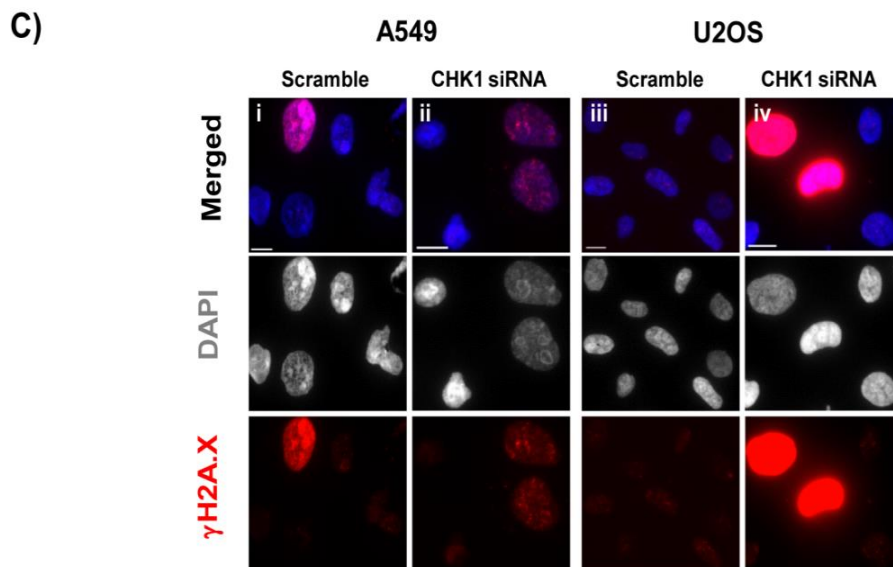
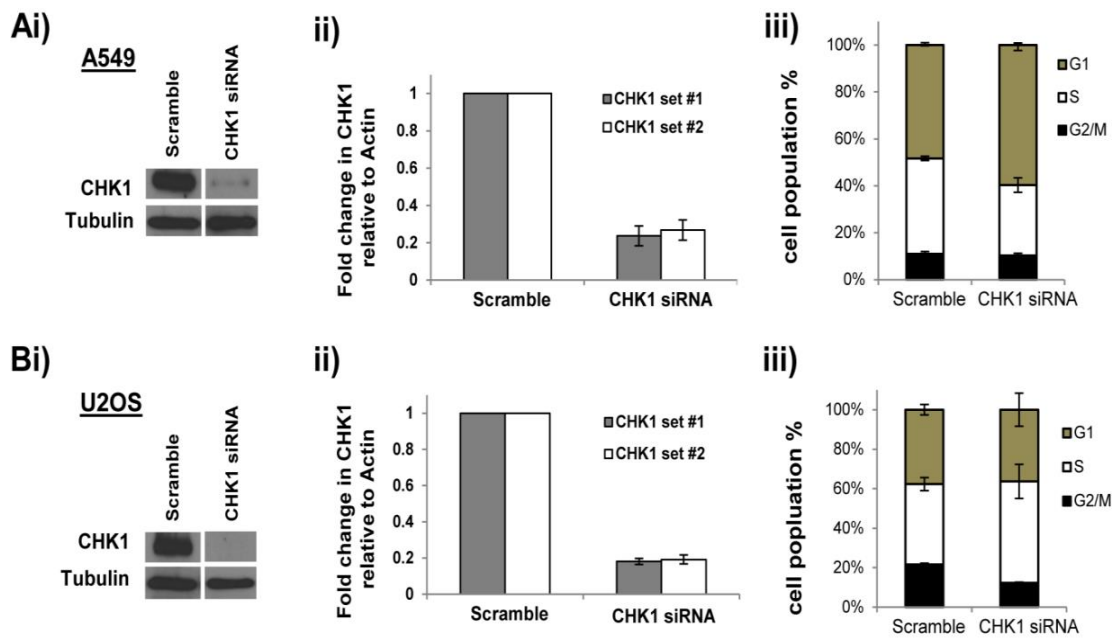
Figure 3.11 Depletion of CHK1 affects the cell-cycle distribution in ALT cancer cells

(A) Lysates were collected from CHK1 depleted (i) non-ALT A549 and (ii) ALT cancer cells U2OS and the level of CHK1 protein were examined by immunoblotting analysis.

(B) RNA was collected from Scramble control and CHK1 siRNA oligonucleotides transfected (i) A549 and (ii) U2OS and the level of CHK1 mRNA was determined by quantitative RT-PCR. After 48 h, the level of CHK1 mRNA remaining was approximately 20-30% relative to the Actin loading control.

(C) The cell-cycle distribution patterns of CHK1 depleted A549 and U2OS cells were also examined by FACS analysis. (i) In A549 cells, an increase in the G1 cell population was observed after the depletion of CHK1 protein for 48hrs. (ii) In U2OS cells, loss of CHK1 protein led to an increase in the percentage of S-phase cells. In addition, a reduction in the percentage of G2/M population was also observed. Graphs represent an average \pm standard error from three independent experiments.

(D) Immunofluorescence analysis was performed to examine the dynamics of DNA damage in CHK1 depleted A549 and U2OS cells. (i, iii) In the Scramble control siRNA transfected cell population, discrete γ H2AX (red) foci were observed in the interphase cell population. (ii, iv) The frequency and intensity of γ H2AX staining has significantly increased in some interphase cells, particularly in the U2OS cell population when CHK1 was depleted. Scale = 10 μ m.



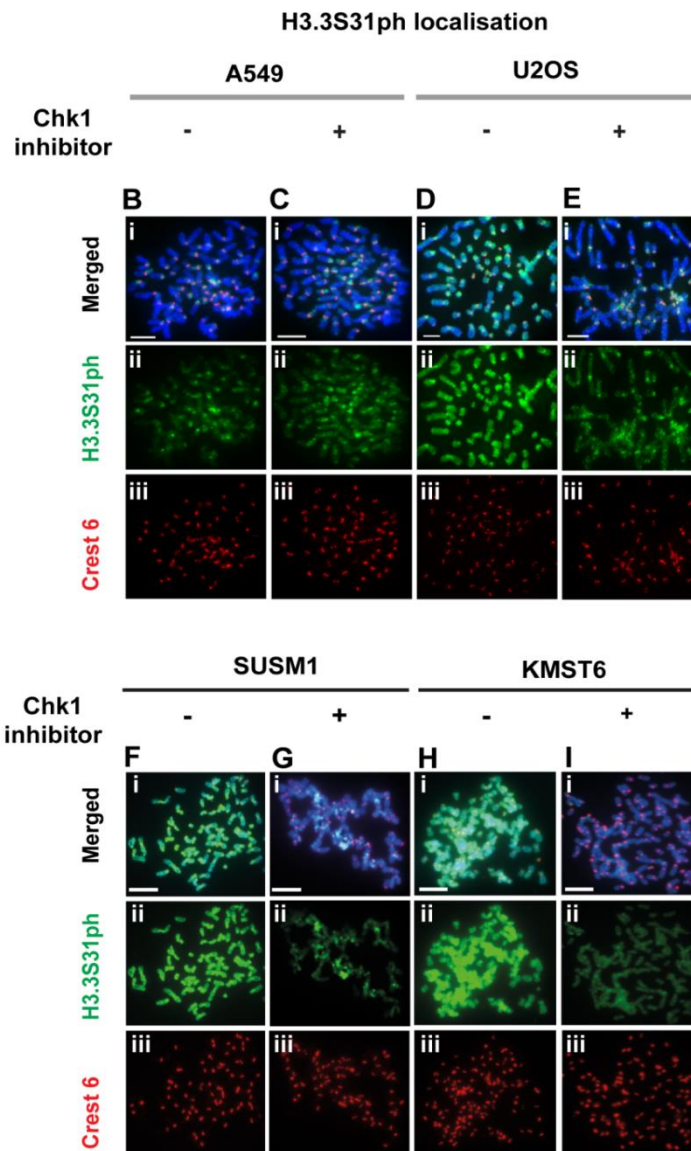
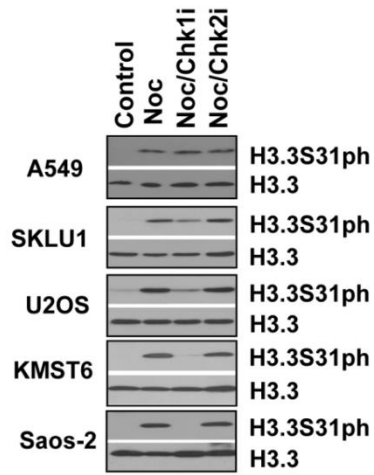
Page intentionally left blank

Page intentionally left blank

Figure 3.12 CHK1 inhibition led to reduced phosphorylation of H3.3S31 in ALT cancer cell lines

(A) Western blot analysis performed on cells arrested at mitosis for 3 h Nocodazole treatment, either in the presence or absence of CHK1 inhibitor. An increase in H3.3S31ph level was detected across all cell lines following Nocodazole treatment. Notably, when cells were treated with Nocodazole in the presence of 2.5 μ M CHK1 inhibitor SB218078, there was a reduction in H3.3S31ph level in all ALT cancer cells. Incubation with 250 μ M of CHK2 inhibitor C3742 did not affect H3.3S31ph levels. *Lane 1*: lysates prepared from asynchronous population; *Lane 2*: lysates from mitotic cells; *Lane 3*: CHK1 inhibitor was co-incubated with mitotic cells; *Lane 4*: CHK2 inhibitor was co-incubated with mitotic cells. Similar observation was made with another CHK1 inhibitor UCN-01 at 1 μ M (data not shown). A549 and ALT positive U2OS, SUSM1 and KMST6 were arrested at G2 boundary using RO-3306. Cells were released either in the presence or absence of CHK1 inhibitor SB218078 for 20 min, followed by Colcemid treatment for 15 min. Immunofluorescence analysis was performed on these G2 released cells. Treatment with 2.5 μ M CHK1 inhibitor SB218078 resulted in a significant reduction in the level of H3.3S31ph (green) in U2OS, SUSM1 and KMST6 ALT cancer cells, but not in non-ALT A549 cells. Centromeres were stained with human CREST antiserum (red). Scale bar = 5 μ m.

A



Page intentionally left blank

3.3.6 Loss of H3.S31 phosphorylation on the chromosome arms affects the viability of ALT cancer cells by the activation of DDR during mitosis

Considering the phosphorylation of histone H3 plays an important role in the maintenance of chromatin structure during mitosis (Sawicka and Seiser, 2012), we also investigated the function of the CHK1 mediated H3.S31 phosphorylation in ALT cancer cell lines. Immunofluorescence analysis was performed on ALT cells that were arrested in mitosis with Colcemid treatment, in the presence or absence of the CHK1 inhibitor SB218078. The distribution and level of the DNA damage chromatin mark γ H2AX were examined. In A549 cells, γ H2AX level was low in both untreated and CHK1 inhibitor-treated cells (Figure 3.12 A, B). In contrast, the treatment of mitotically enriched cells with CHK1 inhibitor had led to the emergence of high levels of γ H2AX signals on chromosome arms in a number of ALT cancer cell lines including the GM847, SUSM1 and W138-VA13/2RA cells. Although the high level of γ H2AX signals on chromosome arms was not observed in the U2OS cells, inhibition of the CHK1 activity led to an increase in the number of telomere associated DNA damage foci (Figure 3.12 I-J). To exclude the possibility that the increase in γ H2AX signal on chromosomes was caused by the Colcemid treatment, we also examined the impact of CHK1 inhibition on a synchronized cell population. Cells were blocked in G2/M using RO-3306 and released into mitosis in the presence of CHK1 inhibitor. There was no increase in the distribution of γ H2AX signal in the non-ALT A549 cancer cells upon released into mitosis (Figure 3.12 K-L). In contrast, an increase in the level of DNA damage was observed on chromosome arms when CHK1 activity was blocked in the GM847 cancer cells upon released into mitosis (Figure 3.12 M-N). This suggests that the change in the γ H2AX distribution was not caused by the Colcemid treatment, but a consequence from the inhibition of CHK1 activity, and that the increase in DNA damage caused by CHK1

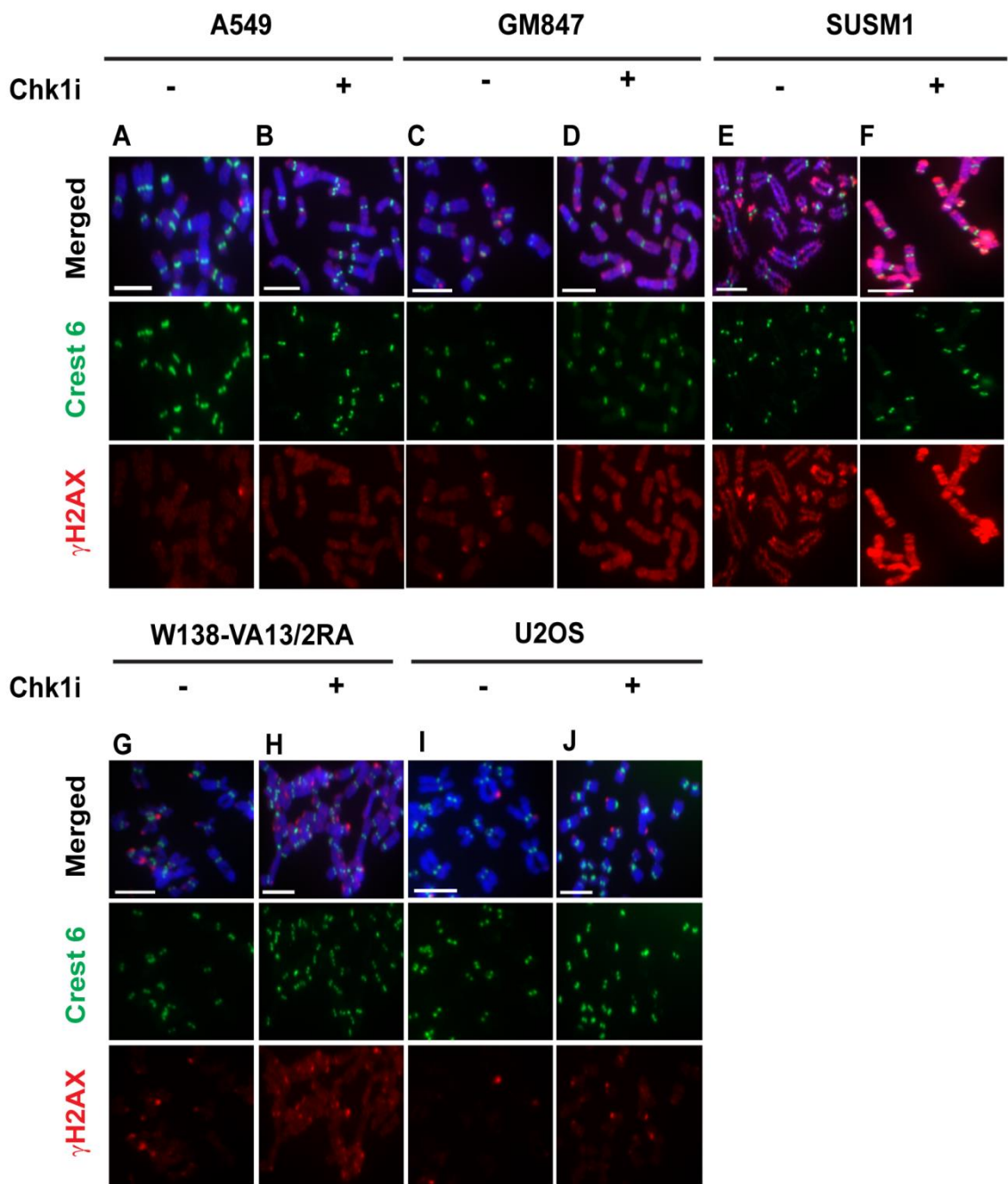
inhibition is a specific observation made in ALT positive cancer cells, but not in telomerase positive cells.

Next, the impact on the inhibition of CHK1 activity on cell viability of ALT cancer cell lines was also examined. Telomerase positive A549 and ALT cancer cell lines including U2OS, G292 and W138-VA13/2RA were arrested in mitosis with nocodazole for 16 h. These mitotic cells were then released in the presence or absence of CHK1 inhibitor for 1 h or 7 h, followed by introduction of a thymidine block to prevent progression from G1 phase into S phase. In A549, CHK1 inhibition did not induce an increase in cell death (Figure 3.12 O). Likewise, in the ALT cancer cell lines, the overall cell viability was also not affected after 1 h of release in the presence of CHK1 inhibitor, except for G292 cells that showed a 15% increase in cell death. However, after 7 h of release in the presence of CHK1 inhibitor, a significant increase in the percentage of cell death was found in all three ALT cell lines. Consistent with the level of γ H2AX acquired upon the inhibition of CHK1 activity, the severity of the percentage of cell death ranged from 25% in U2OS cell line to a 40-50% increase in G292 and W138-VA13/2RA cells, respectively. These results demonstrated that CHK1 activity during mitosis is essential for the survival of ALT cancer cells.

Page intentionally left blank

Figure 3.13 Inhibition of CHK1 activity in mitotic ALT cancer cell lines induces DDR signaling and affects cell viability.

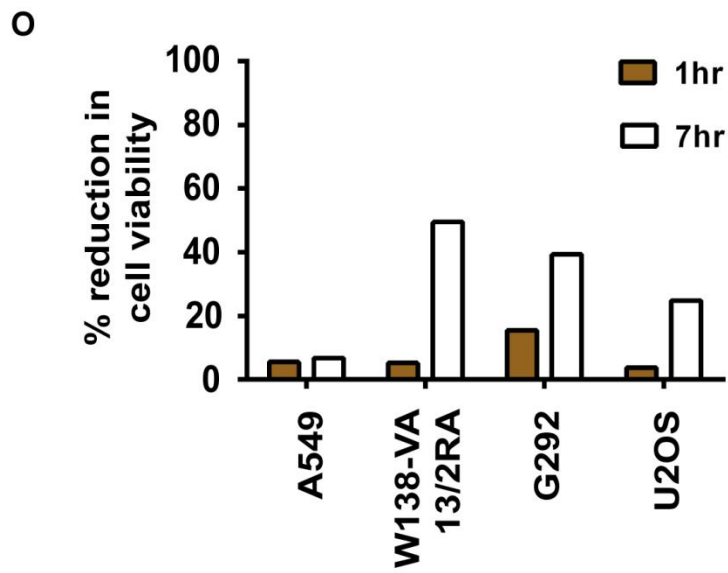
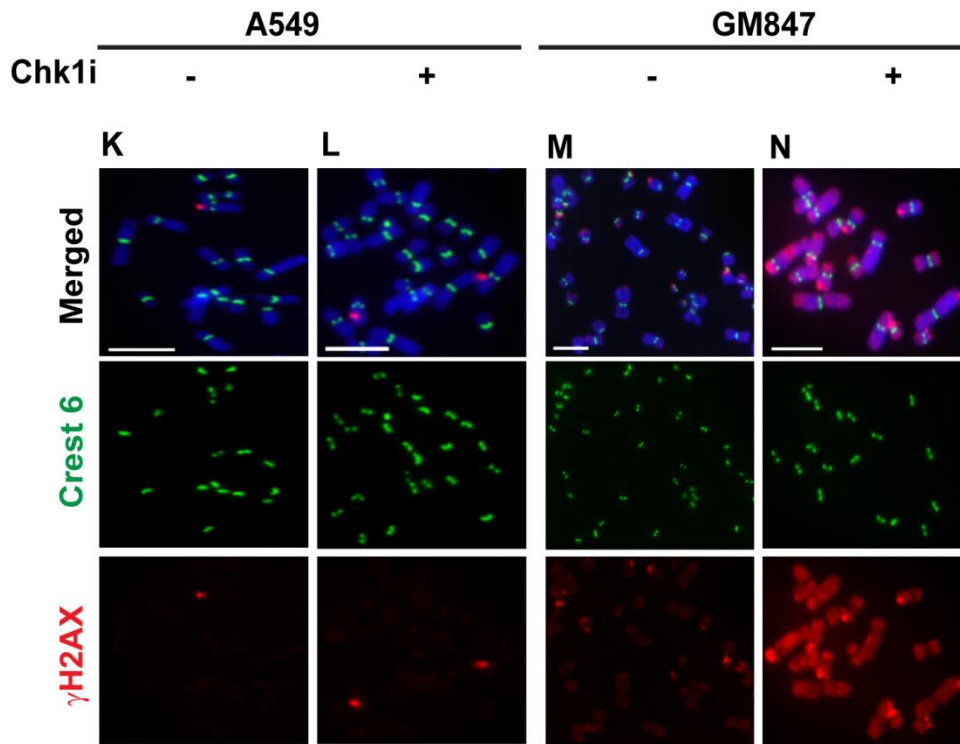
A549, GM847, SUSM1, W138-VA13/2RA and U2OS cells were arrested at mitosis by 3 h treatment with Colcemid, either in the presence or absence of CHK1 inhibitor SB218078. Immunofluorescence analysis was then performed to determine the distribution and level of γ H2AX (red). Centromeres were stained with human CREST antiserum (green). **(A-B)** In A549 cells, γ H2AX was found only at low levels, with occasional staining at telomeric ends. Treatment with CHK1 inhibitor did not cause a significant change to the distribution and level of γ H2AX. **(C-F)** In ALT cell lines including GM847, SUSM1 and W138-VA13/2RA cells, there were significant increases in γ H2AX levels on chromosome arms upon the removal H3.3S31 phosphorylation by inhibiting CHK1 activity during mitosis. In the U2OS cells, only an increase in the frequency of telomeric DNA damage foci was observed. The distribution of γ H2AX was also examined on synchronized cells from the G2 phase with RO-3306. Cells were released in the absence (Control) or presence of CHK1 inhibitor SB218078 (CHK1i) for 50 min, followed by 10 min treatment with Colcemid.



Page intentionally left blank

Page intentionally left blank

(K-L) In the telomerase positive A549 cells, the level of γ H2AX remained low. **(M-N)** In contrast, an increase in the level of γ H2AX on chromosome arms was observed when GM847 cells were treated with CHK1 inhibitor during the release from G2/M block. Representative images of 50 spread. Scale bar = 5 μ m. **(O)** A549 and various ALT cancer cell lines including W138-VA13/2RA, G292 and U2OS cells were arrested at mitosis by overnight treatment with Nocodazole. Cells were released either in the presence or absence of CHK1 inhibitor SB218078 for either 1 h or 7 h, followed by thymidine treatment to prevent cells from progressing through G1/S. Cell viability was determined by staining of cells with 0.4% Trypan blue solution to examine the overall number of live and dead cells. The percentage of cell death was calculated as a percentage of difference between the untreated control and CHK1 inhibited cell populations. No significant change was observed in A549 at both time points. Similarly, there was no significant increase in cell death was observed in ALT cell lines W138-VA13/2RA and U2OS after 1 h of release in the presence of CHK1 inhibitor. However, in G292 cells, there was a 15% increase in cell death. After 7 h of release in the presence of CHK1 inhibitor, all three ALT cancer cell lines showed increased cell death, ranging from 25 to 50%. An average of two independent experiments was presented in graph.



Page intentionally left blank

3.3.7 Substitution of the Serine with an Alanine residue at Position 31 led to an increase in DNA damage on chromosome arms in ALT cancer cells

To further understand the role of H3.3 Serine 31 phosphorylation in the maintenance of chromatin integrity in ALT cancer cells, we expressed a myc-tagged H3.3 protein carrying a substitution at the Serine 31 position with an Alanine that can not be phosphorylated (known as S31A) to examine the impact on the staining pattern of H3.3S31ph and the dynamics of γ H2AX distribution on the mitotic chromatin in ALT cancer cells. The level of myc expression in the transfected cell population was confirmed with immunoblotting analysis using an antibody against the myc-tag. After 96 h of transient expression, there was no perturbation to the cell-cycle distribution was observed in both the wild-type and the mutant S31A transfected cell populations. Furthermore, exogenous expression of the S31A did not alter the number of APB in ALT positive W138-VA13/2RA cancer cells (data not shown). In non-ALT HeLa cells, the level of H3.3S31ph staining at the pericentric satellite repeats was found to be lower on the mitotic chromosomes that were positive for the myc-tagged S31A in comparison to the wild-type control (Figure 3.14 B-C). In the ALT positive W138-VA13/2RA cancer cells, the intense phosphorylation staining of H3.3 Serine 31 on chromosome arms was also reduced when myc-tagged S31A was expressed (Figure 3.14 D-E). Next, we investigated the dynamics of the γ H2AX on mitotic chromosomes. In HeLa cells, the γ H2AX level remained low in both wild-type H3.3 and mutant S31A transfected cell population. Consistent with the observation made with the inhibition of CHK1 activity in ALT cancer cells (Figure 3.13), the substitution of the Serine to Alanine residue resulted in a reduced level of H3.3S31ph on chromosome arms. This also leads to an increase in the frequency of γ H2AX signals in the telomere damage foci in the U2OS cells (Figure 3.14 H-I). In the wild-type transfected W138-VA13/2RA cells, the distribution of

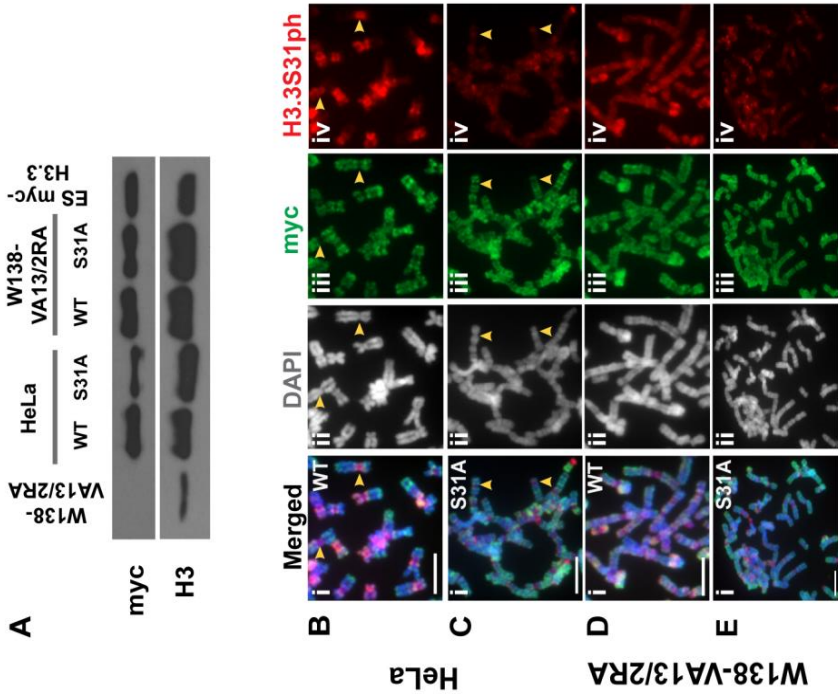
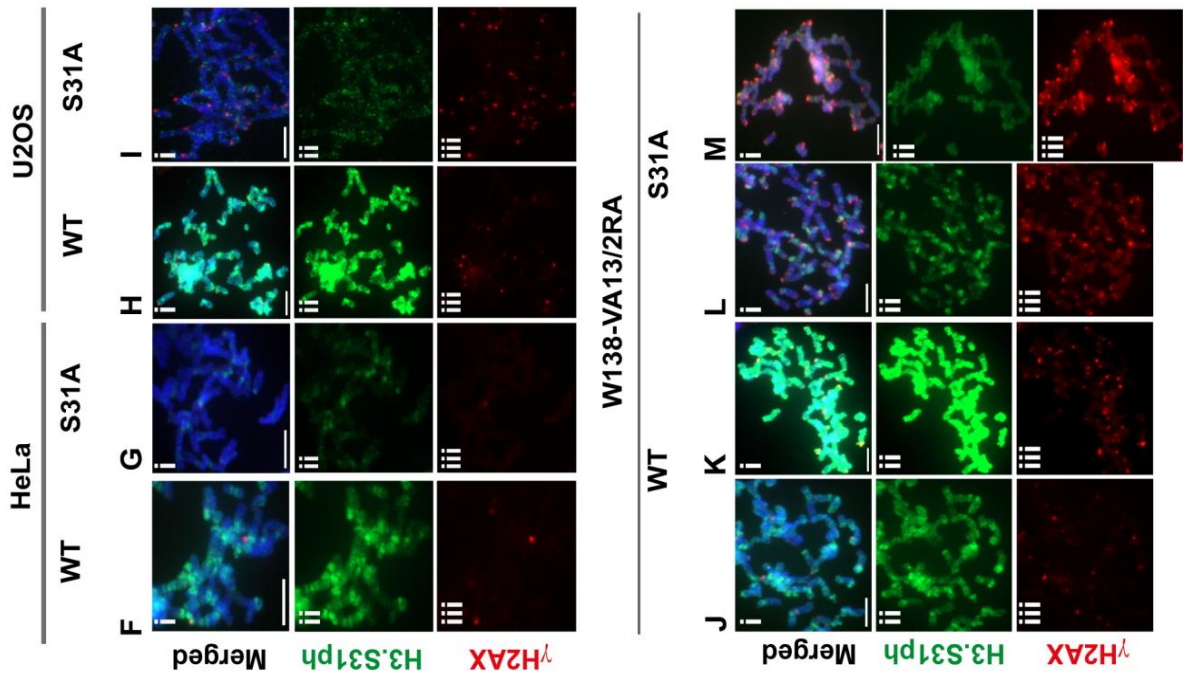
γ H2AX was observed at the telomeres and on chromosome arms (Figure 3.14 J-K). In contrast, the substitution of the Serine 31 residue led to a further increase in the level of γ H2AX on chromosome arms (Figure 3.14 L-M). Collectively, these findings suggest that inhibition of CHK1 activity and loss of H3.3S31 phosphorylation during mitosis lead to DNA damage induction in ALT cancer cells. Based on these findings, we hypothesize that CHK1-mediated H3.3S31 phosphorylation acts as a mark to regulate chromatin integrity by suppressing the high levels of DNA damage or γ H2AX in ALT cells. This then facilitates mitotic progression of ALT cells by preventing the induction of global DDR signaling in chromatin.

Figure 3.14 Substitution of the H3.3 Serine to an Alanine residue alters the staining level of H3.3S31ph and induces DDR signaling in ALT cancer cells

(A) Lysates were prepared from pcDNA4/myc-tagged H3.3 WT and S31A transfected HeLa and W138-VA13/2RA cells after 96 h. The untransfected W138-VA13/2RA cell line and the mouse embryonic stem cell line with a stable expression of the myc tagged H3.3 were used as negative and positive controls respectively. Immunoblotting analysis performed with antibodies against the myc tag; histone H3 was used as a loading control. Cells that are positive for the wild-type protein is labelled as WT; the substitution from Serine to Alanine residue is marked as S31A. Immunofluorescence analysis was performed with antibodies against myc (green) and H3.3 S31ph (red) on myc-tagged H3.3 transfected HeLa and W138-VA13/2RA cells after 96 h. (A) In the myc-tagged WT positive HeLa cells, phosphorylated H3.3S31 localised at the pericentric satellite repeats on mitotic chromosomes. (B) When the Serine 31 is substituted with an Alanine, the level of H3.3S31ph at the pericentric satellite repeats was reduced. (C-D) In ALT positive W138-VA13/2RA, over-expression of the S31A protein led to a significant reduction in the level of H3.3S31ph that was found at the pericentric region and on chromosome arms compared to the wild-type control. The association between the H3.3S31ph level and the distribution of the γ H2AX levels was also examined in the wild-type or S31A transfected cells. Immunofluorescence analysis with antibodies against H3.3S31ph (green) and γ H2AX (red) was performed on myc-tagged wild-type or H3.3S31A transfected HeLa, U2OS and W138-VA13/2RA cell lines after 96 h. (E-F) In telomerase positive HeLa cells, the intensity of DNA damage remained low in both wild-type and S31A transfected mitotic chromosomes. In the ALT cancer cells, the reduction in the phosphorylation of H3.3 Serine 31 led to an increase in the frequency and intensity of γ H2AX signals at the telomere when the myc-tagged S31A was over-expressed in the

U2OS (**I**). In W138-VA13/2RA cells, an increase in the level of γ H2AX was observed on chromosome arms (**L-M**). Representative images of 50 chromosome spreads are shown.

Scale bar =5 μ m.



Page intentionally left blank

3.4 Discussion

The deposition of histone variants by specific chaperones, and associated PTMs on the histone tails, can significantly impact chromatin structure and function. Recent studies have reported that human ALT cancers show a high frequency of mutations in H3.3 and in its chaperones ATRX and DAXX (Bower et al., 2012; Jiao et al., 2010; Lovejoy et al., 2012; Schwartzenuber et al., 2012). Considering the importance of ATRX/DAXX/H3.3 in the maintenance of chromatin repression in heterochromatin (Drane et al., 2010; Goldberg et al., 2010), ALT cancer cells expectedly show severe telomere dysfunction and global genome instability. In these cells, ATRX/DAXX mutations are also likely to affect the deposition pattern of H3.3 and its PTM profile in ALT cells. Indeed, despite the absence of H3.3 over-expression, the findings in this study show greatly elevated H3.3S31ph levels at pericentric DNA repeats, along with aberrant H3.3S31ph localisation on chromosome arms in ALT cancer cells. Furthermore, this study has also unveiled CHK1, a serine/threonine kinase that is linked to the DNA damage response as a novel H3.3S31 kinase. In these ALT cancer cells, the elevated levels of activated CHK1 elicit high levels of H3.3S31ph and its mis-localisation on chromosome arms. Importantly, inhibition of CHK1 activity during mitosis induces an increase in γ H2AX levels on mitotic chromosome arms and compromises the viability of these ALT cancer cells. Lastly, over-expression of H3.3S31A mutant affects H3.3S31ph levels and induces γ H2AX on chromosome arms and at the telomeres in these cells. Altogether, this suggests the importance of CHK1-mediated H3.3S31ph in chromatin maintenance and cell survival in ALT cancer cells.

All ALT cell lines tested in this study, except one, show remarkable up-regulation in H3.3S31ph and mis-localization on chromosome arms. The aberrant localization of the

H3.3S31ph on chromosome arms is also induced following the siRNA knockdown of ATRX in the non-ALT A549 and ALT cancer SKLU1 cells. Indeed, a similar delocalization of the H3.3S31ph onto chromosome arms has also been reported when another H3.3 histone chaperone, DEK was depleted in mESCs (Ivanauskiene et al., 2014). In ALT cells, the failure of H3.3 to be deposited to the heterochromatin in the absence of the ATRX/DAXX may therefore allow the mis-targeting of H3.3 by other chaperones, such as the HIRA complex to different genomic regions. Considering the link between HIRA-mediated H3.3 deposition and transcription regulation following DNA damage (Adam et al., 2013), future investigations are required to examine whether the high levels of DNA damage in ALT cells promotes the mis-loading of H3.3 by HIRA, or whether the inactivation of ATRX function affecting the balance and therefore the mis-localization of H3.3 in these cancers. Nevertheless, the extent of the H3.3S31ph staining that we observed in the ATRX siRNA transfected cells is less intense compared to the ATRX null ALT cancer cells. This suggests that the loss of ATRX is unlikely to be sole factor that drives the altered H3.3S31ph distribution in ALT cancer cells. Indeed, the observation is in line with a recent proposition that a singular dominant mutation in ATRX or DAXX may be insufficient to elicit an ALT phenotype (Bower et al., 2012; Lovejoy et al., 2012), and would likely involved that an unidentified cooperating genetic or epigenetic changes. Consistent with the recent study that suggested that beyond initial activation of ALT activity induced by depletion of histone chaperone anti-silencing factor 1 (ASF1), ALT activity might be maintained via currently unidentified, cooperating epigenetic alterations (O'Sullivan et al., 2014). These findings have indeed provided the first evidence of the existence of aberrant epigenetic histone modification profiles in ALT cells. It is currently unclear whether abnormal H3.3S31ph dynamics reported here is a consequence of ALT activation, or if it contributes to the ALT

phenotype. Nevertheless, these findings suggest that telomere dysfunction and subsequent genome instability could promote a global change in chromatin status, due to elevated DDR signalling. In addition, we propose that aberrant H3.3S31ph labelling may constitute another marker of ALT activation in cancer cells. CHK1-mediated aberrant H3.3S31ph dynamics may be unique to ALT cells and represent a putative therapeutic target for treatment of ALT cancers.

Previous studies have identified the role of CHK1 as a histone kinase that mediates phosphorylation of Ser10 and Thr11 on histone H3, an interaction involved in transcription regulation (Liokatis et al., 2012; Metzger et al., 2008). From this study, the novel function CHK1 in phosphorylating H3.3S31 further implicates the regulatory role of CHK1 in chromatin metabolism. Although the H3.3S31ph PTM was first reported almost a decade ago (Hake et al., 2005), this study is to our knowledge, the first identification of an H3.3S31 kinase *in vitro* and in cells. It is important to note that CHK1 inhibition does not result in a complete loss of the H3.3S31ph signal, particularly at pericentric satellite DNA repeats. This indicates CHK1 is unlikely the kinase that phosphorylates H3.3S31 at the heterochromatin during mitosis and other potential kinase(s) remain to be discovered. Besides the up-regulation of the kinase activity, an imbalance in the kinase/phosphatase axis can also be an underlying factor that promotes the intense H3.3S31ph on chromosome arms in ALT cancer cells. Previous studies have shown that the CHK1/protein phosphatase 1 γ (PP1 γ) axis is involved in the phosphorylation regulation on H3T11 in response to DNA damage (Shimada et al., 2010; Shimada et al., 2008). It is possible that the PP1 γ is a phosphatase that regulates H3.3S31 phosphorylation, and in ALT cancers, the aberrant activity of this phosphatase affects the regulation of H3.3S31 de-phosphorylation status on chromosome arms.

As shown above, the ALT cancer cells show significant up-regulation of activated CHK1, even though global CHK1 levels are unaltered, compared to non-ALT cells. This finding is consistent with the previous data of high basal levels of DNA damage and DDR signalling (as evidenced by high levels of γ H2AX and activated CHK2) in these cells (Lovejoy et al., 2012). Additionally, the impaired G2/M checkpoint in ALT cancer cells has been speculated to permit continued proliferation despite a considerable burden of DNA damage both at telomeres and elsewhere in the genome (Lovejoy et al., 2012).

In a previous study, CHK1 has been shown to regulate spindle assembly checkpoint (SAC) (Zachos et al., 2007). Further analyses may be performed to examine if the elevated CHK1 activity may affect G2/M checkpoint or activity of SAC proteins such as Aurora B kinase in ALT cells. It is also important to determine if H3.3S31ph induced by CHK1 may affect G2/M checkpoint and mitotic progression in these cells. Several recent studies showed that DNA damage including at the telomeres (Cesare et al., 2013; Giunta et al., 2010; Lukas et al., 2011) do not induce a full DDR response during mitosis. Considering the high level of telomere DNA damage in ALT cancer cells and the protective role of H3.3S31ph against DNA damage that was recently reported (Frey et al., 2014), one possibility is that H3.3S31ph induced by CHK1 may be essential for blocking a full DDR during mitosis. This would help ALT cells progress through mitosis without the induction of DDR, which can affect the maintenance of chromatin stability. Indeed, when CHK1 is inhibited in ALT cancer cells, the decrease in H3.3S31ph is accompanied by the appearance of increased levels of γ H2AX at telomeres and on chromosome arms, indicating a wide-spread increase in DNA damage level across (mitotic) chromosomes. It has previously been shown that DNA damage occurring during mitosis is being marked by γ H2AX for subsequent repair in G1 (Giunta et al., 2010; Lukas et al., 2011). Interestingly, the binding of another DNA damage marker, 53BP1 is prevented from

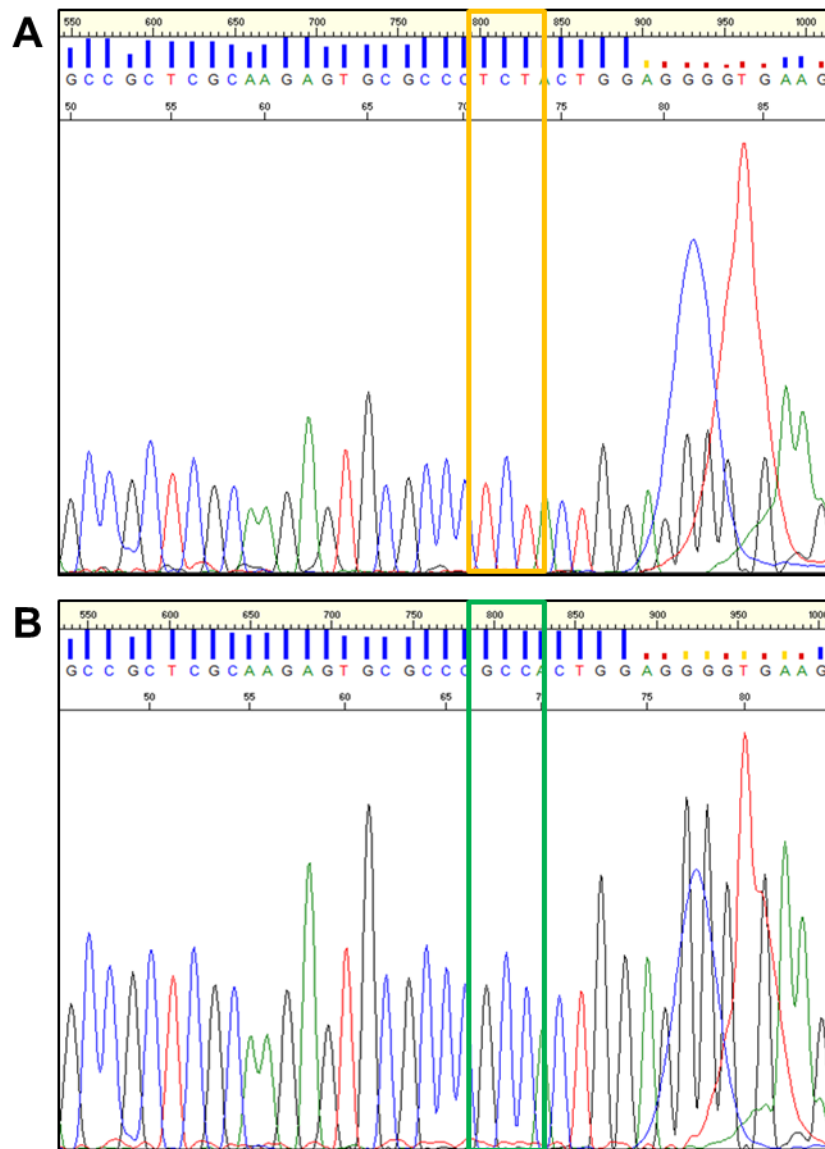
binding to the mitotic chromatin to prevent the full activation of DDR during mitosis, which is detrimental to genome stability (Giunta et al., 2010; Lee et al., 2014). Here in this study, we have shown that CHK1-mediated H3.3S31ph suppresses γ H2AX in these ALT cells; however, the effect on the recruitment of 53BP1 has not been examined. As the binding of 53BP1 to the mitotic chromatin is negatively regulated by the phosphorylation state (Lee et al., 2014), future investigations are needed to determine whether the high levels of H3.3S31ph directly affects the association of 53BP1 with the mitotic chromatin in ALT cells. More importantly, the de-regulation in the timing of 53BP1 localisation may offer a plausible explanation to the poor survival of ALT cancers following the loss of H3.3S31 phosphorylation with CHK1 inhibitor treatment. Besides its known role in the DNA damage signaling mechanism, a recent study has established a function of CHK1 kinase to regulate the expression of transcription factors in brain tumours with specific mutation at the Glycine 34 residue on H3.3. In this study, the findings have uncovered a novel ability of CHK1 to catalyse H3.3S31 phosphorylation *in vitro*, and more importantly, that elevated levels of activated CHK1 drive the aberrant H3.3S31ph dynamics in ALT cells. Interestingly, it was evident that phosphorylation on the Serine 31 residue can affect the binding of a reader protein to its neighbouring Lysine 36 residue (Guo et al., 2014). As CHK1 phosphorylation of H3 Ser10 and Thr11 can influence the establishment of PTM profiles of adjacent residues on H3 (Liokatis et al., 2012; Metzger et al., 2008), it will be interesting to determine whether the aberrant H3.3S31ph influences PTMs on neighbouring residues, and affects the global PTM profile in ALT cells. For example, changes to the methylation/acetylation dynamics of the neighbouring Lys27 and Lys36 may have drastic consequences for the cellular transcription profile. Our finding of H3.3S31 as a new substrate for CHK1 phosphorylation further implicates a regulatory role of CHK1 in chromatin metabolism,

and shows for the first time how mis-regulation of CHK1 activity in a diseased state, such as in ALT cancers, may affect global chromatin regulation.

Supplementary information

Supplementary Figure 2 Sequencing chromatograms of the pcDNA4/TO/HisA myc-tagged H3.3S31A construct

DNA sequencing of was performed using BigDye v3.1 to validate the substitution of the pcDNA4/TO/HISA myc-tagged S31A constructs. (A) The wild-type H3.3 residue is encoded by the TCT base pairs; (B) Substitution is denoted by a GCC coding for an alanine residue.



Supplementary Table 1 ALT cancer cells have elevated CHK1 activity compared to non-ALT cells.

Cell Line	Intensity level of CHK1 S317 against levels of Tubulin (rCHK1S317)	Intensity levels of CHK1 against levels of Tubulin (rCHK1)	Levels of rCHK1S317 against levels of rCHK1 (rCHK1 S317/rCHK1)	Fold of difference in rCHK1 S317/rCHK1 relative to A549 cells
A549	0.1	1.6	0.0625	1
SKLU1	0.2	1	0.2	3.2
W138-VA13/2RA	0.5	1	0.5	8
GM847	0.5	1	0.5	8
KMST6	0.3	1	0.3	4.8
G292	0.9	1.5	0.6	9.6
U2-OS	1.1	1.1	1	16
Saos2	0.9	1.2	0.75	12

Supplementary Table 2 CHK2 activity is higher in some ALT cancer cells.

Cell Line	Intensity level of CHK2 T68 against levels of Tubulin (rCHK2 T68)	Intensity levels of CHK2 against levels of Tubulin (rCHK2)	Levels of rCHK2 T68 against levels of rCHK2 (rCHK2 T68/rCHK2)	Fold of difference in rCHK2 T68/rCHK2 relative to A549 cells
A549	0.01	0.5	0.02	1
SKLU1	0.5	0.2	2.5	125
W138-VA13/2RA	0.1	0.5	0.2	10
GM847	0.01	0.6	0.02	1
KMST6	1.0	0.7	1.43	70
G292	0.6	0.3	2.0	100
U2-OS	0.1	0.5	0.2	10
Saos2	0.01	0.3	0.03	1.5

Chapter 4

Conclusion and Future directions

The deposition of H3.3 by the ATRX protein is important to the regulation of telomere integrity. In this project, we provide a detailed account on how the role of H3.3 and ATRX in the context of the maintenance of telomere dynamics and genome stability can differ between a normal cellular state and a disease environment. In pluripotent mES cells, we show that the loading of ATRX/H3.3 to the telomere chromatin is mediated by the assembly of PML-NB at the telomeres. Despite the similarity between the telomere associated PML-NB and the APB in ALT cancers, our findings indicate that these are functionally distinct entities that are recruited to the telomeres to serve different aspects of the telomere regulation (i.e. propagation of the epigenetic chromatin state versus homologous recombination for telomere lengthening and cellular propagation). Nevertheless, the importance of the deposition of H3.3 by ATRX to maintain the telomere chromatin integrity has not altered.

The frequent inactivation of the ATRX protein is shown to be strongly correlated with the ALT phenotype. It is known that the incorporation of H3.3 to the heterochromatin is affected by the loss of the ATRX protein. In our study, we show that the aberrant CHK1 kinase activity, together with the loss of ATRX function contributes to the up-regulation and re-distribution of the phosphorylated Serine 31 residue of H3.3 on chromosome arms in ALT cancers. Besides this, we have also examined the importance of this histone mark to the maintenance of chromatin by regulating the DDR signaling. As H3.3S31ph is important to ALT cell survival, these findings have further our understanding on how the loss of ATRX alters the PTM on H3.3 to maintain the cell propagation in a disease state.

(i) **Future studies to determine the prevalence of aberrant chromosomal localization of H3.3S31ph in osteosarcoma cell lines**

Osteosarcoma (OS) is a form of bone tumour that is highly prevalent in young children. The molecular aetiology of OS remains undefined; however, high levels of genome instability including telomere dysfunction and multiple chromosomal fusions are commonly detected in OS cell lines (Selvarajah et al., 2006). Unlike other forms of sarcoma, the activation of the ALT pathway to maintain the telomere integrity is prevalent in OS cells (Heaphy et al., 2011b; Selvarajah et al., 2006). Among the seven ALT cancer cell lines that showed aberrant H3.3S31ph localization on chromosome arms, three of those are derived from osteosarcoma. As these OS cells show a high potential for positive ALT activities and harboring high levels of genome instability (Heaphy et al., 2011b), this therefore provides an ideal model for studying H3.3S31ph dynamics, and to study association between aberrant H3.3S31ph staining and ALT activity in cancer cells.

To achieve this, we extended a preliminary investigation into a range of human OS cancer cell lines. Immunofluorescence analysis was performed to examine the distribution of H3.3S31ph. Among the eight human OS cell lines tested, we detected the aberrant staining of H3.3S31ph on chromosome arms in all cell lines, including the non-ALT HOS and MG63 cells (Supplementary Figure 3). Considering our findings that the aberrant localization of H3.3S31ph is a hallmark of ALT cancer cells, we next determined the ALT status in these cells. In these cell lines, ALT status was examined by staining for the presence of APB (Supplementary Figure 4).

In Saos2 ALT positive cells, there was a clear presence of APB, as indicated by the co-staining with antibodies against PML and TERF2. However, many of the cell lines also showed aberrant staining of H3.3S31ph on chromosome arms despite the lack of a clear presence of APB (Supplementary Figure 3 and 4). Our immunoblotting results also show

the normal expression of ATRX in these OS cells (Supplementary 4); however, the proper function of this histone chaperone remains to be examined in a greater detail. Future experiments by immunofluorescence and chromatin immunoprecipitation assays are required to investigate the localization of ATRX in the nucleus, and its ability to deposit H3.3 at telomeres and pericentric DNA repeats in these cells. It is also important to determine if ATRX and/or DAXX are mutated in these cell lines (by performing DNA sequencing analysis). Furthermore, the ALT status of these OS cancers needs to be further re-examined by telomere co-FISH and C-circle assays, which are highly sensitive assays for ALT activity.

It has been well documented that telomeres in ALT cancer cells show a high level of DNA damage, as indicated by the presence of γ H2AX. It is interesting that these OS cells also show high levels of γ H2AX at telomeres (Supplementary Figure 6). This high level of γ H2AX at telomeres appears to correlate with the strong staining of H3.3S31ph on the entire chromosome arms in these OS cells- a phenomenon that is also observed in ATRX-defective ALT cancer cells. As future studies, it is important to investigate if H3.3 deposition or heterochromatin assembly is affected in these cells- this may be caused by the loss of function of other factors that interact with the ATRX/DAXX/H3.3 pathway to regulate heterochromatin assembly at telomeres. To determine this possibility, the chromatin status and transcription activity at telomeres in these cells are also required to be examined in a great detail. The altered H3.3S31ph distribution may not be exclusively unique to ALT cancers, or simply caused by a loss of ATRX function. Instead, it may be a hallmark that is prevalent in cancers that suffer high levels of telomere damage and genome instability. As future studies, it is also important to identify the kinases including CHK1 that promote H3.3 Serine 31 phosphorylation in these cells. In light of the importance of H3.3S31ph in the maintenance of cell survival in ALT

cancers, the targeting of the candidate kinase(s) that drive H3.3S31ph would offer a promising therapeutic strategy for OS cancers.

(ii) Future studies to determine function of H3.3S31ph in normal cells, and in regulating transcription activity in the global genome.

Our findings have demonstrated the role of CHK1 as the kinase that drives the aberrant H3.3S31ph in ALT cells. In ES cells, it is interesting to note that the localization of H3.3S31ph at the telomeres is not affected following the inhibition of CHK1 activity (Supplementary Figure 6). This suggests that the kinase and the role of H3.3S31ph in the normal mESCs could be potentially distinct from its function in a cancer state. We have examined the Aurora kinase family as it is a kinase that phosphorylates both the Serine 10 and 28 residues on histone H3 at mitosis. Indeed, our preliminary data has suggested that the Aurora B kinase, and to a lesser extent, Aurora A can phosphorylate H3.3 Serine 31 *in vitro* (Supplementary Figure 7). The reduction in H3.3S31ph localization at the repetitive regions following the inhibition of Aurora B activity in non-ALT and ALT cancer cells has also confirmed the ability of Aurora B to promote phosphorylation on the Serine 31 of H3.3 at the repetitive regions (Supplementary Figure 7). Although the function of Aurora B-mediated H3.3S31ph remains to be examined, our findings suggest that the role of H3.3S31ph is likely to be different depending on the kinase that promotes the phosphorylation in these normal cell types.

The H3.3-containing nucleosome is associated with the dynamic regulation of transcription activation (McKittrick et al., 2004). A recent study shows that the Serine 31 residue on H3.3 can regulate the binding of the gene regulatory protein, ZMYND11 to its neighbouring Lysine 36 residue (Guo et al., 2014). It is interesting to note that this H3.3K36 histone 'reader' belongs to the PWWP domain family, which also includes the family of DNA methyltransferases (reviewed in (Qin and Min, 2014). It remains to be

investigated if H3.3S31ph affects ZMYND11 binding or transcription activity at telomeres. A recent study by Sturm et al (2012) shows a global alternation to the methylation state in tumors that harbor mutations at the Glycine 34 residue. Considering the close correlation of H3.3G34R/V mutation with ATRX loss (>90% correlation) in ALT tumours (Schwartzentruber et al., 2012), it is possible that the loss of ATRX function and the aberrant H3.3S31ph level may lead to a de-regulated control of transcription activity in ALT cancers (Flynn et al., 2015; Yu et al., 2014). Furthermore, the G34 mutation may further aggravate the transcriptional deregulation by affecting the maintenance of H3K36 methylation in ALT cancers. Future experiments to determine the relationship between ATRX/G34 mutation and the gain in H3.3S31ph, and the impact of the loss of H3.3S31ph on the global transcription profile will provide further insight into the regulatory role of H3.3S31ph in these ALT cancer cells.

Moreover, it will be interesting to determine how this aberrant distribution of H3.3S31 can affect the transcription profile, which could potentially be an underlying factor that contributes to the induction of ALT in ATRX-defective cells (Figure 4.1). Indeed, this could be accomplished by the generation of ALT cell lines carrying the endogenous mutation of H3.3 S31A which would allow the examination on the impact of H3.3S31ph on the genome-wide transcription profile, as well as the chromatin integrity by examining the presence of DNA damage.

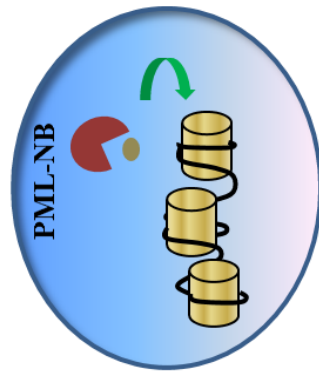
Besides the analysis in ALT cell lines, it will also be useful to determine the genome-wide localization of H3.3 and the phosphorylated Serine 31 histone mark in the absence of ATRX and the impact on global transcription profile at both unique DNA binding and repetitive DNA sites in normal cells. Finally, a better understanding of the function of H3.3S31ph could also be attained by the identification of candidate proteins that bind

H3.3S31ph (in both normal telomerase positive cells and ALT cancer cells) by mass spectrometry or proteomic analysis. In addition, the identification of chromatin enriched with H3.3S31ph by ChIP sequencing analysis and the correlation with the presence of MRN complex or γ H2AX will also unveil the distinct function of H3.3S31ph in the normal and abnormal ALT cancer cells.

Figure 4.1 Proposed model of H3.3S31ph in the regulation of chromatin integrity

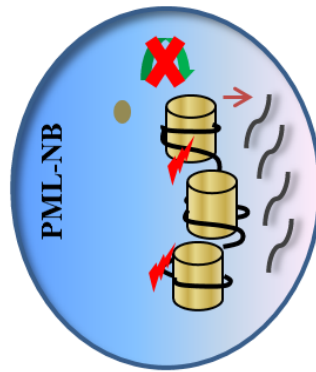
(Top) In normal cells, the PML-NB facilitates the incorporation of H3.3/ATRX/DAXX to maintain the telomere epigenetic state during DNA synthesis. During mitosis, the phosphorylation on the Serine 31 residue of H3.3 by Aurora kinase B ensures that the telomere chromatin state is maintained; however, the underlying mechanism of this pathway remains to be determined. **(Bottom)** The inactivation of ATRX expression affects the normal deposition of H3.3 to the heterochromatin, resulting in telomere damage and could affect the re-establishment of the epigenetic state. Further loss of function, including p53 and other unknown factors allows these cells to progress into mitosis with persistent presence of telomere damage. The highly activated CHK1 kinase can therefore drive the aberrant phosphorylation of H3.3 Serine 31 across the entire chromosomes.

Interphase



Normal

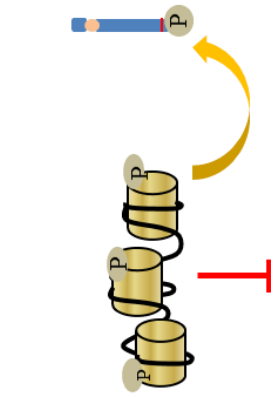
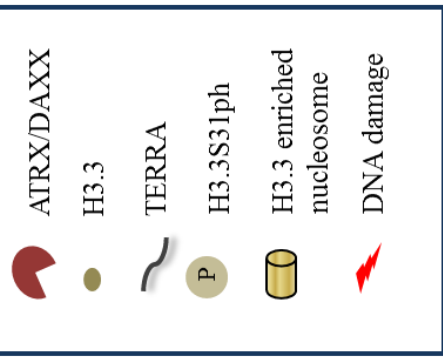
Maintenance of telomere chromatin and organization
Regulates telomere transcription and integrity



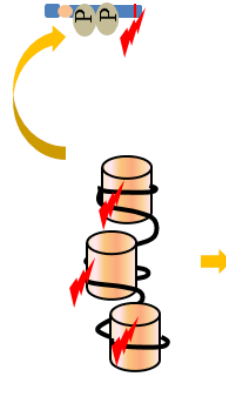
ATRX and p53 inactivation and possible loss of function of unknown factors

Loss of ATRX affects H3.3 deposition and alter the epigenetic state at heterochromatin (telomeres). This leads to aberrant telomere transcription and telomere dysfunction (DNA damage)

Mitosis



Phosphorylated state on H3.3 Serine 31 to maintain chromatin integrity



Disassembly of PML-NB during mitosis

High levels of DNA damage at heterochromatin following the loss of ATRX. This results in a delay in mitotic progression which promotes the aberrant phosphorylation of H3.3S31 by CHK1 kinase

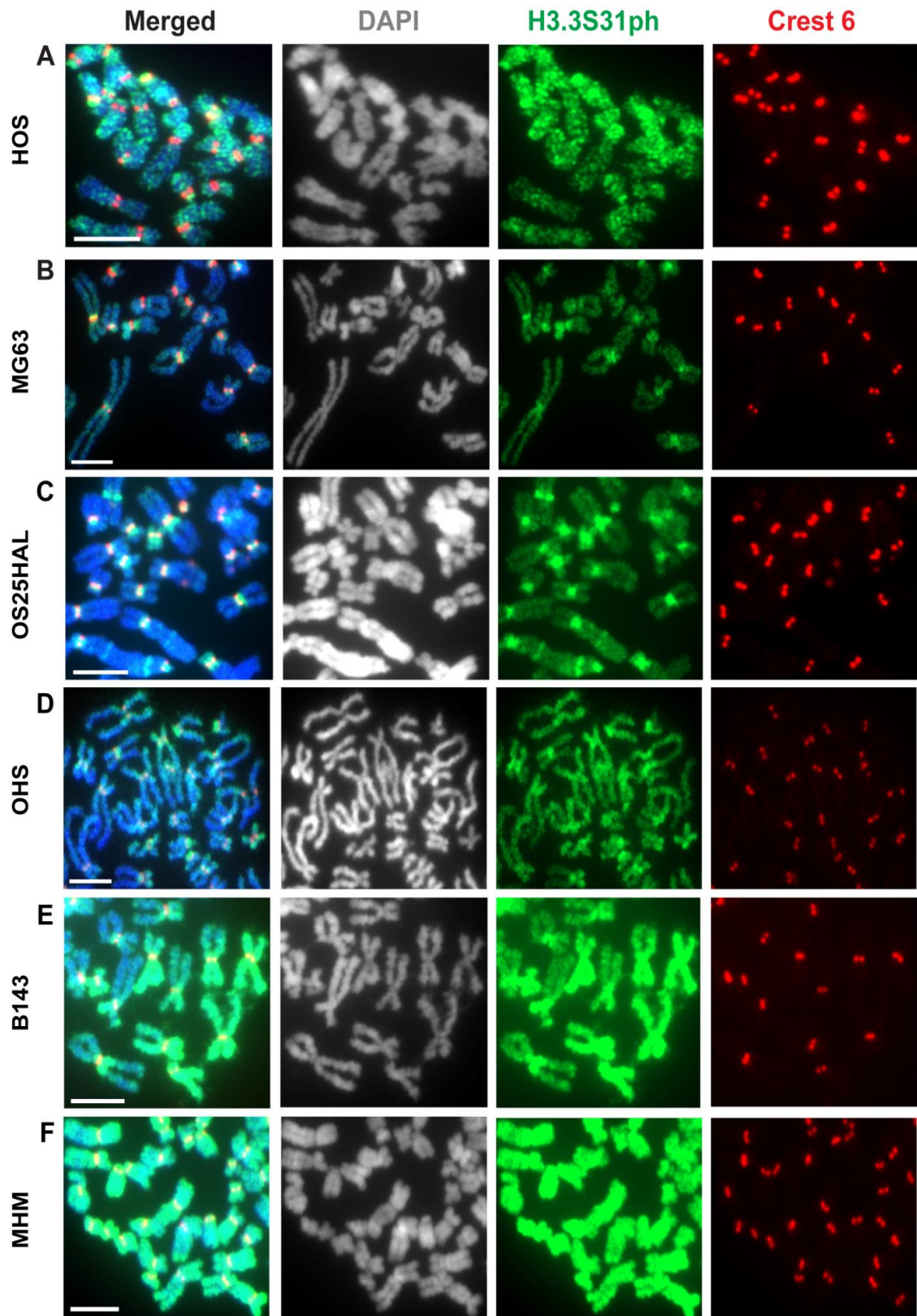
Page intentionally left blank

Page intentionally left blank

Supplementary Information

Supplementary Figure 3 The localization of H3.3S31ph on chromosome arm in OS cancer cells

Immunofluorescence analysis with antibodies against H3.3S31ph (green) and the centromere (anti-CREST serum; red) was performed on OS cells that were treated with Colcemid for 1 h to enrich for mitotic cells (A-B) In non-ALT HOS cells H3.3 S31ph is present on chromosome arms at a low intensity. No enrichment of the H3.3S31ph staining on pericentric satellite repeats was observed. In addition to the pericentric enrichment of H3.3S31ph, low levels of the phosphorylation mark was detected in MG-63 cells (C-D) In OS25HAL and OHS cells, H3.3S31ph is enriched at the pericentric region, accompanied by an up-regulation on chromosome arms. (E-F) The H3.3S31ph staining is more intense on chromosome arms in MHM and B143 cells. Representative images from 50 chromosome spreads. Scale = 5 μ m.

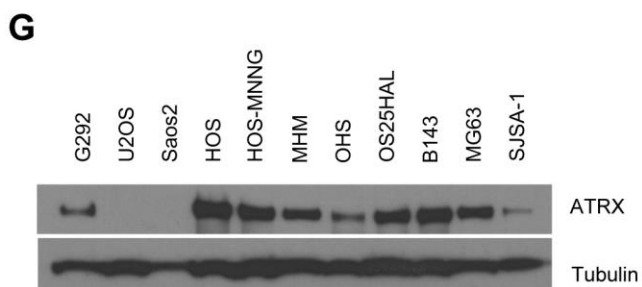
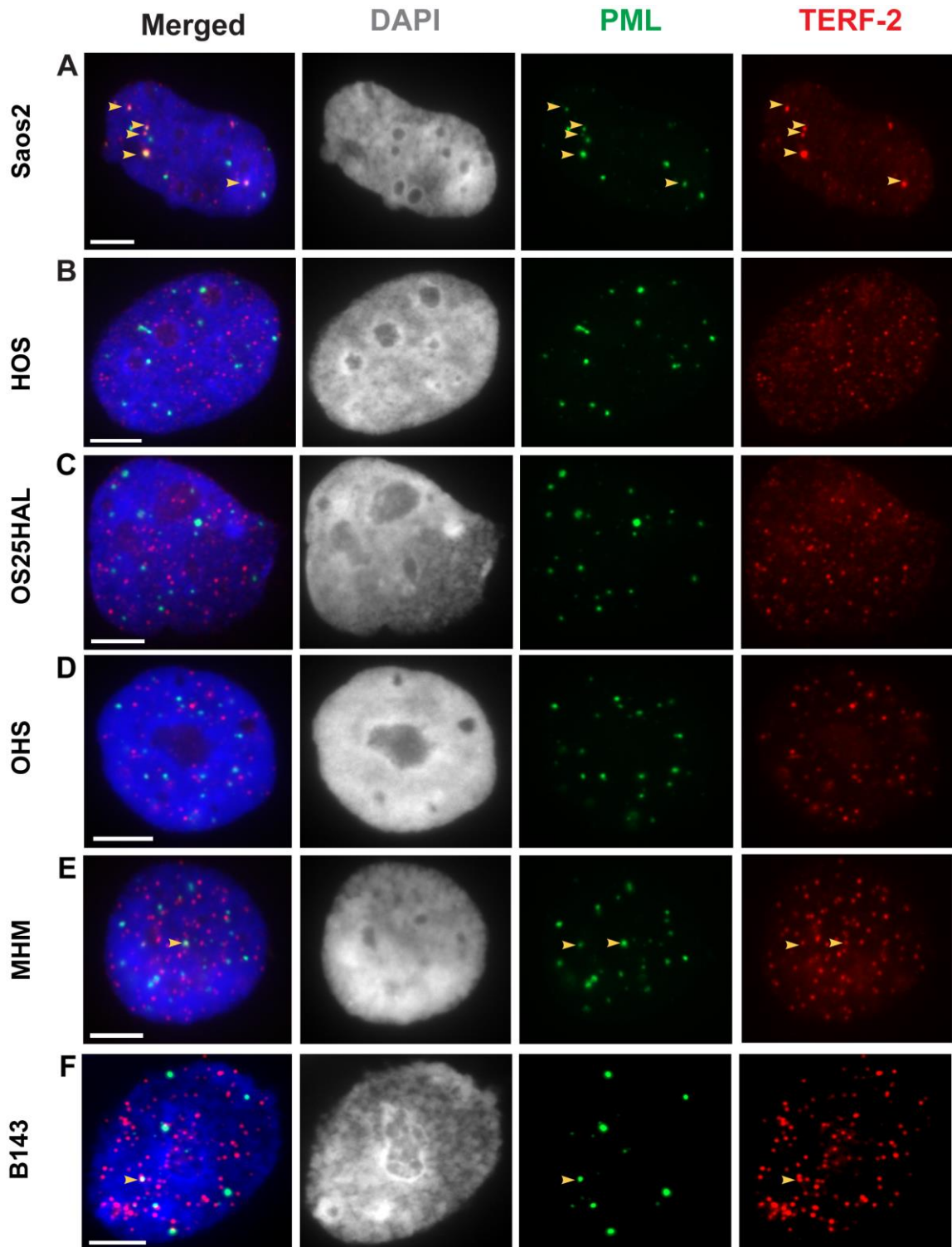


Page intentionally left blank

Page intentionally left blank

Supplementary Figure 4 Low levels of APB in OS cancer cell lines

Immunostaining was performed to examine the distribution of PML enrichment at the telomeres. Antibodies against the PML protein (green) and the telomere marker TERF-2 (red) was used. **(A)** In ALT positive osteosarcoma cancer cells, Saos-2, high frequency of PML targeting at the telomeric region was observed, indicating the presence of ALT-associated PML bodies (APB). **(B)** In non-ALT HOS cancer cells, no co-localization foci were detected. **(C-D)** Low levels of overlapping signals between the PML and TERF-2 protein was found in B143 and MHM cells; however, the low frequency of this co-localization suggests that these cells are unlikely to be ALT positive. **(E-F)** Likewise, there are no overlapping foci observed in the OHS and OS25HAL cancer cells. Representative images from 50 interphase cells. Scale = 5 μ m. **(G)** Immunoblotting with antibody against ATRX was performed on whole cell lysates prepared from OSA cancer cell lines. The ATRX protein is absent in ALT positive U2OS and Saos2 cells; however, ATRX expression was clearly detectable in ALT positive G292 cells and all OSA cell lines.

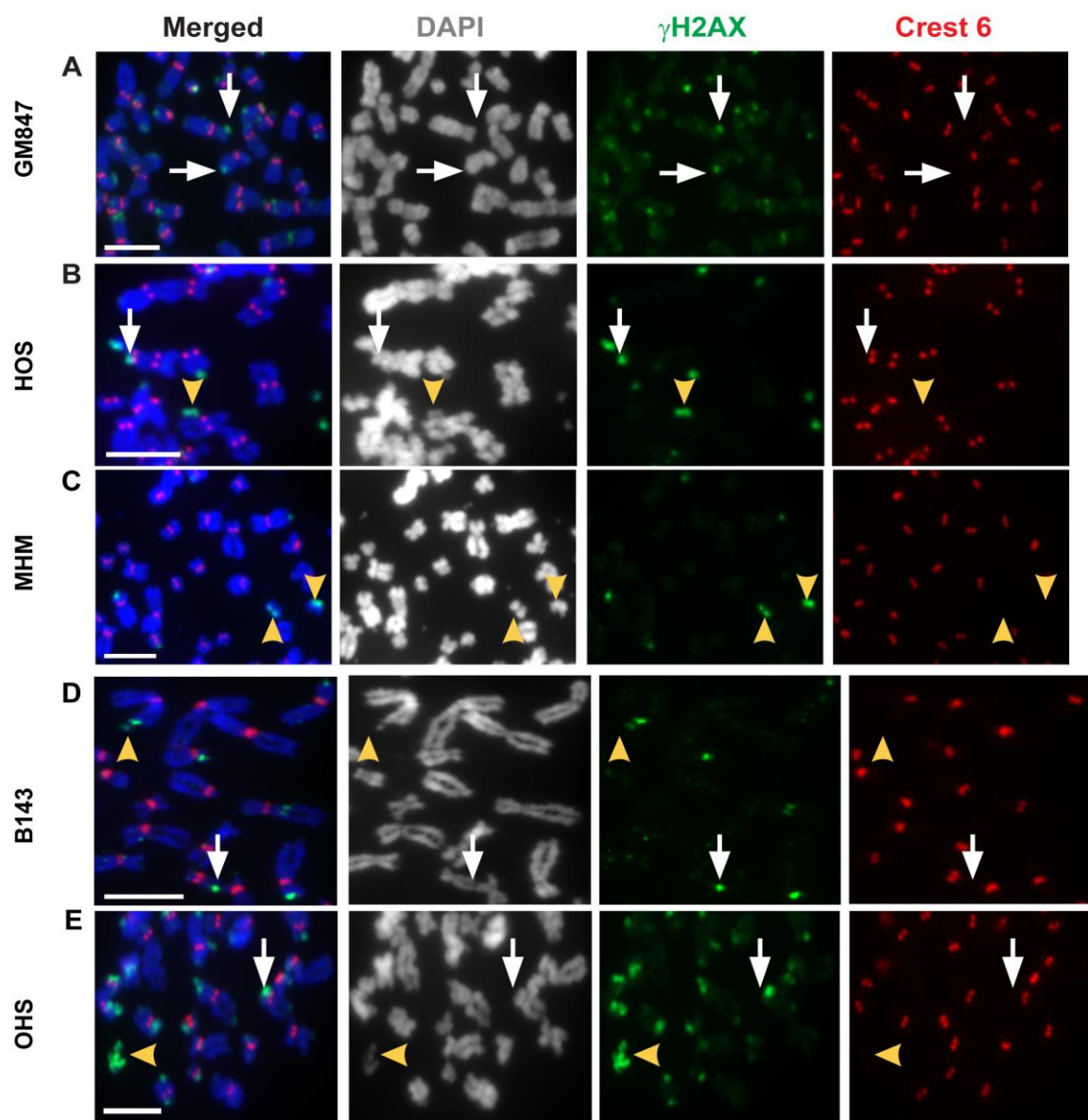


Page intentionally left blank

Page intentionally left blank

Supplementary Figure 5 OS cancer cells are burdened with high levels of DNA damage

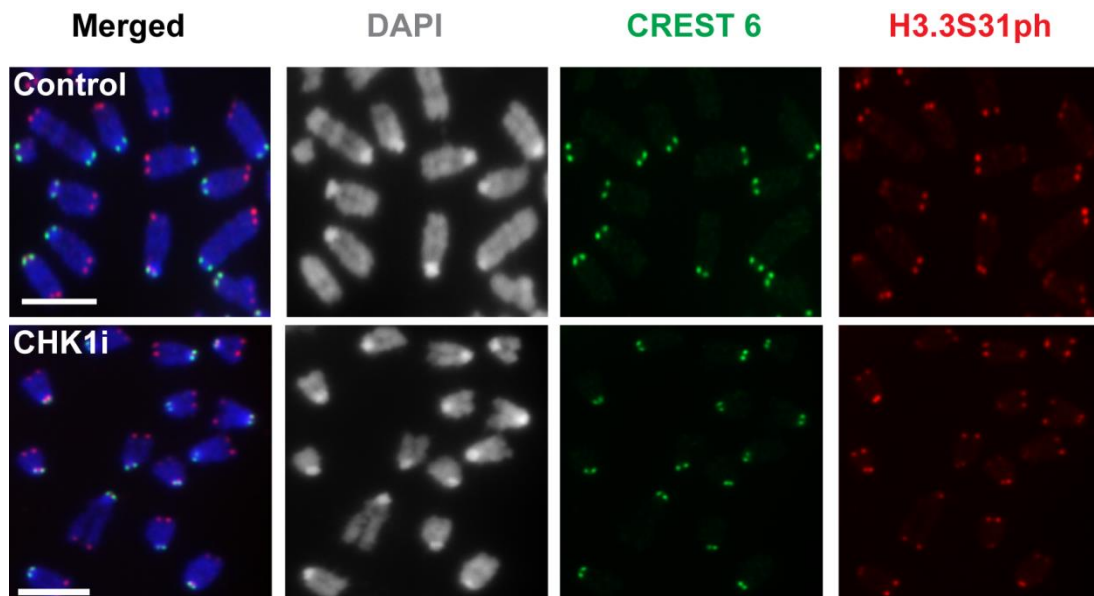
Immunofluorescence analysis was performed to examine the distribution of DNA damage in OS cancer cells. Antibodies against the DNA damage marker, γ H2AX (green) and the centromere (CREST serum; red) was used. **(A-D)** In ALT positive GM847 cells, OS cancer cells HOS, MHM and B143, DNA damage was observed at the telomeric region (arrow) and on DNA fragments that without the Centromere staining (arrowhead). **(E)** High levels of DNA damage at the telomeric region was detected in the OHS cancer cells. Representative images from 50 chromosome spreads. Scale = 5 μ m.



Page intentionally left blank

Supplementary Figure 6 Inhibition of CHK1 activity does not lead to a significant reduction of H3.3S31ph at the telomeres

ES129.1 mESCs were treated with Colcemid for 2 h in the presence of the CHK1 inhibitor, SB218078. Immunofluorescence analysis was performed against the Centromere (green) and the H3.3S31ph (red). (A) In the control cells, the enrichment of H3.3S31ph was observed at the telomere heterochromatin. (B) Treatment with the CHK1 inhibitor only slightly reduces the intensity of H3.3S31ph staining at the telomeres.

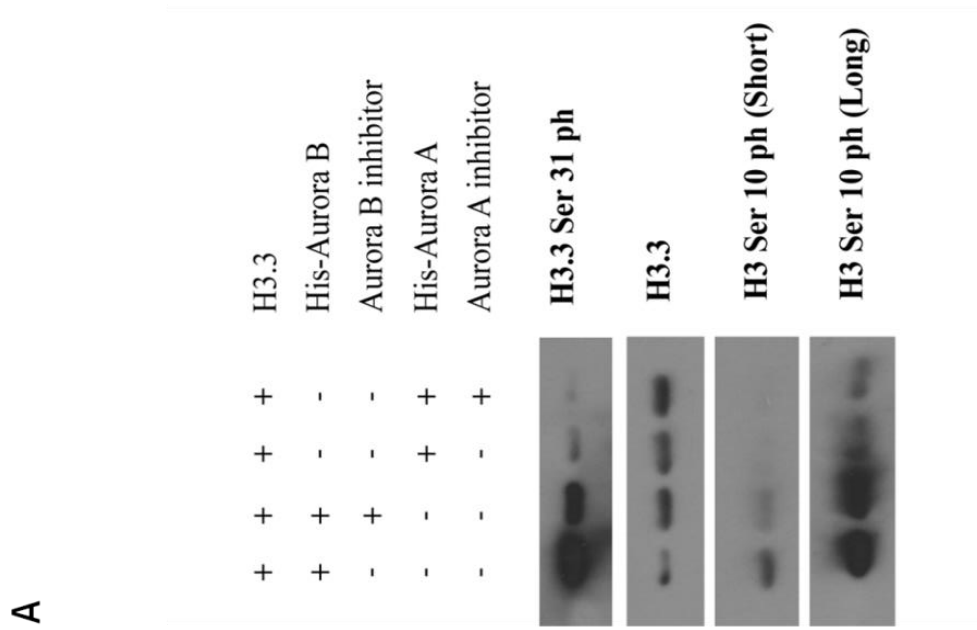
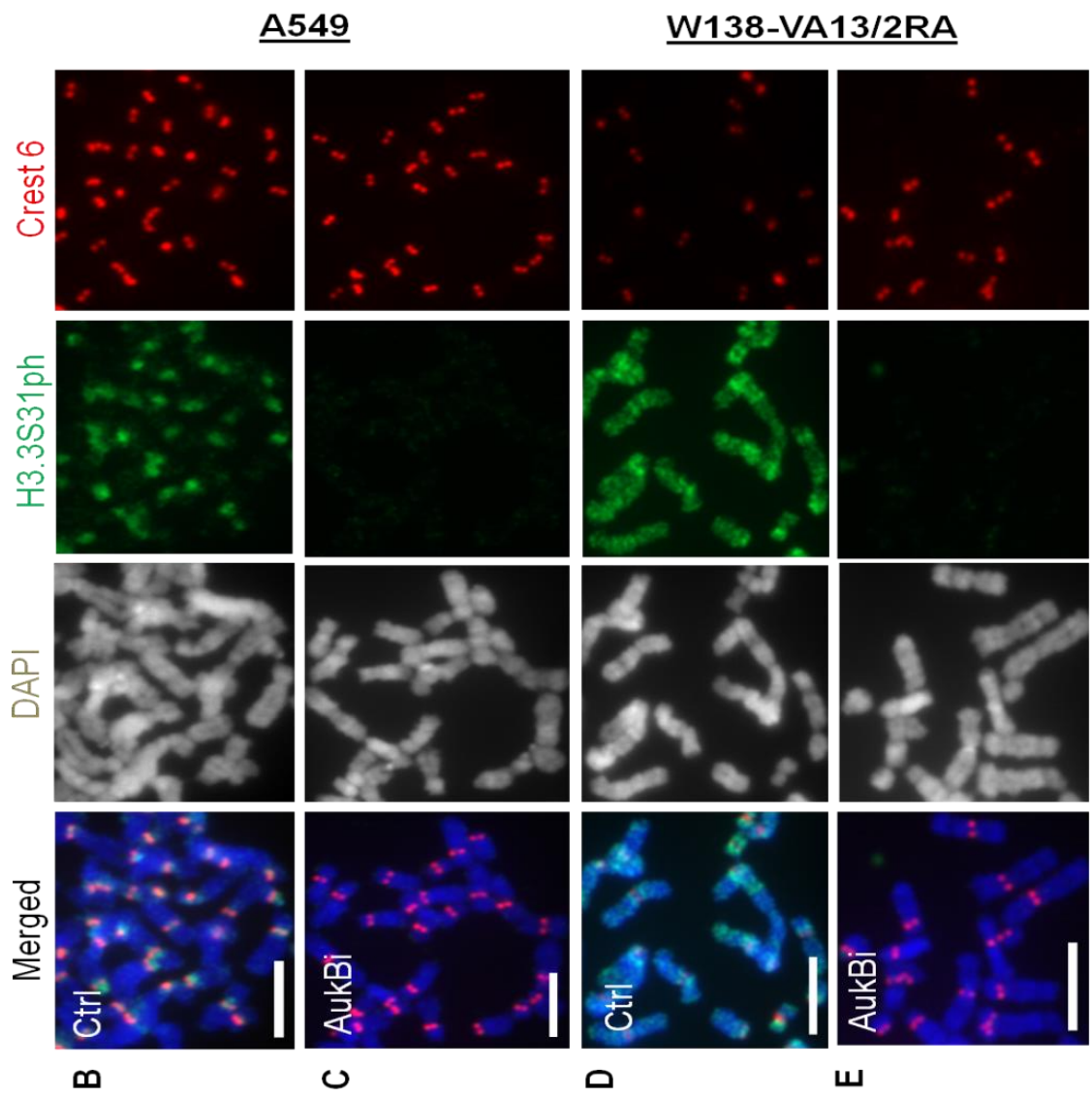


Page intentionally left blank

Page intentionally left blank

Supplementary Figure 7 Phosphorylation of H3.3 Serine 31 residue by the Aurora A and Aurora B kinases

(A) *In vitro* kinase reaction was also performed using the recombinant His-tagged Aurora A or the Aurora B with the H3.3 protein, followed by Western blot analysis with the anti-H3.3S31ph antibody. A strong 17 kDa band was observed when the Aurora B was incubated with the H3.3 protein. The intensity of the H3.3S31ph band was reduced significantly when the Aurora B inhibitor, Hesperadin was added to the reaction. Likewise, a less intense band was detected when the recombinant tagged Aurora A kinase was incubated with the H3.3 protein. Immunoblotting with the antibody against H3S10ph was included as a positive control for the kinase reaction. In the presence of the Aurora B specific inhibitor, a significant reduction in the H3S10 ph intensity was detected (Short exposure time) *Lane 1*: 1 μ g recombinant H3.1 with 0.5 μ g His-tagged Aurora B; *lane 2*: 1 μ g recombinant H3.3 with 0.5 μ g His-tagged Aurora B and 250 nM Hesperadin; *lane 3*: 1 μ g recombinant H3.3 with 0.5 μ g His-tagged Aurora 1; *lane 4*: 1 μ g recombinant H3.3 with 0.5 μ g His-tagged Aurora A and 2 μ M ZM447493. Immunofluorescence analysis with antibodies against H3.3S31ph (green) and Crest 6 (red) was performed to examine the distribution of H3.3S31ph. Cells were treated with Colcemid in the presence or absence of 250 nM (Ctrl) or Hesperadin (AukBi) for 2 h. (B-C) In non-ALT A549 cells, treatment with AukBi led to the removal of H3.3S31ph staining on pericentric satellite repeats. (D-E) Treatment with AukBi also led to a significant reduction in the level of H3.3S31ph staining on chromosome arms, as well as the pericentric region in ALT positive W138-VA13/2RA cells. Scale = 5 μ m. Representative images of 30 chromosome spreads.



Page intentionally left blank

REFERENCES

Abreu, E., Aritonovska, E., Reichenbach, P., Cristofari, G., Culp, B., Terns, R.M., Lingner, J., and Terns, M.P. (2010). TIN2-Tethered TPP1 Recruits Human Telomerase to Telomeres In Vivo. *Molecular and Cellular Biology* 30, 2971-2982.

Adam, S., Polo, S.E., and Almouzni, G. (2013). Transcription recovery after DNA damage requires chromatin priming by the H3.3 histone chaperone HIRA. *Cell* 155, 94-106.

Aguilera, A., and Garcia-Muse, T. (2012). R loops: from transcription byproducts to threats to genome stability. *Molecular cell* 46, 115-124.

Ahmad, K., and Henikoff, S. (2002). The histone variant H3.3 marks active chromatin by replication-independent nucleosome assembly. *Molecular cell* 9, 1191-1200.

Arnoult, N., Van Beneden, A., and Decottignies, A. (2012). Telomere length regulates TERRA levels through increased trimethylation of telomeric H3K9 and HP1 α . *Nature structural & molecular biology* 19, 948-956.

Arora, R., Lee, Y., Wischnewski, H., Brun, C.M., Schwarz, T., and Azzalin, C.M. (2014). RNaseH1 regulates TERRA-telomeric DNA hybrids and telomere maintenance in ALT tumour cells. *Nat Commun* 5.

Ayrapetov, M.K., Gursoy-Yuzugullu, O., Xu, C., Xu, Y., and Price, B.D. (2014). DNA double-strand breaks promote methylation of histone H3 on lysine 9 and transient formation of repressive chromatin. *Proceedings of the National Academy of Sciences of the United States of America* 111, 9169-9174.

Azzalin, C.M., Reichenbach, P., Khoriantuli, L., Giulotto, E., and Lingner, J. (2007). Telomeric repeat-containing RNA and RNA surveillance factors at mammalian chromosome ends. *Science* 318, 798-801.

Bakhoun, S.F., Kabeche, L., Murnane, J.P., Zaki, B.I., and Compton, D.A. (2014). DNA-Damage Response during Mitosis Induces Whole-Chromosome Missegregation. *Cancer discovery*.

Balk, B., Maicher, A., Dees, M., Klermund, J., Luke-Glaser, S., Bender, K., and Luke, B. (2013). Telomeric RNA-DNA hybrids affect telomere-length dynamics and senescence. *Nature structural & molecular biology* 20, 1199-1205.

Baur, J.A., Zou, Y., Shay, J.W., and Wright, W.E. (2001). Telomere position effect in human cells. *Science* 292, 2075-2077.

Beier, F., Foronda, M., Martinez, P., and Blasco, M.A. (2012). Conditional TRF1 knockout in the hematopoietic compartment leads to bone marrow failure and recapitulates clinical features of dyskeratosis congenita. *Blood* 120, 2990-3000.

Bender, S., Tang, Y., Lindroth, A.M., Hovestadt, V., Jones, D.T., Kool, M., Zapatka, M., Northcott, P.A., Sturm, D., Wang, W., *et al.* (2013). Reduced H3K27me3 and DNA hypomethylation are major drivers of gene expression in K27M mutant pediatric high-grade gliomas. *Cancer cell* 24, 660-672.

Benetti, R., Gonzalo, S., Jaco, I., Schotta, G., Klatt, P., Jenuwein, T., and Blasco, M.A. (2007). Suv4-20h deficiency results in telomere elongation and derepression of telomere recombination. *The Journal of cell biology* 178, 925-936.

Bernardi, R., and Pandolfi, P.P. (2007). Structure, dynamics and functions of promyelocytic leukaemia nuclear bodies. *Nat Rev Mol Cell Bio* 8, 1006-1016.

Bernstein, B.E., Mikkelsen, T.S., Xie, X.H., Kamal, M., Huebert, D.J., Cuff, J., Fry, B., Meissner, A., Wernig, M., Plath, K., *et al.* (2006). A bivalent chromatin structure marks key developmental genes in embryonic stem cells. *Cell* 125, 315-326.

Bischof, O., Kim, S.H., Irving, J., Beresten, S., Ellis, N.A., and Campisi, J. (2001). Regulation and localization of the Bloom syndrome protein in response to DNA damage. *Journal of Cell Biology* 153, 367-380.

Bjerke, L., Mackay, A., Nandhabalan, M., Burford, A., Jury, A., Popov, S., Bax, D.A., Carvalho, D., Taylor, K.R., Vinci, M., *et al.* (2013). Histone H3.3 mutations drive pediatric glioblastoma through upregulation of MYCN. *Cancer discovery* 3, 512-519.

- Blanco, R., Munoz, P., Flores, J.M., Klatt, P., and Blasco, M.A. (2007). Telomerase abrogation dramatically accelerates TRF2-induced epithelial carcinogenesis. *Genes & development* 21, 206-220.
- Blasco, M.A. (2005). Telomeres and human disease: Ageing, cancer and beyond. *Nat Rev Genet* 6, 611-622.
- Blasco, M.A. (2007). The epigenetic regulation of mammalian telomeres. *Nat Rev Genet* 8, 299-309.
- Bohr, V.A. (2008). Rising from the RecQ-age: the role of human RecQ helicases in genome maintenance. *Trends in Biochemical Sciences* 33, 609-620.
- Bombarde, O., Boby, C., Gomez, D., Frit, P., Giraud-Panis, M.J., Gilson, E., Salles, B., and Calsou, P. (2010). TRF2/RAP1 and DNA-PK mediate a double protection against joining at telomeric ends. *Embo Journal* 29, 1573-1584.
- Bower, K., Napier, C.E., Cole, S.L., Dagg, R.A., Lau, L.M., Duncan, E.L., Moy, E.L., and Reddel, R.R. (2012). Loss of wild-type ATRX expression in somatic cell hybrids segregates with activation of Alternative Lengthening of Telomeres. *PloS one* 7, e50062.
- Broccoli, D., Smogorzewska, A., Chong, L., and de Lange, T. (1997). Human telomeres contain two distinct Myb-related proteins, TRF1 and TRF2. *Nature genetics* 17, 231-235.
- Bryan, T.M., Englezou, A., Dalla-Pozza, L., Dunham, M.A., and Reddel, R.R. (1997). Evidence for an alternative mechanism for maintaining telomere length in human tumors and tumor-derived cell lines. *Nature medicine* 3, 1271-1274.
- Cai, L., Rothbart, S.B., Lu, R., Xu, B.W., Chen, W.Y., Tripathy, A., Rockowitz, S., Zheng, D.Y., Patel, D.J., Allis, C.D., *et al.* (2013). An H3K36 Methylation-Engaging Tudor Motif of Polycomb-like Proteins Mediates PRC2 Complex Targeting. *Molecular cell* 49, 571-582.
- Cann, K.L., and Dellaire, G. (2011). Heterochromatin and the DNA damage response: the need to relax. *Biochem Cell Biol* 89, 45-60.

Canudas, S., Houghtaling, B.R., Bhanot, M., Sasa, G., Savage, S.A., Bertuch, A.A., and Smith, S. (2011). A role for heterochromatin protein 1gamma at human telomeres. *Genes & development* 25, 1807-1819.

Carmena, M., Ruchaud, S., and Earnshaw, W.C. (2009). Making the Auroras glow: regulation of Aurora A and B kinase function by interacting proteins. *Current opinion in cell biology* 21, 796-805.

Cesare, A.J., Hayashi, M.T., Crabbe, L., and Karlseder, J. (2013). The telomere deprotection response is functionally distinct from the genomic DNA damage response. *Molecular cell* 51, 141-155.

Chan, F.L., Marshall, O.J., Saffery, R., Kim, B.W., Earle, E., Choo, K.H., and Wong, L.H. (2012). Active transcription and essential role of RNA polymerase II at the centromere during mitosis. *Proceedings of the National Academy of Sciences of the United States of America* 109, 1979-1984.

Chang, C.C., Naik, M.T., Huang, Y.S., Jeng, J.C., Liao, P.H., Kuo, H.Y., Ho, C.C., Hsieh, Y.L., Lin, C.H., Huang, N.J., *et al.* (2011). Structural and functional roles of Daxx SIM phosphorylation in SUMO paralog-selective binding and apoptosis modulation. *Molecular cell* 42, 62-74.

Chang, F.T., McGhie, J.D., Chan, F.L., Tang, M.C., Anderson, M.A., Mann, J.R., Andy Choo, K.H., and Wong, L.H. (2013). PML bodies provide an important platform for the maintenance of telomeric chromatin integrity in embryonic stem cells. *Nucleic acids research* 41, 4447-4458.

Cho, S., Park, J.S., and Kang, Y.K. (2011). Dual Functions of Histone-Lysine N-Methyltransferase Setdb1 Protein at Promyelocytic Leukemia-Nuclear Body (PML-NB) maintaining PML-NB and regulating the expression of its associated genes.

. *Journal of Biological Chemistry* 286, 41115-41124.

Chueh, A.C., Wong, L.H., Wong, N., and Choo, K.H. (2005). Variable and hierarchical size distribution of L1-retroelement-enriched CENP-A clusters within a functional human neocentromere. *Human molecular genetics* 14, 85-93.

Clynes, D., and Gibbons, R.J. (2013). ATRX and the replication of structured DNA. *Current opinion in genetics & development* 23, 289-294.

Clynes, D., Higgs, D.R., and Gibbons, R.J. (2013). The chromatin remodeller ATRX: a repeat offender in human disease. *Trends Biochem Sci* 38, 461-466.

Corpet, A., Olbrich, T., Gwerder, M., Fink, D., and Stucki, M. (2014). Dynamics of histone H3.3 deposition in proliferating and senescent cells reveals a DAXX-dependent targeting to PML-NBs important for pericentromeric heterochromatin organization. *Cell Cycle* 13, 249-267.

Crabbe, L., Verdun, R.E., Haggblom, C.I., and Karlseder, J. (2004). Defective telomere lagging strand synthesis in cells lacking WRN helicase activity. *Science* 306, 1951-1953.

Crosio, C., Fimia, G.M., Loury, R., Kimura, M., Okano, Y., Zhou, H., Sen, S., Allis, C.D., and Sassone-Corsi, P. (2002). Mitotic Phosphorylation of Histone H3: Spatio-Temporal Regulation by Mammalian Aurora Kinases. *Molecular and Cellular Biology* 22, 874-885.

Dai, J., Sultan, S., Taylor, S.S., and Higgins, J.M.G. (2005). The kinase haspin is required for mitotic histone H3 Thr 3 phosphorylation and normal metaphase chromosome alignment. *Genes & Development* 19, 472-488.

Dan, J., Liu, Y., Liu, N., Chiourea, M., Okuka, M., Wu, T., Ye, X., Mou, C., Wang, L., Wang, L., *et al.* (2014). Rif1 Maintains Telomere Length Homeostasis of ESCs by Mediating Heterochromatin Silencing. *Developmental Cell* 29, 7-19.

Davoli, T., Denchi, E.L., and de Lange, T. (2010). Persistent telomere damage induces by-pass of mitosis and tetraploidy. *Cell* 141, 81-93.

de Lange, T. (2005). Shelterin: the protein complex that shapes and safeguards human telomeres. *Genes & Development* 19, 2100-2110.

Delbarre, E., Ivanauskiene, K., Kuntziger, T., and Collas, P. (2013). DAXX-dependent supply of soluble (H3.3-H4) dimers to PML bodies pending deposition into chromatin. *Genome Res* 23, 440-451.

Dellaire, G., Ching, R.W., Ahmed, K., Jalali, F., Tse, K.C.K., Bristow, R.G., and Bazett-Jones, D.P. (2006a). Promyelocytic leukemia nuclear bodies behave as DNA damage sensors whose response to DNA double-strand breaks is regulated by NBS1 and the kinases ATM, Chk2, and ATR. *Journal of Cell Biology* 175, 55-66.

Dellaire, G., Ching, R.W., Dehghani, H., Ren, Y., and Bazett-Jones, D.P. (2006b). The number of PML nuclear bodies increases in early S phase by a fission mechanism. *J Cell Sci* 119, 1026-1033.

Denchi, E.L., and de Lange, T. (2007). Protection of telomeres through independent control of ATM and ATR by TRF2 and POT1. *Nature* 448, 1068-1071.

Deng, Z., Glousker, G., Molczan, A., Fox, A.J., Lamm, N., Dheekollu, J., Weizman, O.E., Schertzer, M., Wang, Z., Vladimirova, O., *et al.* (2013). Inherited mutations in the helicase RTEL1 cause telomere dysfunction and Hoyeraal-Hreidarsson syndrome. *Proceedings of the National Academy of Sciences of the United States of America* 110, E3408-E3416.

Deng, Z., Norseen, J., Wiedmer, A., Riethman, H., and Lieberman, P.M. (2009). TERRA RNA Binding to TRF2 Facilitates Heterochromatin Formation and ORC Recruitment at Telomeres. *Molecular cell* 35, 403-413.

Dhayalan, A., Tamas, R., Bock, I., Tattermusch, A., Dimitrova, E., Kudithipudi, S., Ragozin, S., and Jeltsch, A. (2011). The ATRX-ADD domain binds to H3 tail peptides and reads the combined methylation state of K4 and K9. *Human Molecular Genetics* 20, 2195-2203.

Dimitrova, N., Chen, Y.C.M., Spector, D.L., and de Lange, T. (2008). 53BP1 promotes non-homologous end joining of telomeres by increasing chromatin mobility. *Nature* 456, 524-U551.

Dorris, K., Sobo, M., Onar-Thomas, A., Panditharatna, E., Stevenson, C.B., Gardner, S.L., Dewire, M.D., Pierson, C.R., Olshefski, R., Rempel, S.A., *et al.* (2014). Prognostic significance of telomere maintenance mechanisms in pediatric high-grade gliomas. *Journal of neuro-oncology* 117, 67-76.

Drane, P., Ouararhni, K., Depaux, A., Shuaib, M., and Hamiche, A. (2010). The death-associated protein DAXX is a novel histone chaperone involved in the replication-independent deposition of H3.3. *Genes & Development* 24, 1253-1265.

Draskovic, I., Arnoult, N., Steiner, V., Bacchetti, S., Lomonte, P., and Londono-Vallejo, A. (2009). Probing PML body function in ALT cells reveals spatiotemporal requirements for telomere recombination. *Proceedings of the National Academy of Sciences of the United States of America* 106, 15726-15731.

Dunham, M.A., Neumann, A.A., Fasching, C.L., and Reddel, R.R. (2000). Telomere maintenance by recombination in human cells. *Nat Genet* 26, 447-450.

Dunleavy, E.M., Roche, D., Tagami, H., Lacoste, N., Ray-Gallet, D., Nakamura, Y., Daigo, Y., Nakatani, Y., and Almouzni-Pettinotti, G. (2009). HJURP is a cell-cycle-dependent maintenance and deposition factor of CENP-A at centromeres. *Cell* 137, 485-497.

Elsaesser, S.J., and Allis, C.D. (2010). HIRA and Daxx constitute two independent histone H3.3-containing predeposition complexes. *Cold Spring Harbor symposia on quantitative biology* 75, 27-34.

Episkopou, H., Draskovic, I., Van Beneden, A., Tilman, G., Mattiussi, M., Gobin, M., Arnoult, N., Londono-Vallejo, A., and Decottignies, A. (2014). Alternative Lengthening of Telomeres is characterized by reduced compaction of telomeric chromatin. *Nucleic Acids Research* 42, 4391-4405.

Eustermann, S., Yang, J.C., Law, M.J., Amos, R., Chapman, L.M., Jelinska, C., Garrick, D., Clynes, D., Gibbons, R.J., Rhodes, D., *et al.* (2011). Combinatorial readout of histone H3 modifications specifies localization of ATRX to heterochromatin. *Nature structural & molecular biology* 18, 777-U750.

Fischle, W., Tseng, B.S., Dormann, H.L., Ueberheide, B.M., Garcia, B.A., Shabanowitz, J., Hunt, D.F., Funabiki, H., and Allis, C.D. (2005). Regulation of HP1-chromatin binding by histone H3 methylation and phosphorylation. *Nature* 438, 1116-1122.

Fischle, W., Wang, Y., and Allis, C.D. (2003). Binary switches and modification cassettes in histone biology and beyond. *Nature* 425, 475-479.

Flynn, R.L., Centore, R.C., O'Sullivan, R.J., Rai, R., Tse, A., Songyang, Z., Chang, S., Karlseder, J., and Zou, L. (2011). TERRA and hnRNPA1 orchestrate an RPA-to-POT1 switch on telomeric single-stranded DNA. *Nature* 471, 532-536.

Flynn, R.L., Cox, K.E., Jeitany, M., Wakimoto, H., Bryll, A.R., Ganem, N.J., Bersani, F., Pineda, J.R., Suva, M.L., Benes, C.H., *et al.* (2015). Alternative lengthening of telomeres renders cancer cells hypersensitive to ATR inhibitors. *Science* 347, 273-277.

Foltman, M., Evrin, C., De Piccoli, G., Jones, R.C., Edmondson, R.D., Katou, Y., Nakato, R., Shirahige, K., and Labib, K. (2013). Eukaryotic replisome components cooperate to process histones during chromosome replication. *Cell reports* 3, 892-904.

Foltz, D.R., Jansen, L.E., Bailey, A.O., Yates, J.R., 3rd, Bassett, E.A., Wood, S., Black, B.E., and Cleveland, D.W. (2009). Centromere-specific assembly of CENP-a nucleosomes is mediated by HJURP. *Cell* 137, 472-484.

Fong, J.J., Nguyen, B.L., Bridger, R., Medrano, E.E., Wells, L., Pan, S.J., and Sifers, R.N. (2012). beta-N-Acetylglucosamine (O-GlcNAc) Is a Novel Regulator of Mitosis-specific Phosphorylations on Histone H3. *Journal of Biological Chemistry* 287, 12195-12203.

Fonseca, J.P., Steffen, P.A., Muller, S., Lu, J., Sawicka, A., Seiser, C., and Ringrose, L. (2012). In vivo Polycomb kinetics and mitotic chromatin binding distinguish stem cells from differentiated cells. *Genes & development* 26, 857-871.

Fradet-Turcotte, A., Canny, M.D., Escribano-Diaz, C., Orthwein, A., Leung, C.C.Y., Huang, H., Landry, M.C., Kitevski-LeBlanc, J., Noordermeer, S.M., Sicheri, F., *et al.* (2013). 53BP1 is a reader of the DNA-damage-induced H2A Lys 15 ubiquitin mark. *Nature* 499, 50-+.

Frescas, D., and de Lange, T. (2014). TRF2-tethered TIN2 can mediate telomere protection by TPP1/POT1. *Molecular and cellular biology* 34, 1349-1362.

Frey, A., Listovsky, T., Guilbaud, G., Sarkies, P., and Sale, J.E. (2014). Histone H3.3 Is Required to Maintain Replication Fork Progression after UV Damage. *Curr Biol* 24, 2195-2201.

Gagos, S., Chiourea, M., Christodoulidou, A., Apostolou, E., Raftopoulou, C., Deustch, S., Jefford, C.-E., Irminger-Finger, I., Shay, J.W., and Antonarakis, S.E. (2008). Pericentromeric Instability and Spontaneous Emergence of Human Neoacrocentric and Minute Chromosomes in the Alternative Pathway of Telomere Lengthening. *Cancer Res* 68, 8146-8155.

Garcia-Cao, M., O'Sullivan, R., Peters, A.H., Jenuwein, T., and Blasco, M.A. (2004). Epigenetic regulation of telomere length in mammalian cells by the Suv39h1 and Suv39h2 histone methyltransferases. *Nature genetics* 36, 94-99.

Gehani, S.S., Agrawal-Singh, S., Dietrich, N., Christophersen, N.S., Helin, K., and Hansen, K. (2010). Polycomb Group Protein Displacement and Gene Activation through MSK-Dependent H3K27me3S28 Phosphorylation. *Molecular cell* 39, 886-900.

Gibbons, R.J., McDowell, T.L., Raman, S., O'Rourke, D.M., Garrick, D., Ayyub, H., and Higgs, D.R. (2000). Mutations in ATRX, encoding a SWI/SNF-like protein, cause diverse changes in the pattern of DNA methylation. *Nat Genet* 24, 368-371.

Giraud-Panis, M.J., Pisano, S., Benarroch-Popivker, D., Pei, B., Le Du, M.H., and Gilson, E. (2013). One identity or more for telomeres? *Frontiers in oncology* 3, 48.

Giunta, S., Belotserkovskaya, R., and Jackson, S.P. (2010). DNA damage signaling in response to double-strand breaks during mitosis. *The Journal of cell biology* 190, 197-207.

Goldberg, A.D., Banaszynski, L.A., Noh, K.M., Lewis, P.W., Elsaesser, S.J., Stadler, S., Dewell, S., Law, M., Guo, X.Y., Li, X., *et al.* (2010). Distinct Factors Control Histone Variant H3.3 Localization at Specific Genomic Regions. *Cell* 140, 678-691.

Gonzalo, S., Jaco, I., Fraga, M.F., Chen, T., Li, E., Esteller, M., and Blasco, M.A. (2006). DNA methyltransferases control telomere length and telomere recombination in mammalian cells. *Nature cell biology* 8, 416-424.

Goto, H., Yasui, Y., Nigg, E.A., and Inagaki, M. (2002). Aurora-B phosphorylates histone H3 at serine28 with regard to the mitotic chromosome condensation. *Genes Cells* 7, 11-17.

Griffith, J.D., Comeau, L., Rosenfield, S., Stansel, R.M., Bianchi, A., Moss, H., and de Lange, T. (1999). Mammalian telomeres end in a large duplex loop. *Cell* 97, 503-514.

Guo, R., Zheng, L., Park, J.W., Lv, R., Chen, H., Jiao, F., Xu, W., Mu, S., Wen, H., Qiu, J., *et al.* (2014). BS69/ZMYND11 Reads and Connects Histone H3.3 Lysine 36 Trimethylation-Decorated Chromatin to Regulated Pre-mRNA Processing. *Molecular cell* 56, 298-310.

Hake, S.B., Garcia, B.A., Kauer, M., Baker, S.P., Shabanowitz, J., Hunt, D.F., and Allis, C.D. (2005). Serine 31 phosphorylation of histone variant H3.3 is specific to regions bordering centromeres in metaphase chromosomes. *Proc Natl Acad Sci U S A* 102, 6344-6349.

Hayashi, M.T., Cesare, A.J., Fitzpatrick, J.A., Lazzerini-Denchi, E., and Karlseder, J. (2012). A telomere-dependent DNA damage checkpoint induced by prolonged mitotic arrest. *Nature structural & molecular biology* 19, 387-394.

Heaphy, C.M., de Wilde, R.F., Jiao, Y.C., Klein, A.P., Edil, B.H., Shi, C.J., Bettgowda, C., Rodriguez, F.J., Eberhart, C.G., Hebbar, S., *et al.* (2011a). Altered Telomeres in Tumors with ATRX and DAXX Mutations. *Science* 333, 425-425.

Heaphy, C.M., Subhawong, A.P., Hong, S.M., Goggins, M.G., Montgomery, E.A., Gabrielson, E., Netto, G.J., Epstein, J.I., Lotan, T.L., Westra, W.H., *et al.* (2011b). Prevalence of the alternative lengthening of telomeres telomere maintenance mechanism in human cancer subtypes. *The American journal of pathology* 179, 1608-1615.

Henzel, M.J., Wei, Y., Mancini, M.A., VanHooser, A., Ranalli, T., Brinkley, B.R., BazettJones, D.P., and Allis, C.D. (1997). Mitosis-specific phosphorylation of histone H3 initiates primarily within pericentromeric heterochromatin during G2 and spreads in an ordered fashion coincident with mitotic chromosome condensation. *Chromosoma* 106, 348-360.

Henson, J.D., Cao, Y., Huschtscha, L.I., Chang, A.C., Au, A.Y.M., Pickett, H.A., and Reddel, R.R. (2009). DNA C-circles are specific and quantifiable markers of alternative-lengthening-of-telomeres activity. *Nat Biotechnol* 27, 1181-U1148.

Hirashima, K., and Seimiya, H. (2015). Telomeric repeat-containing RNA/G-quadruplex-forming sequences cause genome-wide alteration of gene expression in human cancer cells in vivo. *Nucleic acids research* *43*, 2022-2032.

Hirota, T., Lipp, J.J., Toh, B.H., and Peters, J.M. (2005). Histone H3 serine 10 phosphorylation by Aurora B causes HP1 dissociation from heterochromatin. *Nature* *438*, 1176-1180.

Hockemeyer, D., Palm, W., Else, T., Daniels, J.P., Takai, K.K., Ye, J.Z.S., Keegan, C.E., de Lange, T., and Hammer, G.D. (2007). Telomere protection by mammalian Pot1 requires interaction with Tpp1. *Nature structural & molecular biology* *14*, 754-761.

Hockemeyer, D., Sfeir, A.J., Shay, J.W., Wright, W.E., and de Lange, T. (2005). POT1 protects telomeres from a transient DNA damage response and determines how human chromosomes end. *Embo Journal* *24*, 2667-2678.

Hollenbach, A.D., McPherson, C.J., Mientjes, E.J., Iyengar, R., and Grosveld, G. (2002). Daxx and histone deacetylase II associate with chromatin through an interaction with core histones and the chromatin-associated protein Dek. *J Cell Sci* *115*, 3319-3330.

Huang, X., Tran, T., Zhang, L., Hatcher, R., and Zhang, P. (2005). DNA damage-induced mitotic catastrophe is mediated by the Chk1-dependent mitotic exit DNA damage checkpoint. *Proc Natl Acad Sci U S A* *102*, 1065-1070.

Huh, M.S., O'Dea, T.P., Ouazia, D., McKay, B.C., Parise, G., Parks, R.J., Rudnicki, M.A., and Picketts, D.J. (2012). Compromised genomic integrity impedes muscle growth after Atrx inactivation. *J Clin Invest* *122*, 4412-4423.

Ishov, A.M., Sotnikov, A.G., Negorev, D., Vladimirova, O.V., Neff, N., Kamitani, T., Yeh, E.T., Strauss, J.F., 3rd, and Maul, G.G. (1999). PML is critical for ND10 formation and recruits the PML-interacting protein daxx to this nuclear structure when modified by SUMO-1. *The Journal of cell biology* *147*, 221-234.

Ivanauskiene, K., Delbarre, E., McGhie, J., Küntziger, T., Wong, L.H., and Collas, P. (2014). The PML-associated protein DEK regulates the balance of H3.3 loading on chromatin and is important for telomere integrity. *Genome Res*.

Jiang, W.Q., Nguyen, A., Cao, Y., Chang, A.C., and Reddel, R.R. (2011). HP1-mediated formation of alternative lengthening of telomeres-associated PML bodies requires HIRA but not ASF1a. *Plos One* 6, e17036.

Jiang, W.Q., Zhong, Z.H., Henson, J.D., Neumann, A.A., Chang, A.C., and Reddel, R.R. (2005). Suppression of alternative lengthening of telomeres by Sp100-mediated sequestration of the MRE11/RAD50/NBS1 complex. *Molecular and cellular biology* 25, 2708-2721.

Jiao, Y., Shi, C., Edil, B.H., de Wilde, R.F., Klimstra, D.S., Maitra, A., Schulick, R.D., Tang, L.H., Wolfgang, C.L., Choti, M.A., *et al.* (2011). DAXX/ATRX, MEN1, and mTOR pathway genes are frequently altered in pancreatic neuroendocrine tumors. *Science* 331, 1199-1203.

Jiao, Y., Shi, C., Edil, B.H., de Wilde, R.F., Klimstra, D.S., Maitra, A., Schulick, R.D., Tang, L.H., Wolfgang, C.L., Choti, M.A., *et al.* (2010). DAXX/ATRX, MEN1, and mTOR Pathway Genes Are Frequently Altered in Pancreatic Neuroendocrine Tumors. *Science* 331, 1199-1203.

Jin, C., and Felsenfeld, G. (2007). Nucleosome stability mediated by histone variants H3.3 and H2A.Z. *Genes & development* 21, 1519-1529.

Kabir, S., Hockemeyer, D., and de Lange, T. (2014). TALEN gene knockouts reveal no requirement for the conserved human shelterin protein Rap1 in telomere protection and length regulation. *Cell reports* 9, 1273-1280.

Kannan, K., Inagaki, A., Silber, J., Gorovets, D., Zhang, J., Kasthuber, E.R., Heguy, A., Petrini, J.H., Chan, T.A., and Huse, J.T. (2012). Whole-exome sequencing identifies ATRX mutation as a key molecular determinant in lower-grade glioma. *Oncotarget* 3, 1194-1203.

Kappes, F., Waldmann, T., Mathew, V., Yu, J.D., Zhang, L., Khodadoust, M.S., Chinnaiyan, A.M., Luger, K., Erhardt, S., Schneider, R., *et al.* (2011). The DEK oncoprotein is a Su(var) that is essential to heterochromatin integrity. *Genes & Development* 25, 673-678.

Karlseder, J., Hoke, K., Mirzoeva, O.K., Bakkenist, C., Kastan, M.B., Petrini, J.H., and de Lange, T. (2004). The telomeric protein TRF2 binds the ATM kinase and can inhibit the ATM-dependent DNA damage response. *PLoS biology* 2, E240.

Karlseder, J., Kachatrian, L., Takai, H., Mercer, K., Hingorani, S., Jacks, T., and de Lange, T. (2003). Targeted deletion reveals an essential function for the telomere length regulator Trf1. *Molecular and cellular biology* 23, 6533-6541.

Khuong-Quang, D.A., Buczkowicz, P., Rakopoulos, P., Liu, X.Y., Fontebasso, A.M., Bouffet, E., Bartels, U., Albrecht, S., Schwartzentruber, J., Letourneau, L., *et al.* (2012). K27M mutation in histone H3.3 defines clinically and biologically distinct subgroups of pediatric diffuse intrinsic pontine gliomas. *Acta neuropathologica* 124, 439-447.

Kim, S.H., Beausejour, C., Davalos, A.R., Kaminker, P., Heo, S.J., and Campisi, J. (2004). TIN2 mediates functions of TRF2 at human telomeres. *Journal of Biological Chemistry* 279, 43799-43804.

Konev, A.Y., Tribus, M., Park, S.Y., Podhraski, V., Lim, C.Y., Emelyanov, A.V., Vershilova, E., Pirrotta, V., Kadonaga, J.T., Lusser, A., *et al.* (2007). CHD1 motor protein is required for deposition of histone variant h3.3 into chromatin in vivo. *Science* 317, 1087-1090.

Kouzarides, T. (2007). Chromatin modifications and their function. *Cell* 128, 693-705.

Kraushaar, D.C., Jin, W., Maunakea, A., Abraham, B., Ha, M., and Zhao, K. (2013). Genome-wide incorporation dynamics reveal distinct categories of turnover for the histone variant H3.3. *Genome biology* 14, R121.

Lacoste, N., Woolfe, A., Tachiwana, H., Garea, A.V., Barth, T., Cantaloube, S., Kurumizaka, H., Imhof, A., and Almouzni, G. (2014). Mislocalization of the Centromeric Histone Variant CenH3/CENP-A in Human Cells Depends on the Chaperone DAXX. *Molecular cell* 53, 631-644.

Law, M.J., Lower, K.M., Voon, H.P., Hughes, J.R., Garrick, D., Viprakasit, V., Mitson, M., De Gobbi, M., Marra, M., Morris, A., *et al.* (2010). ATR-X syndrome protein targets tandem repeats and influences allele-specific expression in a size-dependent manner. *Cell* 143, 367-378.

Lee, D.H., Acharya, S.S., Kwon, M., Drane, P., Guan, Y.H., Adelmant, G., Kalev, P., Shah, J., Pellman, D., Marto, J.A., *et al.* (2014). Dephosphorylation Enables the Recruitment of 53BP1 to Double-Strand DNA Breaks. *Molecular cell* *54*, 512-525.

Leung, J.W.C., Ghosal, G., Wang, W.Q., Shen, X., Wang, J.D., Li, L., and Chen, J.J. (2013). Alpha Thalassemia/Mental Retardation Syndrome X-linked Gene Product ATRX Is Required for Proper Replication Restart and Cellular Resistance to Replication Stress. *Journal of Biological Chemistry* *288*, 6342-6350.

Levy, M.A., Kernohan, K.D., Jiang, Y., and Bérubé, N.G. (2014). ATRX promotes gene expression by facilitating transcriptional elongation through guanine-rich coding regions. *Human Molecular Genetics*.

Lewis, P.W., Elsaesser, S.J., Noh, K.M., Stadler, S.C., and Allis, C.D. (2010). Daxx is an H3.3-specific histone chaperone and cooperates with ATRX in replication-independent chromatin assembly at telomeres. *Proceedings of the National Academy of Sciences of the United States of America* *107*, 14075-14080.

Lewis, P.W., Muller, M.M., Koletsky, M.S., Cordero, F., Lin, S., Banaszynski, L.A., Garcia, B.A., Muir, T.W., Becher, O.J., and Allis, C.D. (2013). Inhibition of PRC2 activity by a gain-of-function H3 mutation found in pediatric glioblastoma. *Science* *340*, 857-861.

Lin, C.J., Conti, M., and Ramalho-Santos, M. (2013). Histone variant H3.3 maintains a decondensed chromatin state essential for mouse preimplantation development. *Development* *140*, 3624-3634.

Lin, C.J., Koh, F.M., Wong, P., Conti, M., and Ramalho-Santos, M. (2014). Hira-Mediated H3.3 Incorporation Is Required for DNA Replication and Ribosomal RNA Transcription in the Mouse Zygote. *Developmental cell*.

Liokatis, S., Stutzer, A., Elsaesser, S.J., Theillet, F.X., Klingberg, R., van Rossum, B., Schwarzer, D., Allis, C.D., Fischle, W., and Selenko, P. (2012). Phosphorylation of histone H3 Ser10 establishes a hierarchy for subsequent intramolecular modification events. *Nature structural & molecular biology* *19*, 819-823.

Lipps, H.J., and Rhodes, D. (2009). G-quadruplex structures: in vivo evidence and function. *Trends Cell Biol* *19*, 414-422.

Lovejoy, C.A., Li, W., Reisenweber, S., Thongthip, S., Bruno, J., de Lange, T., De, S., Petrini, J.H., Sung, P.A., Jasin, M., *et al.* (2012). Loss of ATRX, genome instability, and an altered DNA damage response are hallmarks of the alternative lengthening of telomeres pathway. *Plos Genet* *8*, e1002772.

Loyola, A., and Almouzni, G. (2007). Marking histone H3 variants: how, when and why? *Trends Biochem Sci* *32*, 425-433.

Luciani, J.J., Depetris, D., Usson, Y., Metzler-Guillemain, C., Mignon-Ravix, C., Mitchell, M.J., Megarbane, A., Sarda, P., Sirma, H., Moncla, A., *et al.* (2006). PML nuclear bodies are highly organised DNA-protein structures with a function in heterochromatin remodelling at the G2 phase. *J Cell Sci* *119*, 2518-2531.

Lukas, C., Savic, V., Bekker-Jensen, S., Doil, C., Neumann, B., Pedersen, R.S., Grofte, M., Chan, K.L., Hickson, I.D., Bartek, J., *et al.* (2011). 53BP1 nuclear bodies form around DNA lesions generated by mitotic transmission of chromosomes under replication stress. *Nature cell biology* *13*, 243-U380.

Maicher, A., Kastner, L., Dees, M., and Luke, B. (2012). Deregulated telomere transcription causes replication-dependent telomere shortening and promotes cellular senescence. *Nucleic Acids Research* *40*, 6649-6659.

Mangerel, J., Price, A., Castelo-Branco, P., Brzezinski, J., Buczkowicz, P., Rakopoulos, P., Merino, D., Baskin, B., Wasserman, J., Mistry, M., *et al.* (2014). Alternative lengthening of telomeres is enriched in, and impacts survival of TP53 mutant pediatric malignant brain tumors. *Acta Neuropathol* *128*, 853-862.

Margueron, R., and Reinberg, D. (2010). Chromatin structure and the inheritance of epigenetic information. *Nat Rev Genet* *11*, 285-296.

Marion, R.M., Schotta, G., Ortega, S., and Blasco, M.A. (2011). Suv4-20h abrogation enhances telomere elongation during reprogramming and confers a higher tumorigenic potential to iPS cells. *PloS one* *6*, e25680.

Martinez, P., Thanasoula, M., Carlos, A.R., Gomez-Lopez, G., Tejera, A.M., Schoeftner, S., Dominguez, O., Pisano, D.G., Tarsounas, M., and Blasco, M.A. (2010). Mammalian Rap1 controls telomere function and gene expression through binding to telomeric and extratelomeric sites. *Nature cell biology* 12, 768-780.

Martinez, P., Thanasoula, M., Munoz, P., Liao, C., Tejera, A., McNees, C., Flores, J.M., Fernandez-Capetillo, O., Tarsounas, M., and Blasco, M.A. (2009). Increased telomere fragility and fusions resulting from TRF1 deficiency lead to degenerative pathologies and increased cancer in mice. *Genes & development* 23, 2060-2075.

Metzger, E., Yin, N., Wissmann, M., Kunowska, N., Fischer, K., Friedrichs, N., Patnaik, D., Higgins, J.M., Potier, N., Scheidtmann, K.H., *et al.* (2008). Phosphorylation of histone H3 at threonine 11 establishes a novel chromatin mark for transcriptional regulation. *Nature cell biology* 10, 53-60.

Mikhailov, A., Cole, R.W., and Rieder, C.L. (2002). DNA damage during mitosis in human cells delays the metaphase/anaphase transition via the spindle-assembly checkpoint. *Current biology : CB* 12, 1797-1806.

Mohaghegh, P., Karow, J.K., Brosh, R.M., Jr., Bohr, V.A., and Hickson, I.D. (2001). The Bloom's and Werner's syndrome proteins are DNA structure-specific helicases. *Nucleic acids research* 29, 2843-2849.

Morozov, V.M., Gavrilova, E.V., Ogryzko, V.V., and Ishov, A.M. (2012). Dualistic function of Daxx at centromeric and pericentromeric heterochromatin in normal and stress conditions. *Nucleus-Austin* 3, 276-285.

Muñoz , P., Blanco, R., de Carcer, G., Schoeftner, S., Benetti, R., Flores, J.M., Malumbres, M., and Blasco, M.A. (2009). TRF1 Controls Telomere Length and Mitotic Fidelity in Epithelial Homeostasis. *Molecular and Cellular Biology* 29, 1608-1625.

Munoz, P., Blanco, R., Flores, J.M., and Blasco, M.A. (2005). XPF nuclease-dependent telomere loss and increased DNA damage in mice overexpressing TRF2 result in premature aging and cancer. *Nature genetics* 37, 1063-1071.

Nabetani, A., and Ishikawa, F. (2009). Unusual telomeric DNAs in human telomerase-negative immortalized cells. *Molecular and cellular biology* 29, 703-713.

Nakamura, M., Zhou, X.Z., Kishi, S., Kosugi, I., Tsutsui, Y., and Lu, K.P. (2001). A specific interaction between the telomeric protein Pin2/TRF1 and the mitotic spindle. *Current biology : CB* 11, 1512-1516.

Napier, C.E., Huschtscha, L.I., Harvey, A., Bower, K., Noble, J.R., Hendrickson, E.A., and Reddel, R.R. (2015). ATRX represses alternative lengthening of telomeres. *Oncotarget*.

Newhart, A., Rafalska-Metcalf, I.U., Yang, T., Negorev, D.G., and Janicki, S.M. (2012). Single-cell analysis of Daxx and ATRX-dependent transcriptional repression. *J Cell Sci* 125, 5489-5501.

Nguyen, D.N., Heaphy, C.M., de Wilde, R.F., Orr, B.A., Odia, Y., Eberhart, C.G., Meeker, A.K., and Rodriguez, F.J. (2013). Molecular and morphologic correlates of the alternative lengthening of telomeres phenotype in high-grade astrocytomas. *Brain Pathol* 23, 237-243.

Nie, X., Wang, H., Li, J., Holec, S., and Berger, F. (2014). The HIRA complex that deposits the histone H3.3 is conserved in Arabidopsis and facilitates transcriptional dynamics. *Biology open* 3, 794-802.

Noh, K.-M., Maze, I., Zhao, D., Xiang, B., Wenderski, W., Lewis, P.W., Shen, L., Li, H., and Allis, C.D. (2014). ATRX tolerates activity-dependent histone H3 methyl/phosphorylation switching to maintain repetitive element silencing in neurons. *Proceedings of the National Academy of Sciences*.

O'Sullivan, R.J., Arnoult, N., Lackner, D.H., Oganessian, L., Haggblom, C., Corpet, A., Almouzni, G., and Karlseder, J. (2014). Rapid induction of alternative lengthening of telomeres by depletion of the histone chaperone ASF1. *Nature structural & molecular biology* 21, 167-174.

Ohishi, T., Hirota, T., Tsuruo, T., and Seimiya, H. (2010). TRF1 mediates mitotic abnormalities induced by Aurora-A overexpression. *Cancer Res* 70, 2041-2052.

Ohishi, T., Muramatsu, Y., Yoshida, H., and Seimiya, H. (2014). TRF1 Ensures the Centromeric Function of Aurora-B and Proper Chromosome Segregation. *Molecular and Cellular Biology* 34, 2464-2478.

Okamoto, K., Bartocci, C., Ouzounov, I., Diedrich, J.K., Yates, J.R., 3rd, and Denchi, E.L. (2013). A two-step mechanism for TRF2-mediated chromosome-end protection. *Nature* *494*, 502-505.

Opresko, P.L., Otterlei, M., Graakjaer, J., Bruheim, P., Dawut, L., Kolvraa, S., May, A., Seidman, M.M., and Bohr, V.A. (2004). The Werner syndrome helicase and exonuclease cooperate to resolve telomeric D loops in a manner regulated by TRF1 and TRF2. *Molecular cell* *14*, 763-774.

Orthwein, A., Fradet-Turcotte, A., Noordermeer, S.M., Canny, M.D., Brun, C.M., Strecker, J., Escibano-Diaz, C., and Durocher, D. (2014). Mitosis Inhibits DNA Double-Strand Break Repair to Guard Against Telomere Fusions. *Science* *344*, 189-193.

Paeschke, K., McDonald, K.R., and Zakian, V.A. (2010). Telomeres: structures in need of unwinding. *FEBS letters* *584*, 3760-3772.

Palm, W., and de Lange, T. (2008). How Shelterin Protects Mammalian Telomeres. *Annual Review of Genetics* *42*, 301-334.

Palm, W., Hockemeyer, D., Kibe, T., and de Lange, T. (2009). Functional dissection of human and mouse POT1 proteins. *Molecular and cellular biology* *29*, 471-482.

Pfister, S.X., Ahrabi, S., Zalmas, L.P., Sarkar, S., Aymard, F., Bachrati, C.Z., Helleday, T., Legube, G., La Thangue, N.B., Porter, A.C.G., *et al.* (2014). SETD2-Dependent Histone H3K36 Trimethylation Is Required for Homologous Recombination Repair and Genome Stability. *Cell Rep* *7*, 2006-2018.

Pickett, H.A., Henson, J.D., Au, A.Y.M., Neumann, A.A., and Reddel, R.R. (2011). Normal mammalian cells negatively regulate telomere length by telomere trimming. *Human Molecular Genetics* *20*, 4684-4692.

Preuss, U., Landsberg, G., and Scheidtmann, K.H. (2003). Novel mitosis-specific phosphorylation of histone H3 at Thr11 mediated by Dlk/ZIP kinase. *Nucleic Acids Research* *31*, 878-885.

Qin, S., and Min, J. (2014). Structure and function of the nucleosome-binding PWWP domain. *Trends in Biochemical Sciences* *39*, 536-547.

Ratnakumar, K., Duarte, L.F., LeRoy, G., Hasson, D., Smeets, D., Vardabasso, C., Bonisch, C., Zeng, T.Y., Xiang, B., Zhang, D.Y., *et al.* (2012). ATRX-mediated chromatin association of histone variant macroH2A1 regulates alpha-globin expression. *Genes & Development* 26, 433-438.

Ray-Gallet, D., Woolfe, A., Vassias, I., Pellentz, C., Lacoste, N., Puri, A., Schultz, D.C., Pchelintsev, N.A., Adams, P.D., Jansen, L.E., *et al.* (2011). Dynamics of histone H3 deposition in vivo reveal a nucleosome gap-filling mechanism for H3.3 to maintain chromatin integrity. *Molecular cell* 44, 928-941.

Redon, S., Reichenbach, P., and Lingner, J. (2010). The non-coding RNA TERRA is a natural ligand and direct inhibitor of human telomerase. *Nucleic Acids Research* 38, 5797-5806.

Rizzo, A., Salvati, E., Porru, M., D'Angelo, C., Stevens, M.F., D'Incalci, M., Leonetti, C., Gilson, E., Zupi, G., and Biroccio, A. (2009). Stabilization of quadruplex DNA perturbs telomere replication leading to the activation of an ATR-dependent ATM signaling pathway. *Nucleic Acids Research* 37, 5353-5364.

Sabbattini, P., Canzonetta, C., Sjoberg, M., Nikic, S., Georgiou, A., Kemball-Cook, G., Auner, H.W., and Dillon, N. (2007). A novel role for the Aurora B kinase in epigenetic marking of silent chromatin in differentiated postmitotic cells. *The EMBO journal* 26, 4657-4669.

Sabbattini, P., Sjoberg, M., Nikic, S., Frangini, A., Holmqvist, P.-H., Kunowska, N., Carroll, T., Brookes, E., Arthur, S.J., Pombo, A., *et al.* (2014). An H3K9/S10 methyl-phospho switch modulates Polycomb and Pol II binding at repressed genes during differentiation. *Molecular Biology of the Cell* 25, 904-915.

Sansoni, V., Casas-Delucchi, C.S., Rajan, M., Schmidt, A., Bonisch, C., Thomae, A.W., Staeger, M.S., Hake, S.B., Cardoso, M.C., and Imhof, A. (2014). The histone variant H2A.Bbd is enriched at sites of DNA synthesis. *Nucleic Acids Research* 42, 6405-6420.

Santenard, A., Ziegler-Birling, C., Koch, M., Tora, L., Bannister, A.J., and Torres-Padilla, M.E. (2010). Heterochromatin formation in the mouse embryo requires critical residues of the histone variant H3.3. *Nature cell biology* 12, 853-862.

Sarek, G., Vannier, J.B., Panier, S., Petrini, J.H., and Boulton, S.J. (2015). TRF2 recruits RTEL1 to telomeres in S phase to promote t-loop unwinding. *Molecular cell* *57*, 622-635.

Sarkies, P., Reams, C., Simpson, L.J., and Sale, J.E. (2010). Epigenetic instability due to defective replication of structured DNA. *Molecular cell* *40*, 703-713.

Sarma, K., Cifuentes-Rojas, C., Ergun, A., del Rosario, A., Jeon, Y., White, F., Sadreyev, R., and Lee, Jeannie T. (2014). ATRX Directs Binding of PRC2 to Xist RNA and Polycomb Targets. *Cell* *159*, 869-883.

Sawatsubashi, S., Murata, T., Lim, J., Fujiki, R., Ito, S., Suzuki, E., Tanabe, M., Zhao, Y., Kimura, S., Fujiyama, S., *et al.* (2012). A histone chaperone, DEK, transcriptionally coactivates a nuclear receptor (vol 24, pg 159, 2010). *Genes & Development* *26*, 2118-2118.

Sawicka, A., and Seiser, C. (2012). Histone H3 phosphorylation - a versatile chromatin modification for different occasions. *Biochimie* *94*, 2193-2201.

Scheel, C., Schaefer, K.L., Jauch, A., Keller, M., Wai, D., Brinkschmidt, C., van Valen, F., Boecker, W., Dockhorn-Dworniczak, B., and Poremba, C. (2001). Alternative lengthening of telomeres is associated with chromosomal instability in osteosarcomas. *Oncogene* *20*, 3835-3844.

Schneiderman, J.I., Orsi, G.A., Hughes, K.T., Loppin, B., and Ahmad, K. (2012). Nucleosome-depleted chromatin gaps recruit assembly factors for the H3.3 histone variant. *Proc Natl Acad Sci U S A* *109*, 19721-19726.

Schoeftner, S., and Blasco, M.A. (2008). Developmentally regulated transcription of mammalian telomeres by DNA-dependent RNA polymerase II. *Nature cell biology* *10*, 228-236.

Schoeftner, S., and Blasco, M.A. (2010). Chromatin regulation and non-coding RNAs at mammalian telomeres. *Semin Cell Dev Biol* *21*, 186-193.

Schwartz, B.E., and Ahmad, K. (2005). Transcriptional activation triggers deposition and removal of the histone variant H3.3. *Genes & development* *19*, 804-814.

Schwartzentruber, J., Korshunov, A., Liu, X.Y., Jones, D.T.W., Pfaff, E., Jacob, K., Sturm, D., Fontebasso, A.M., Quang, D.A.K., Tonjes, M., *et al.* (2012). Driver mutations in histone H3.3 and chromatin remodelling genes in paediatric glioblastoma. *Nature* *482*, 226-U119.

Selvarajah, S., Yoshimoto, M., Park, P.C., Maire, G., Paderova, J., Bayani, J., Lim, G., Al-Romaih, K., Squire, J.A., and Zielenska, M. (2006). The breakage-fusion-bridge (BFB) cycle as a mechanism for generating genetic heterogeneity in osteosarcoma. *Chromosoma* *115*, 459-467.

Sfeir, A., and de Lange, T. (2012). Removal of Shelterin Reveals the Telomere End-Protection Problem. *Science* *336*, 593-597.

Sfeir, A., Kabir, S., van Overbeek, M., Celli, G.B., and de Lange, T. (2010). Loss of Rap1 induces telomere recombination in the absence of NHEJ or a DNA damage signal. *Science* *327*, 1657-1661.

Sfeir, A., Kosiyatrakul, S.T., Hockemeyer, D., MacRae, S.L., Karlseder, J., Schildkraut, C.L., and de Lange, T. (2009). Mammalian Telomeres Resemble Fragile Sites and Require TRF1 for Efficient Replication. *Cell* *138*, 90-103.

Shay, J.W., and Bacchetti, S. (1997). A survey of telomerase activity in human cancer. *Eur J Cancer* *33*, 787-791.

Shi, L.L., Wang, J., Hong, F., Spector, D.L., and Fang, Y.D. (2011). Four amino acids guide the assembly or disassembly of Arabidopsis histone H3.3-containing nucleosomes. *Proceedings of the National Academy of Sciences of the United States of America* *108*, 10574-10578.

Shiloh, Y. (2003). ATM and related protein kinases: Safeguarding genome integrity. *Nat Rev Cancer* *3*, 155-168.

Shimada, M., Haruta, M., Niida, H., Sawamoto, K., and Nakanishi, M. (2010). Protein phosphatase 1gamma is responsible for dephosphorylation of histone H3 at Thr 11 after DNA damage. *EMBO reports* *11*, 883-889.

Shimada, M., Niida, H., Zineldeen, D.H., Tagami, H., Tanaka, M., Saito, H., and Nakanishi, M. (2008). Chk1 is a histone H3 threonine 11 kinase that regulates DNA damage-induced transcriptional repression. *Cell* *132*, 221-232.

Smogorzewska, A., van Steensel, B., Bianchi, A., Oelmann, S., Schaefer, M.R., Schnapp, G., and de Lange, T. (2000). Control of human telomere length by TRF1 and TRF2. *Molecular and cellular biology* *20*, 1659-1668.

Soboleva, T.A., Nekrasov, M., Pahwa, A., Williams, R., Huttley, G.A., and Tremethick, D.J. (2012). A unique H2A histone variant occupies the transcriptional start site of active genes. *Nature structural & molecular biology* *19*, 25-U37.

Stagno d'Alcontres, M., Palacios, A., Mejias, D., and Blasco, M.A. (2014). TopoII α prevents telomere fragility and formation of ultra thin DNA bridges during mitosis through TRF1-dependent binding to telomeres. *Cell Cycle* *13*, 1463-1481.

Stephan, H., Concannon, C., Kremmer, E., Carty, M.P., and Nasheuer, H.P. (2009). Ionizing radiation-dependent and independent phosphorylation of the 32-kDa subunit of replication protein A during mitosis. *Nucleic acids research* *37*, 6028-6041.

Sturm, D., Witt, H., Hovestadt, V., Khuong-Quang, D., Jones, D.T.W., Korshunov, A., Tonjes, M., Plass, C., Jabado, N., and Pfister, S.M. (2012). Hotspot mutations in H3F3A and IDH1 define distinct epigenetic and biological subgroups of glioblastoma. *Neuro-Oncology* *14*, 15-15.

Szenker, E., Ray-Gallet, D., and Almouzni, G. (2011). The double face of the histone variant H3.3. *Cell research* *21*, 421-434.

Tagami, H., Ray-Gallet, D., Almouzni, G., and Nakatani, Y. (2004). Histone H3.1 and H3.3 complexes mediate nucleosome assembly pathways dependent or independent of DNA synthesis. *Cell* *116*, 51-61.

Takai, H., Smogorzewska, A., and de Lange, T. (2003). DNA damage foci at dysfunctional telomeres. *Curr Biol* *13*, 1549-1556.

Takai, K.K., Kibe, T., Donigian, J.R., Frescas, D., and de Lange, T. (2011). Telomere Protection by TPP1/POT1 Requires Tethering to TIN2. *Molecular cell* *44*, 647-659.

Tang, M.C., Binos, S., Ong, E.K., Wong, L.H., and Mann, J.R. (2014). High histone variant H3.3 content in mouse prospermatogonia suggests a role in epigenetic reformatting. *Chromosoma*.

Thompson, R., Montano, R., and Eastman, A. (2012). The Mre11 Nuclease Is Critical for the Sensitivity of Cells to Chk1 Inhibition. *PLoS one* 7, e44021.

Tomonaga, T., Matsushita, K., Yamaguchi, S., Oohashi, T., Shimada, H., Ochiai, T., Yoda, K., and Nomura, F. (2003). Overexpression and mistargeting of centromere protein-A in human primary colorectal cancer. *Cancer Res* 63, 3511-3516.

Ulbricht, T., Alzrigat, M., Horch, A., Reuter, N., von Mikecz, A., Steimle, V., Schmitt, E., Kramer, O.H., Stamminger, T., and Hemmerich, P. (2012). PML promotes MHC class II gene expression by stabilizing the class II transactivator. *The Journal of cell biology* 199, 49-63.

Uren, A.G., Wong, L., Pakusch, M., Fowler, K.J., Burrows, F.J., Vaux, D.L., and Choo, K.H. (2000). Survivin and the inner centromere protein INCENP show similar cell-cycle localization and gene knockout phenotype. *Curr Biol* 10, 1319-1328.

van der Heijden, G.W., Dieker, J.W., Derijck, A.A.H.A., Muller, S., Berden, J.H.M., Braat, D.D.M., van der Vlag, J., and de Boer, P. (2005). Asymmetry in Histone H3 variants and lysine methylation between paternal and maternal chromatin of the early mouse zygote. *Mech Develop* 122, 1008-1022.

van Steensel, B., and de Lange, T. (1997). Control of telomere length by the human telomeric protein TRF1. *Nature* 385, 740-743.

van Steensel, B., Smogorzewska, A., and de Lange, T. (1998). TRF2 protects human telomeres from end-to-end fusions. *Cell* 92, 401-413.

Vannier, J.B., Pavicic-Kaltenbrunner, V., Petalcorin, M.I., Ding, H., and Boulton, S.J. (2012). RTEL1 dismantles T loops and counteracts telomeric G4-DNA to maintain telomere integrity. *Cell* 149, 795-806.

Vassilev, L.T., Tovar, C., Chen, S., Knezevic, D., Zhao, X., Sun, H., Heimbrook, D.C., and Chen, L. (2006). Selective small-molecule inhibitor reveals critical mitotic functions of human CDK1. *Proceedings of the National Academy of Sciences* *103*, 10660-10665.

Verdun, R.E., Crabbe, L., Haggblom, C., and Karlseder, J. (2005). Functional human telomeres are recognized as DNA damage in G2 of the cell cycle. *Molecular cell* *20*, 551-561.

Verdun, R.E., and Karlseder, J. (2007). Replication and protection of telomeres. *Nature* *447*, 924-931.

Voigt, P., LeRoy, G., Drury, W.J., Zee, B.M., Son, J., Beck, D.B., Young, N.L., Garcia, B.A., and Reinberg, D. (2012). Asymmetrically Modified Nucleosomes. *Cell* *151*, 181-193.

Wang, C., Cai, W., Li, Y., Deng, H., Bao, X., Girton, J., Johansen, J., and Johansen, K.M. (2011). The epigenetic H3S10 phosphorylation mark is required for counteracting heterochromatic spreading and gene silencing in *Drosophila melanogaster*. *J Cell Sci* *124*, 4309-4317.

Watson, L.A., Solomon, L.A., Li, J.R., Jiang, Y., Edwards, M., Shin-ya, K., Beier, F., and Berube, N.G. (2013). Atrx deficiency induces telomere dysfunction, endocrine defects, and reduced life span. *J Clin Invest* *123*, 2049-2063.

Wei, Y., Yu, L.L., Bowen, J., Gorovsky, M.A., and Allis, C.D. (1999). Phosphorylation of histone H3 is required for proper chromosome condensation and segregation. *Cell* *97*, 99-109.

Wen, H., Li, Y., Xi, Y., Jiang, S., Stratton, S., Peng, D., Tanaka, K., Ren, Y., Xia, Z., Wu, J., *et al.* (2014). ZMYND11 links histone H3.3K36me3 to transcription elongation and tumour suppression. *Nature* *508*, 263-268.

Weth, O., Paprotka, C., Günther, K., Schulte, A., Baierl, M., Leers, J., Galjart, N., and Renkawitz, R. (2014). CTCF induces histone variant incorporation, erases the H3K27me3 histone mark and opens chromatin. *Nucleic Acids Research* *42*, 11941-11951.

Wiestler, B., Capper, D., Holland-Letz, T., Korshunov, A., von Deimling, A., Pfister, S.M., Platten, M., Weller, M., and Wick, W. (2013). ATRX loss refines the classification of anaplastic gliomas and identifies a subgroup of IDH mutant astrocytic tumors with better prognosis. *Acta neuropathologica* 126, 443-451.

Wong, L.H., McGhie, J.D., Sim, M., Anderson, M.A., Ahn, S., Hannan, R.D., George, A.J., Morgan, K.A., Mann, J.R., and Choo, K.H. (2010). ATRX interacts with H3.3 in maintaining telomere structural integrity in pluripotent embryonic stem cells. *Genome research* 20, 351-360.

Wong, L.H., Ren, H., Williams, E., McGhie, J., Ahn, S., Sim, M., Tam, A., Earle, E., Anderson, M.A., Mann, J., *et al.* (2009). Histone H3.3 incorporation provides a unique and functionally essential telomeric chromatin in embryonic stem cells. *Genome research* 19, 404-414.

Wong, L.H., Saffery, R., Anderson, M.A., Earle, E., Quach, J.M., Stafford, A.J., Fowler, K.J., and Choo, K.H. (2005). Analysis of mitotic and expression properties of human neocentromere-based transchromosomes in mice. *J Biol Chem* 280, 3954-3962.

Wu, G., Broniscer, A., McEachron, T.A., Lu, C., Paugh, B.S., Beckfort, J., Qu, C., Ding, L., Huether, R., Parker, M., *et al.* (2012). Somatic histone H3 alterations in pediatric diffuse intrinsic pontine gliomas and non-brainstem glioblastomas. *Nature genetics* 44, 251-253.

Wu, G.K., Jiang, X.Z., Lee, W.H., and Chen, P.L. (2003). Assembly of functional ALT-associated promyelocytic leukemia bodies requires Nijmegen breakage syndrome 1. *Cancer Res* 63, 2589-2595.

Wu, L., Multani, A.S., He, H., Cosme-Blanco, W., Deng, Y., Deng, J.M., Bachilo, O., Pathak, S., Tahara, H., Bailey, S.M., *et al.* (2006). Pot1 deficiency initiates DNA damage checkpoint activation and aberrant homologous recombination at telomeres. *Cell* 126, 49-62.

Xu, M., Long, C., Chen, X., Huang, C., Chen, S., and Zhu, B. (2010). Partitioning of histone H3-H4 tetramers during DNA replication-dependent chromatin assembly. *Science* 328, 94-98.

Yang, Q., Zheng, Y.L., and Harris, C.C. (2005). POT1 and TRF2 cooperate to maintain telomeric integrity. *Molecular and cellular biology* 25, 1070-1080.

Yang, X., Li, L., Liang, J., Shi, L., Yang, J., Yi, X., Zhang, D., Han, X., Yu, N., and Shang, Y. (2013). Histone Acetyltransferase 1 Promotes Homologous Recombination in DNA Repair by Facilitating Histone Turnover. *Journal of Biological Chemistry* 288, 18271-18282.

Yeager, T.R., Neumann, A.A., Englezou, A., Huschtscha, L.I., Noble, J.R., and Reddel, R.R. (1999). Telomerase-negative immortalized human cells contain a novel type of promyelocytic leukemia (PML) body. *Cancer Res* 59, 4175-4179.

Yehezkel, S., Segev, Y., Viegas-Pequignot, E., Skorecki, K., and Selig, S. (2008). Hypomethylation of subtelomeric regions in ICF syndrome is associated with abnormally short telomeres and enhanced transcription from telomeric regions. *Human molecular genetics* 17, 2776-2789.

Yeung, P.L., Denissova, N.G., Nasello, C., Hakhverdyan, Z., Chen, J.D., and Brenneman, M.A. (2012). Promyelocytic leukemia nuclear bodies support a late step in DNA double-strand break repair by homologous recombination. *Journal of Cellular Biochemistry* 113, 1787-1799.

Yu, J., Lan, J.P., Wang, C., Wu, Q., Zhu, Y.Y., Lai, X.Y., Sun, J., Jin, C.J., and Huang, H. (2010). PML3 interacts with TRF1 and is essential for ALT-associated PML bodies assembly in U2OS cells. *Cancer Lett* 291, 177-186.

Yu, T.Y., Kao, Y.W., and Lin, J.J. (2014). Telomeric transcripts stimulate telomere recombination to suppress senescence in cells lacking telomerase. *Proceedings of the National Academy of Sciences of the United States of America* 111, 3377-3382.

Yuen, B.T.K., Bush, K.M., Barrilleaux, B.L., Cotterman, R., and Knoepfler, P.S. (2014). Histone H3.3 regulates dynamic chromatin states during spermatogenesis. *Development* 141, 3483-3494.

Zachos, G., Black, E.J., Walker, M., Scott, M.T., Vagnarelli, P., Earnshaw, W.C., and Gillespie, D.A. (2007). Chk1 is required for spindle checkpoint function. *Developmental cell* 12, 247-260.

Zentner, G.E., and Henikoff, S. (2013). Regulation of nucleosome dynamics by histone modifications. *Nature structural & molecular biology* 20, 259-266.

Zhang, Y., and Hunter, T. (2014). Roles of Chk1 in cell biology and cancer therapy. *International journal of cancer Journal international du cancer* 134, 1013-1023.

Zhong, Z.H., Jiang, W.Q., Cesare, A.J., Neumann, A.A., Wadhwa, R., and Reddel, R.R. (2007). Disruption of telomere maintenance by depletion of the MRE11/RAD50/NBS1 complex in cells that use alternative lengthening of telomeres. *Journal of Biological Chemistry* 282, 29314-29322.

Zhu, X.D., Kuster, B., Mann, M., Petrini, J.H., and de Lange, T. (2000). Cell-cycle-regulated association of RAD50/MRE11/NBS1 with TRF2 and human telomeres. *Nature genetics* 25, 347-352.

Zimmermann, M., Kibe, T., Kabir, S., and de Lange, T. (2014). TRF1 negotiates TTAGGG repeat-associated replication problems by recruiting the BLM helicase and the TPP1/POT1 repressor of ATR signaling. *Genes & Development* 28, 2477-2491.